T-CELL DYNAMICS IN CHRONIC VIRAL INFECTION

Nieuwe inzichten in de dynamiek van T cellen tijdens chronische virale infecties
(met een samenvatting in het Nederlands)

Proefschrift

ter verkrijging van de graad van doctor
aan de Universiteit Utrecht op gezag
van de rector magnificus, prof.dr. G.J. van der Zwaan,
ingevolge het besluit van het college voor promoties
in het openbaar te verdedigen op donderdag
30 januari 2014 des middags te 12.45 uur

door

Elisabeth Maria Veel

geboren op 9 maart 1982 te Alkmaar

Promotor: Prof.dr. F. Miedema

Co-promotoren: Dr. K. Tesselaar
                    Dr. J.A.M. Borghans

CONTENTS

CHAPTER

GENERAL INTRODUCTION

1

CHRONIC VIRAL INFECTIONS AND THE IMMUNE SYSTEM

Viruses are pathogens that replicate within host cells. Many virus infections are self-limited because the host immune system eliminates the virus. Infections with certain viruses, however, fail to resolve and become chronic. Such infections can continue for prolonged periods and often result in a life-long infection. Some of these infections may cause serious progressive disease and early death while others only cause disease in immune-compromised individuals. Examples of chronic infections are herpes virus- and human immunodeficiency virus (HIV) infections. Herpes viruses are chronic latent viruses, which means that, at some stage, they enter a phase in which viral reactivation occurs only sporadically (1). By contrast, HIV is a persistent virus that continuously produces new virus particles (1).

Chronic viruses usually exploit multiple mechanisms to evade the immune system (1-5) and are often capable of substantially altering the this system. Which modifications chronic viruses cause to the human immune system is currently not completely understood for every virus. In this thesis, the alterations that chronic viral infections cause within the human immune system are subject of investigation.

T-LYMPHOCYTE DEVELOPMENT

T cells play a central role in adaptive immunity and are of particular importance in eliminating and/or controlling viruses that have infected a host. A unique characteristic of adaptive immunity is the presence of antigen receptors on individual cells with distinct specificities, which allows for the recognition of a wide range of pathogens in a specific manner and fine tuning of the response. The T-cell compartment consists of approximately 25×10^6 unique T cells, which should be sufficient to fight most pathogens an individual encounters (6).

The distinct T-cell receptors (TCR) are formed by recombination of the TCR genes during T-cell development in the thymus. After completion of TCR rearrangement, αβ T cells, which are investigated in depth in this thesis, commit to either the CD4$^+$ or the CD8$^+$ T-cell lineage. Upon completion of T-cell maturation, they leave the thymus and move to the peripheral lymphoid organs were they can differentiate.

DIFFERENTIATION OF T CELLS

In this thesis, in depth analysis of several T-cell subsets, which are being distinguished based on phenotype, is described. Different subsets of CD4$^+$ and CD8$^+$ T cells can be phenotypically distinguished, based on their differentiation status. Phenotype analysis is a widely used and straightforward way to show whether a T cell is naive or antigen experienced. Also, other characteristics, such as longevity or the ability to proliferate, have been associated with certain phenotypical characteristics. T cells that have migrated to the periphery, but have not yet recognized their antigen are termed naive. Upon the first encounter between naive T cells and their antigen, presented on major histocompatibility complex (MHC) molecules, they become activated and differentiate into effector cells (7). CD8$^+$ T cells mainly interact with presented peptides from intracellular pathogens, such as viruses, while CD4$^+$ T cells mainly interact with presented peptides from extracellular pathogens, such as bacteria. CD4$^+$ and CD8$^+$ effector

T cells that are generated upon activation are functionally distinct. CD8+ effector T cells are capable of directly killing infected cells by the secretion of perforins and granzymes (7). CD4+ effector T cells secrete cytokines that have a direct effect on target cells or that have an indirect effect by activating different arms of the immune system (7). Antigen specific T cells that survive after a primary infection are termed antigen experienced or memory T cells (7;8). They are capable of generating a fast and vigorous response upon a second encounter with the same antigen. Two types of memory cells have been identified, central memory T cells and effector memory T cells. Central memory T cells reside in secondary lymphoid organs, have diminished cytolytic potential and limited migratory properties. Effector memory T cells are located in non-lymphoid tissues, have cytolytic activity and better circulatory potential (7;8).

ALTERATIONS OF THE IMMUNE SYSTEM INDUCED BY CHRONIC VIRAL INFECTIONS

The scenario described above typically occurs following acute infections. When a pathogen persists, the course of T-cell responses can be substantially modified and the immune system may be activated chronically. The effects of chronic immune activation by HIV and CMV on the human T-cell compartment are investigated in chapter 2 – 6. Chronic activation of the immune system, caused by persisting virus infections, but also cancers and overwhelming bacterial infections, may lead to impaired immune responses to other pathogens (9;10). Functional and phenotypical alterations during chronic immune activation have often been attributed to repeated stimulation with antigen, a process called replicative senescence (11;12). This can lead to functional exhaustion of both CD4+ and CD8+ T cells, which is characterized by a diminished proliferative capacity and failure to produce effector cytokines (12;13). Phenotypical alterations during chronic immune activation have also been described (12). T cells upregulate markers of exhaustion and terminal differentiation, which indicates that they have undergone extensive replicative senescence (13-15). T-cell turnover and life span are also altered during chronic viral infection (16;17). Labeling with the stable isotope deuterium is a unique tool to determine T-cell turnover and T-cell life span *in vivo*. Individuals receive deuterium for a certain period, varying from hours to weeks. This label is built in to the DNA of dividing or newly synthesized T cells and by frequent blood sampling the amount of T-cell DNA that contains deuterium can be measured. Mathematical modeling is subsequently applied to determine the actual turnover and life span of the T-cell subsets that are studied (chapter 2 and 3, (18-20).

KNOWN EFFECTS OF HIV INFECTION

HIV is a retrovirus that specifically targets CD4+ T cells and causes generalized immune activation. The virus cannot be eradicated and establishes a chronic infection. Chapter 2 – 5 show how HIV infection affects different aspects of the human immune system. Adaptive immunity develops during the first weeks of infection, and HIV-1 specific CD8+ T-cell responses are initiated (21). The association between the rise of HIV-1 specific CD8+ T-cell responses and the decrease in plasma viral load during acute HIV infection suggests that CD8+ T cells are important in the initial control of viral replication (22-25). Even in the acute phase of infection, effective HIV-1

specific CD4$^+$ T-cell responses are absent (26). Activated CD4$^+$ T cells are the main target of HIV-1 and are lost already early during HIV-infection. After the acute phase of HIV infection, the plasma viral load is reduced to a "set point" level. This viral set point, together with the degree of immune activation, is highly predictive for the later course of disease progression (21). Viral load in HIV infected individuals may remain at the set point for prolonged periods. The clinical and immunological changes during this phase are highly variable between different individuals (27). Due to continuous activation by the virus, memory and effector CD8$^+$ T-cell numbers generally increase during untreated HIV infection. Whether these CD8$^+$ T-cell expansions contract after cessation of HIV replication during antiretroviral treatment is explored in chapter 5. CD4$^+$ T cells are gradually lost during the chronic phase of HIV infection (28;29). Many infected CD4$^+$ T cells die from viral cytopathicity and cytotoxic intervention mediated by HIV-specific CD8$^+$ T cells and natural killer (NK) cells (30-32). Furthermore, bystander activation-induced cell death, that is programmed cell death resulting from sustained activation of non-infected CD4$^+$ T cells, contributes substantially to depletion of CD4$^+$ T cells (33;34). Due to ongoing recombination and mutations, HIV-1 permanently escapes from the recognition by CD8$^+$ T cells of the host (35). Loss of viral control is accompanied by a rise in HIV viral load, and a rapid loss of CD4$^+$ T cells.

Effects of HIV treatment. Typically, when HIV is not properly controlled CD4$^+$ T-cell numbers drop and patients become immunodeficient. To prevent immunodeficiency, combination antiretroviral therapy (cART) is initiated at a certain threshold number of CD4$^+$ T cells. In chapter 3 – 5, the effects of cART on the T-cell compartment of HIV infected individuals are described. cART is a combination of three different antiretroviral drugs, usually from two different drug classes. cART is aimed at inhibiting HIV replication at multiple levels, which include inhibition of enzymes required for virus replication, integration and prevention of HIV entry into the host cell. The latter is one of the newest drug classes and includes CCR5 antagonists. Currently, Maraviroc (celsentry ®) is the only registered CCR5 antagonist for the treatment of HIV-1 infected individuals (36). Chapter 3 focusses on the effect of Maraviroc on the turnover of T cells and chapter 4 describes the functional and phenotypical changes that treatment with Maraviroc induces in T cells. The success rate of cART is high. Individuals that adhere to treatment often show a good response, which is defined by a decrease in viral load and normalization of CD4$^+$ T-cell numbers (37;38). CD8$^+$ T-cell numbers have been described to increase during short-term cART (39-42).What happens to CD8$^+$ T cells during long-term cART is less well understood and is investigated in chapter 5.

KNOWN EFFECTS OF CMV INFECTION

The impact of cytomegalovirus (CMV) infection on the subset distribution and phenotypical characteristics of the T-cell compartment is presented in chapter 6. Similar to HIV, infection with CMV often becomes chronic. CMV, however, establishes clinical latency, whereas HIV is persistent. These two virus infections provide an opportunity to compare how persistent and latent viruses alter the human immune system. CMV is a member of the human herpes virus family. Once infection has occurred, CMV resides in an individual throughout life, but is controlled by CD8$^+$ T cells (43). The virus typically does not cause any symptoms in healthy,

immunocompetent individuals. CMV has a high infection rate, with 50–90% of the population becoming seropositive at some point in life (44;45). During the chronic phase of infection, the virus remains present, but usually dormant, and resides inside cells without causing detectable damage or clinical symptoms (45). CMV reactivation occurs predominantly in immunocompromised individuals, but has also been described in asymptomatic healthy individuals (43). It has previously been shown that a large part of CD8^{+} T cells in healthy CMV seropositive individuals is specific for CMV (46) and that the majority of CMV specific CD8^{+} T cells has a terminally differentiated phenotype (47-49). The high frequency of CMV specific effector CD8^{+} T cells in healthy, CMV seropositive individuals suggests that CMV may, in fact, frequently reactivate in this group, but these reactivations are well controlled and remain asymptomatic (46).

SCOPE OF THIS THESIS

In this thesis we investigate how chronic HIV and CMV infections impact on the human T-cell compartment.

How untreated HIV infection affects the turnover of human CD4^{+} and CD8^{+} T cells is described in chapter 2. In this chapter, T-cell turnover in untreated HIV infected individuals is compared to that in healthy individuals. To investigate whether certain HIV-induced alterations in the human T-cell compartment are reversible during therapy, we analyze T-cell turnover during cART with an in depth investigation of the role of the HIV entry inhibitor Maraviroc in immunological non-responders, a specific group of HIV infected individuals in which viral replication is controlled but immune recovery is slow, in chapter 3. Maraviroc and placebo treated individuals within the same clinical trial were compared in terms of T-cell turnover and life span. Functional and phenotypical changes in T cells during cART intensification with Maraviroc are characterized in chapter 4. In this placebo controlled clinical trial, Maraviroc treated individuals were followed longitudinally for 48 weeks, from the start of Maraviroc treatment intensification. Chapter 5 explores whether CD8^{+} T-cell numbers, which are expanded in untreated HIV infected individuals normalize during cART. This is investigated cross-sectionally after at least 5 years of successful cART. Chapter 6 covers the changes that chronic CMV infection induces in the CD8^{+} T-cell compartment. In a large cohort of children and adults, phenotypical characteristics of T cells from CMV seropositive and CMV seronegative individuals were compared. Chapter 7 focuses on the measurement of TCR diversity since this is an important tool to analyze the functionality of the human T-cell compartment. We optimized the AmpliCot method for the measurement of TCR diversity with mathematical modeling in this chapter.

REFERENCE LIST

1. Nikolich-Zugich J. Ageing and life-long maintenance of T-cell subsets in the face of latent persistent infections. Nat Rev Immunol **2008 Jul**;8(7):512-22.

2. Stern-Ginossar N, Elefant N, Zimmermann A, et al. Host immune system gene targeting by a viral miRNA. Science **2007 Jul 20**;317(5836):376-81.

3. Sylwester AW, Mitchell BL, Edgar JB, et al. Broadly targeted human cytomegalovirus-specific CD4+ and CD8+ T cells dominate the memory compartments of exposed subjects. J Exp Med **2005 Sep 5**;202(5):673-85.

4. Manel N, Littman DR. Hiding in plain sight: how HIV evades innate immune responses. Cell **2011 Oct 14**;147(2):271-4.

5. Whitney JB, Lim SY, Wainberg MA. Evolutionary mechanisms of retroviral persistence. AIDS Rev **2011 Oct**;13(4):234-9.

6. Arstila TP, Casrouge A, Baron V, Even J, Kanellopoulos J, Kourilsky P. A direct estimate of the human alphabeta T cell receptor diversity. Science **1999 Oct 29**;286(5441):958-61.

7. Schluns KS, Lefrancois L. Cytokine control of memory T-cell development and survival. Nat Rev Immunol **2003 Apr**;3(4):269-79.

8. Ahmed R, Bevan MJ, Reiner SL, Fearon DT. The precursors of memory: models and controversies. Nat Rev Immunol **2009 Sep**;9(9):662-8.

9. Lee PP, Yee C, Savage PA, et al. Characterization of circulating T cells specific for tumor-associated antigens in melanoma patients. Nat Med **1999 Jun**;5(6):677-85.

10. Rocha B, Grandien A, Freitas AA. Anergy and exhaustion are independent mechanisms of peripheral T cell tolerance. J Exp Med **1995 Mar 1**;181(3):993-1003.

11. Effros RB. Genetic alterations in the ageing immune system: impact on infection and cancer. Mech Ageing Dev **2003 Jan**;124(1):71-7.

12. Tarazona R, DelaRosa O, Alonso C, et al. Increased expression of NK cell markers on T lymphocytes in aging and chronic activation of the immune system reflects the accumulation of effector/senescent T cells. Mech Ageing Dev **2000 Dec 20**;121(1-3):77-88.

13. Shin H, Wherry EJ. CD8 T cell dysfunction during chronic viral infection. Curr Opin Immunol **2007 Aug**;19(4):408-15.

14. Batliwalla F, Monteiro J, Serrano D, Gregersen PK. Oligoclonality of CD8+ T cells in health and disease: aging, infection, or immune regulation? Hum Immunol **1996 Jun**;48(1-2):68-76.

15. Monteiro J, Batliwalla F, Ostrer H, Gregersen PK. Shortened telomeres in clonally expanded CD28-CD8+ T cells imply a replicative history that is distinct from their CD28+CD8+ counterparts. J Immunol **1996 May 15**;156(10):3587-90.

16. Hellerstein MK, Hoh RA, Hanley MB, et al. Subpopulations of long-lived and short-lived T cells in advanced HIV-1 infection. J Clin Invest **2003 Sep**;112(6):956-66.

17. Wallace DL, Zhang Y, Ghattas H, et al. Direct measurement of T cell subset kinetics in vivo in elderly men and women. J Immunol **2004 Aug 1**;173(3):1787-94.

18. Busch R, Neese RA, Awada M, Hayes GM, Hellerstein MK. Measurement of cell proliferation by heavy water labeling. Nat Protoc **2007**;2(12):3045-57.

19. Neese RA, Misell LM, Turner S, et al. Measurement in vivo of proliferation rates of slow turnover cells by 2H2O labeling of the deoxyribose moiety of DNA. Proc Natl Acad Sci U S A **2002 Nov 26**;99(24):15345-50.

20. Vrisekoop N, den B, I, de Boer AB, et al. Sparse production but preferential incorporation of recently produced naive T cells in the human peripheral pool. Proc Natl Acad Sci U S A **2008 Apr 22**;105(16):6115-20.

21. Streeck H, Jolin JS, Qi Y, et al. Human immunodeficiency virus type 1-specific CD8+ T-cell responses during primary infection are major determinants of the viral set point and loss of CD4+ T cells. J Virol **2009 Aug**;83(15):7641-8.

22. Borrow P, Lewicki H, Hahn BH, Shaw GM, Oldstone MB. Virus-specific CD8+ cytotoxic T-lymphocyte activity associated with control of viremia in primary human immunodeficiency virus type 1 infection. J Virol **1994 Sep**;68(9):6103-10.

23. Jin X, Bauer DE, Tuttleton SE, et al. Dramatic rise in plasma viremia after CD8(+) T cell depletion in simian immunodeficiency virus-infected macaques. J Exp Med **1999 Mar 15**;189(6):991-8.

24. Koup RA, Safrit JT, Cao Y, et al. Temporal association of cellular immune responses with the initial control of viremia in primary human immunodeficiency virus type 1 syndrome. J Virol **1994 Jul**;68(7):4650-5.

25. Schmitz JE, Kuroda MJ, Santra S, et al. Control of viremia in simian immunodeficiency virus infection by CD8+ lymphocytes. Science **1999 Feb 5**;283(5403):857-60.

26. Altfeld M, Rosenberg ES. The role of CD4(+) T helper cells in the cytotoxic T lymphocyte

response to HIV-1. Curr Opin Immunol **2000 Aug**;12(4):375-80.

27. Carrington M, O'Brien SJ. The influence of HLA genotype on AIDS. Annu Rev Med **2003**;54:535-51.

28. Autran B, Debre P, Walker B, Katlama C. Therapeutic vaccines against HIV need international partnerships. Nat Rev Immunol **2003 Jun**;3(6):503-8.

29. Roederer M, Dubs JG, Anderson MT, Raju PA, Herzenberg LA, Herzenberg LA. CD8 naive T cell counts decrease progressively in HIV-infected adults. J Clin Invest **1995 May**;95(5):2061-6.

30. Brenchley JM, Schacker TW, Ruff LE, et al. CD4+ T cell depletion during all stages of HIV disease occurs predominantly in the gastrointestinal tract. J Exp Med **2004 Sep 20**;200(6):749-59.

31. Cheynier R, Henrichwark S, Hadida F, et al. HIV and T cell expansion in splenic white pulps is accompanied by infiltration of HIV-specific cytotoxic T lymphocytes. Cell **1994 Aug 12**;78(3):373-87.

32. Vieillard V, Strominger JL, Debre P. NK cytotoxicity against CD4+ T cells during HIV-1 infection: a gp41 peptide induces the expression of an NKp44 ligand. Proc Natl Acad Sci U S A **2005 Aug 2**;102(31):10981-6.

33. Appay V, Sauce D. Immune activation and inflammation in HIV-1 infection: causes and consequences. J Pathol **2008 Jan**;214(2):231-41.

34. Gougeon ML, Montagnier L. Programmed cell death as a mechanism of CD4 and CD8 T cell deletion in AIDS. Molecular control and effect of highly active anti-retroviral therapy. Ann N Y Acad Sci **1999**;887:199-212.

35. Coffin JM. HIV population dynamics in vivo: implications for genetic variation, pathogenesis, and therapy. Science **1995 Jan 27**;267(5197):483-9.

36. Gulick RM, Lalezari J, Goodrich J, et al. Maraviroc for previously treated patients with R5 HIV-1 infection. N Engl J Med **2008 Oct 2**;359(14):1429-41.

37. Cameron DW, Heath-Chiozzi M, Danner S, et al. Randomised placebo-controlled trial of ritonavir in advanced HIV-1 disease. The Advanced HIV Disease Ritonavir Study Group. Lancet **1998 Feb 21**;351(9102):543-9.

38. Hammer SM, Squires KE, Hughes MD, et al. A controlled trial of two nucleoside analogues plus indinavir in persons with human immunodeficiency virus infection and CD4 cell counts of 200 per cubic millimeter or less. AIDS Clinical Trials Group 320 Study Team. N Engl J Med **1997 Sep 11**;337(11):725-33.

39. Autran B, Carcelain G, Li TS, et al. Positive effects of combined antiretroviral therapy on CD4+ T cell homeostasis and function in advanced HIV disease. Science **1997 Jul 4**;277(5322):112-6.

40. Di MM, Sereti I, Matthews LT, et al. Naive T-cell dynamics in human immunodeficiency virus type 1 infection: effects of highly active antiretroviral therapy provide insights into the mechanisms of naive T-cell depletion. J Virol **2006 Mar**;80(6):2665-74.

41. Dyrhol-Riise AM, Voltersvik P, Olofsson J, Asjo B. Activation of CD8 T cells normalizes and correlates with the level of infectious provirus in tonsils during highly active antiretroviral therapy in early HIV-1 infection. AIDS **1999 Dec 3**;13(17):2365-76.

42. Pakker NG, Notermans DW, de Boer RJ, et al. Biphasic kinetics of peripheral blood T cells after triple combination therapy in HIV-1 infection: a composite of redistribution and proliferation. Nat Med **1998 Feb**;4(2):208-14.

43. Harari A, Zimmerli SC, Pantaleo G. Cytomegalovirus (CMV)-specific cellular immune responses. Hum Immunol **2004 May**;65(5):500-6.

44. Landolfo S, Gariglio M, Gribaudo G, Lembo D. The human cytomegalovirus. Pharmacol Ther **2003 Jun**;98(3):269-97.

45. Scholz M, Doerr HW, Cinatl J. Human cytomegalovirus retinitis: pathogenicity, immune evasion and persistence. Trends Microbiol **2003 Apr**;11(4):171-8.

46. Reinke P, Prosch S, Kern F, Volk HD. Mechanisms of human cytomegalovirus (HCMV) (re)activation and its impact on organ transplant patients. Transpl Infect Dis **1999 Sep**;1(3):157-64.

47. Aandahl EM, Sandberg JK, Beckerman KP, Tasken K, Moretto WJ, Nixon DF. CD7 is a differentiation marker that identifies multiple CD8 T cell effector subsets. J Immunol **2003 Mar 1**;170(5):2349-55.

48. Appay V, Dunbar PR, Callan M, et al. Memory CD8+ T cells vary in differentiation phenotype in different persistent virus infections. Nat Med **2002 Apr**;8(4):379-85.

49. Ellefsen K, Harari A, Champagne P, Bart PA, Sekaly RP, Pantaleo G. Distribution and functional analysis of memory antiviral CD8 T cell responses in HIV-1 and cytomegalovirus infections. Eur J Immunol **2002 Dec**;32(12):3756-64.

50. Brunner S, Herndler-Brandstetter D, Weinberger B, Grubeck-Loebenstein B. Persistent viral infections and immune aging. Ageing Res Rev **2011 Jul**;10(3):362-9.

CHAPTER

QUANTIFICATION OF NAIVE AND MEMORY T-CELL TURNOVER DURING HIV-1 INFECTION

2

Nienke Vrisekoop[a], Ellen Veel[a], Rogier van Gent[a],
Tendai Mugwagwa[b], Julia Drylewicz[a], Steven F.L. van Lelyveld[c],
Anne Bregje de Boer[a], Sigrid A. Otto[a], An F.C. Ruiter[d],
Mariëtte T. Ackermans[d], Joost N. Vermeulen[e,f],
Hidde H. Huidekoper[g], Koos Gaiser[a], Hans P. Sauerwein[g],
Jan M. Prins[f], Frank Miedema[a], Rob J. de Boer[b], Kiki Tesselaar[a]
and José A.M. Borghans[a]

[a] Laboratory for Translational Immunology, University Medical Center Utrecht,
Lundlaan 6, 3584 EA Utrecht;
[b] Theoretical Biology, Utrecht University, Padualaan 8, 3584 CH Utrecht;
[c] Department of Internal Medicine and Infectious Diseases, University Medical
Center Utrecht;
[d] Laboratory of Endocrinology, Academic Medical Center, Meibergdreef 9, 1105 AZ
Amsterdam;
[e] IATEC, Academic Medical Center, Amsterdam;
[f] Department of Internal Medicine, Academic Medical Center Amsterdam;
[g] Department of Endocrinology and Metabolism, Academic Medical Center,
Amsterdam,
The Netherlands.

ABSTRACT

The cause of the progressive decline of CD4$^+$ T-cell numbers during human immunodeficiency virus (HIV) infection remains debated. Based on different markers and labeling strategies, several studies have shown that T-cell turnover is increased during HIV infection. To understand which processes are responsible for the progressive loss of CD4$^+$ T cells during HIV infection, it is important to have quantitative insights into the life spans of cells constituting the different T-lymphocyte populations. Using long-term *in vivo* D$_2$O labeling, we show that during untreated chronic HIV-1 infection, naive CD4$^+$ and CD8$^+$ T lymphocytes live on average 618 and 271 days, while memory CD4$^+$ and CD8$^+$ T lymphocytes have average life spans of 53 and 43 days, respectively. We show that these average life spans are at least three-fold shorter than in healthy volunteers. While total CD4$^+$ T-cell counts in patients on effective cART were in the normal range, naive CD4$^+$ and CD8$^+$ T-cell lifespans remained affected. Our analyses also point out that while the naive CD8$^+$ T-cell pool in healthy individuals forms a kinetically homogeneous population of long-lived cells, upon HIV-1 infection it becomes kinetically heterogeneous, with some cells acquiring a higher turnover rate. We discuss the implications of such shifts in T-cell dynamics for the different mechanisms that have been held responsible for the changes in the T-cell pool that are typically observed in HIV-1 infected individuals.

INTRODUCTION

The cause of the progressive decline of CD4^{+} T-cell numbers during human immunodeficiency virus (HIV) infection remains debated. Although controversies remain on the role of impaired thymic output in HIV infection, there is ample evidence that the state of chronic immune activation induced by HIV plays a key role in disease progression (1-5). Several studies have shown increased production rates of CD4^{+} and CD8^{+} T cells during HIV-1 infection, measured by different labeling techniques or markers for T-cell proliferation (6-14). These increased turnover rates are not merely due to shifts in the percentages of naive and memory T cells, (15) because studies in separated naive and memory T-cell populations have shown that both naive and memory CD4^{+} and CD8^{+} T cells are turning over more rapidly in HIV-1 infected individuals (16).

To understand how these changes in T-cell turnover in HIV-1 infection cause the gradual depletion of CD4^{+} T cells, it is important to have quantitative insights into T-cell dynamics in healthy and HIV-1 infected individuals. Only once such quantitative insights are available, can one estimate, for example, the expected effect of impaired thymic output on CD4^{+} T-cell loss in HIV-1 infection. Quantitative insights into T-cell life spans are extremely scarce, because of the difficulty to measure cellular turnover rates under normal physiological circumstances. Markers that have been used to quantify T-cell dynamics include Annexin V staining of cells undergoing apoptosis, and measurement of the expression of Ki67, an intracellular marker that is uniquely expressed during the G1, S, G2 and mitotic phase of the cell cycle. Such snapshot markers are, however, hard to translate into the actual parameters of interest, i.e. the fraction of cells that die or proliferate per day. Moreover, it has been suggested that T cells undergoing proliferation in HIV-infected individuals can get stuck in the cell cycle (17), and hence the fraction of Ki67-expressing cells could exceed the fraction of cells that are actually producing progeny. The introduction of stable isotope labeling into the field of immunology has paved the way for reliable quantification of T-cell dynamics. Previous studies based on ^{2}H-glucose or D_2O labeling have demonstrated the great potential of this technique in the field of lymphocyte turnover (7;9;11;12;16;18-23).

Using stable-isotope labeling, we compared the average life spans and total daily production rates (i.e., numbers of cells produced per day) of naive and memory CD4^{+} and CD8^{+} T cells in healthy volunteers and in treatment-naive and combination antiretroviral therapy (cART)-treated HIV-1 infected individuals. We report the first complete up- and down-labeling curves after long-term *in vivo* D_2O labeling in chronic HIV-1 infected individuals. Mathematical analysis of these data reveals that, while total T-cell population sizes are hardly changing, the average life spans of not only memory, but also naive CD4^{+} and CD8^{+} T lymphocytes are at least three-fold shortened during untreated HIV-1 infection. Upon effective cART, the dynamics of naive CD4^{+} and CD8^{+} T cells remain affected, despite good reconstitution of the CD4^{+} T-cell pool. We also show that the naive CD8^{+} T-lymphocyte population, which is kinetically homogeneous in healthy individuals, becomes kinetically heterogeneous upon HIV-1 infection. We discuss the implications of these quantitative changes for the different mechanisms that are held responsible for the changes in the T-cell population that are typically observed in HIV-1 infected individuals.

MATERIAL AND METHODS

Subjects and in vivo D$_2$O labeling protocol. Four HIV-infected and five healthy male volunteers were admitted to the AMC hospital, Amsterdam, the Netherlands to receive the initial dose of 10 ml D$_2$O per kg body water in small portions throughout the day. Three HIV-infected male volunteers were admitted to the UMC Utrecht, the Netherlands to receive the same initial dose. Body water was estimated to be 60% of body weight. As a maintenance dose, the subjects drank 1/8 of their initial dose daily for nine weeks. Blood and urine were collected before labeling (blood), at the end of the first labeling day (urine), four to six times during the rest of the nine-week labeling phase, five to seven during the down-label phase of 16 weeks, and approximately 3 years after stop of label in healthy individuals. Four HIV-patients were treatment-naive at inclusion and did not receive antiretroviral therapy during the whole protocol (CDC class A). Patient B experienced bronchitis (diagnosed and treated by the general practitioner) which started a few days prior to the second visit at day 22. Patient C withdrew from the protocol from day 113 onward, because he was advised to start treatment, and developed a disseminated Varicella shortly after withdrawal. Patient D developed gastro-enteritis (light fever and diarrhea) a few days prior to the visit at day 63. Three HIV-patients were receiving cART treatment at the time of inclusion. All three patients had more than 350 CD4$^+$ T cells / µl blood. They had viral suppression (< 50 copies/ml) and a maximal treatment interruption of two weeks within the six months prior to inclusion. All healthy volunteers were asked to answer a questionnaire to exclude (a high risk of) infections and immunomodulatory medication. Details about the HIV-infected patients are shown in Table 1, while those about the healthy volunteers have been described previously (22). This study was approved by the medical ethical committee of the AMC and written informed consent was obtained from all participants (22).

Flow cytometry and cell sorting. Absolute CD4$^+$ and CD8$^+$ T-cell counts were determined by dual-platform flow cytometry. Peripheral blood mononuclear cells (PBMC) were obtained by Ficoll-Paque density gradient centrifugation from heparinized blood and cryopreserved until further processed. T-cell proliferation in CD4$^+$ and CD8$^+$ T-cell subsets was studied by flow-cytometric measurements of the Ki67 nuclear antigen, as described previously (24). To measure the fraction of labeled cells within the naive (CD45RO$^-$CD27$^+$) and memory (CD45RO$^+$) CD4$^+$ and CD8$^+$ T-cell population, these subsets were isolated by cell sorting on a FACS Aria (BD) as previously described (22). Purity of the sorted cells was on average 99.2% for naive CD4$^+$, 98.7% for naive CD8$^+$ T cells, 98.1% for memory CD4$^+$ T cells and 97.1% for memory CD8$^+$ T cells.

Measurement of D$_2$O enrichment in body water and DNA and mathematical modeling. Deuterium enrichment in urine was measured by a method adopted from Previs et al. (1996) (25). The isotopic enrichment of DNA was measured according to the method described by Neese et al. (2002) (26) with minor modifications (22). We first fitted a simple label enrichment/decay curve to the urine enrichment data of each individual:
during label intake ($t \leq \tau$):

$$U(t) \ = \ f(1 - e^{-\delta t}) + \beta \, e^{-\delta t} \qquad \text{(Equation 1a)}$$

Table 1. Characteristics of HIV-infected individuals

	Treatment naive				cART-treated			Healthy
	A	*B*	*C*	*D*	*IR1*[a]	*IR2*	*IR3*	*Median*[b]
Symbol	▲	●	■	♦	▲	●	■	
Age at start protocol (yrs)	47	63	49	25	63	52	64	22
Time on cART	n/a	n/a	n/a	n/a	15	5	1	
Viral load (log10 cp/mL)[c]	4.04	5.14	4.05	5.13	<1.69	<1.69	<1.69	n/a
	(3.96-4.06)	(5.09-5.17)	(4.04-4.06)	(4.85-5.15)				
CD4$^+$ count (cells/μl blood)[c]	306	182	189	450	1814	677	574	890
	(283-354)	(165-221)	(165-243)	(425-503)	(1805-1932)	(644-720)	(487-586)	
CD8$^+$ count (cells/μl blood)	667	1612	296	532	1248	354	165	470
	(558-816)	(1574-1798)	(259-384)	(489-548)	(1155-1344)	(312-390)	(152-174)	
% naive CD4$^+$	52.8	23.7	23.9	49.0	56.7	44.3	56.5	68
	(51.0-64.5)	(20.3-26.9)	(22.4-24.4)	(45.6-56.5)	(55.6-57.8)	(41.4-47.4)	(55.8-58.1)	
% memory CD4$^+$	42.7	74.7	74.6	42.6	36.1	47.6	38.4	32
	(33.9-46.2)	(71.6-78.8)	(74.0-76.6)	(35.0-45.9)	(35.7-37.6)	(45.1-50.6)	(37.3-41.1)	
% naive CD8$^+$	17.3	8.1	14.0	25.6	26.6	27.0	24.9	59
	(15.4-17.4)	(6.9-10.2)	(13.0-14.6)	(22.8-29.2)	(24.3-28.3)	(24.0-30.5)	(22.5-26.4)	
% memory CD8$^+$	29.6	67.0	58.5	24.9	40.4	31.1	32.4	18
	(28.4-35.5)	(65.1-69.1)	(57.2-63.0)	(20.2-26.7)	(36.4-41.6)	(25.5-32.5)	(28.5-34.9)	
% Ki67$^+$ in CD4$^+$	4.7	7.2	6.4	2.8				1.9
	(3.6-6.4)	(6.3-8.4)	(4.7-8.3)	(2.0-3.6)				
% Ki67$^+$ in naive CD4$^+$	1.3	3.8	4.1	1.4				0.8
	(0.8-1.6)	(3.1-4.3)	(2.9-4.8)	(0.7-2.0)				
% Ki67$^+$ in memory CD4$^+$	7.0	7.7	6.4	4.6				3.4
	(6.2-10.2)	(6.9-9.7)	(4.7-7.9)	(3.0-6.5)				
% Ki67$^+$ in CD8$^+$	2.4	2.6	8.3	4.1				1.5
	(1.4-3.6)	(2.5-3.4)	(6.3-10.2)	(3.4-6.4)				
% Ki67$^+$ in naive CD8$^+$	1.9	2.2	4.7	4.4				0.7
	(0.9-3.2)	(2.1-3.0)	(4.0-5.6)	(2.2-6.9)				
% Ki67$^+$ in memory CD8$^+$	3.8	2.8	9.4	10.8				2.1
	(2.1-5.9)	(2.5-3.7)	(6.8-11.1)	(8.2-13.9)				

[a]IR = immunological responder
[b]Median values from healthy individuals described in Vrisekoop (1)
[c]Depicted are median values and interquartile ranges during the entire follow-up
n/a: not applicable

after label intake ($t > \tau$):

$$U(t) \; = \; \left[f(1 - e^{-\delta\tau}) + \beta \, e^{-\delta\tau} \right] e^{-\delta(t-\tau)} \qquad \text{(Equation 1b)}$$

as described previously (22) (Supplemental fig. S1 and Table S1), where $U(t)$ represents the fraction of D_2O in plasma at time t (in days), f is the fraction of D_2O in the drinking water, labelling was stopped at $t = \tau$ days, δ represents the turnover rate of body water per day, and β is the plasma enrichment attained after the boost of label by the end of day 0. We incorporated these best fits when analyzing the enrichment in the different cell populations. Up- and down-labeling of the granulocyte population of each individual was analyzed as described previously (22) (Supplemental fig. S2 and Table S2), to estimate the maximum level of label intake that cells could possibly attain. The label enrichment data of all cell subsets were subsequently scaled by the granulocyte asymptote of each individual (22).

Labeling data of the different T-cell subsets were fitted with mathematical models that did or did not allow for kinetic heterogeneity between cells of the same population. Each kinetic sub-population i was modelled to contain a fraction α_i of cells with turnover rate p_i. Assuming a steady state for each kinetic sub-population (production equals loss), label enrichment of adenosine in the DNA of each sub-population i was modelled by the following differential equation:

$$\frac{dl_i}{dt} \; = \; p_i c U(t) \alpha_i A - p_i l_i \qquad \text{(Equation 2a)}$$

where l_i is the total amount of labelled adenosine in the DNA of sub-population i and A is the total amount of adenosine in the cell population under investigation, c is an amplification factor that needs to be introduced because the adenosine deoxyribose (dR) moiety contains seven hydrogen atoms that can be replaced by deuterium (22), and p_i is the average turnover rate of sub-population i. Basically, labelled adenosines in sub-population i are gained when a deuterium atom is incorporated with probability $cU(t)$ in the DNA of cells that replicate at rate p_i, and they are lost when cells of sub-population i are lost at rate p_i. For naive T cells this replication may occur both in the periphery and in the thymus. Scaling this equation by the total amount of adenosine in the DNA of sub-population i, i.e., defining $L_i = l_i/(\alpha_i A)$, yields

$$\frac{dL_i}{dt} \; = \; p_i c U(t) - p_i L_i \qquad \text{(Equation 2b)}$$

throughout the up- and down-labelling period, where L_i represents the fraction of labelled adenosine dR moieties in the DNA of sub-population i. The corresponding analytical solutions are

$$L_i(t) \; = \; \frac{c}{\delta - p_i} \left[\delta \, f(1 - e^{-p_i t}) - p_i f(1 - e^{-\delta t}) + \beta \, p_i(e^{-p_i t} - e^{-\delta t}) \right] \qquad \text{(Equation 3a)}$$

during label intake ($t \leq \tau$), and

$$L_i(t) = \frac{c}{\delta - p_i}\left[\delta f(\mathrm{e}^{-p_i(t-\tau)} - \mathrm{e}^{-p_i t}) - p_i f(\mathrm{e}^{-\delta(t-\tau)} - \mathrm{e}^{-\delta t}) + \beta\, p_i(\mathrm{e}^{-p_i t} - \mathrm{e}^{-\delta t})\right]$$

<div align="right">(Equation 3b)</div>

after label intake ($t > \tau$).

The fraction of labelled DNA in the total T-cell population under investigation was subsequently derived from

$$L(t) = \sum \alpha_i L_i(t)$$

and the average turnover rate p was calculated from

$$p = \sum \alpha_i p_i$$

Because all enrichment data were expressed as fractions, labelling data were arcsin(sqrt) transformed before the mathematical model was fitted. As the number of kinetically different sub-populations within a cell population may not be known, one can increase the number of sub-populations in the model until the estimated average turnover rate no longer markedly changes as suggested in Westera et al. (2013) (27).

Each parameter was modeled as the sum of a population (fixed) parameter (a) and a random effect (b_i) allowing each parameter to be different from one patient to another: $\theta_i = a + b_i$. Each random effect was assumed to be normally distributed with a variance to be estimated: $b_i \sim N(0, \sigma_b^2)$. Hence, for each biological parameter, two parameters have to be estimated: one for the average value and one for the variance of the random effect. Parameters were estimated using the R package *nlme* for random effect models. Average lifespans were calculated from the average turnover rates as $1/p$. Memory T-cell compartments were always better described with a model with two kinetic different sub-populations. While naive CD4+ T cells were always described with a single exponential model, naive CD8+ T-cell compartments required a multi-exponential model (including two kinetic different sub-populations) only in untreated HIV-infected individuals.

Statistical Analyses. The likelihood ratio test was used to determine whether the data were significantly better described by a model with kinetic heterogeneity. Significance of the differences in expected life spans and total production rates of T-cell subsets between healthy volunteers and HIV-infected individuals was tested using the Mann-Whitney test. Statistical analyses were performed using R (with package nlme) and Graphpad. Differences with $p < 0.05$ were considered significant.

RESULTS

Patient characteristics. HIV-1 viral loads of the untreated HIV-1 infected individuals were relatively constant during the labeling protocol and varied from 10^4 to 10^5 copies/ml between

individuals (Table 1). In patients on cART, viral loads were undetectable throughout the study. During the entire protocol, absolute CD4$^+$ T-cell counts and fractions of naive CD4$^+$ and CD8$^+$ T cells remained almost constant in all HIV-1 patients (data not shown), which was not unexpected because the 25-week follow-up period of the protocol is rather short compared to the ~10 years of disease progression during which the CD4$^+$ T-cell pool generally gets depleted. Absolute CD4$^+$ T-cell counts were about 3.5-fold lower in untreated HIV-infected individuals compared to healthy volunteers, and numbers of naive CD4$^+$ and CD8$^+$ T cells were about 5-fold and 2-fold lower, respectively (Table 1). CD4$^+$ and CD8$^+$ T-cell counts in patients on effective cART correlated strongly with the number of years on cART. Fractions of Ki67$^+$ CD4$^+$ and CD8$^+$ T cells in treatment-naive HIV patients were also constant during the study and were 2-3 fold higher than in healthy volunteers (Table 1).

Quantification of lymphocyte turnover. T-cell turnover rates were analyzed by administration of D$_2$O during 9 weeks. T cells were isolated and sorted, and the level of deuterium enrichment in the DNA of the naive and memory T-cell populations was measured by GC-MS analysis during and after D$_2$O administration. Since naive and memory CD4$^+$ and CD8$^+$ T-cell counts hardly changed during the study protocol, the label enrichment data of naive and memory CD4$^+$ and CD8$^+$ T cells were fitted with a mathematical model assuming that the size of the cell population under investigation remained constant. Because not every cell in a T-cell population that is sorted on the basis of phenotypic markers may act similarly in terms of T-cell dynamics, the model allowed for kinetic heterogeneity within T-cell populations, i.e. each cell population was modeled as a combination of sub-populations i, with relative size α_i, and turnover rate p_i (see Material and Methods). From the best fit to the data, we subsequently calculated the average lymphocyte turnover rate ($p = \sum \alpha_i p_i$) of the T-cell population under investigation (27). To determine the maximum level of label enrichment in the DNA that could potentially be attained, we measured the label enrichment in granulocytes, a cell population that is thought to turnover completely during the labeling period (26). The granulocytes of treated and untreated HIV-infected individuals reached similar enrichment levels as those of healthy volunteers (supplemental fig. S2) (22). To correct for the actual availability of deuterium for the different cell populations at any point in time, we also determined the label enrichment in urine of the study participants at different time points (see Material and Methods and supplemental fig. S1) (22).

CD4$^+$ and CD8$^+$ T-cell turnover in healthy volunteers. We have previously measured T-lymphocyte turnover rates in 5 healthy volunteers by heavy water labeling (22). After 9 weeks of labeling, enrichment levels reached about 1-5% for naive and 10-20% for memory CD4$^+$ and CD8$^+$ T cells. During the down-labeling phase of 16 weeks we observed no significant loss of label from the naive T-cell populations. To test our previous conclusion that naive T cells in healthy volunteers are extremely long-lived (22), 4 of the 5 healthy volunteers were resampled approximately 3 years after label cessation. When these new samples were analyzed along with a few historic samples, we found that indeed, even 3 years after label cessation, labeled DNA could still be detected in the naive T-cell pools of these individuals. Fitting the complete dataset of the healthy individuals using a mixed effect model yielded no statistical evidence
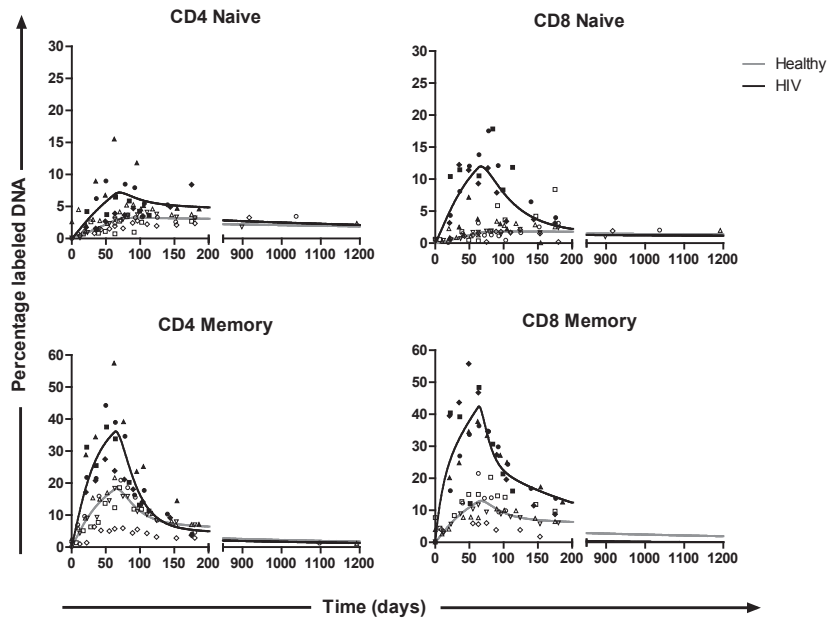
Figure 1. ²H enrichment of naive and memory T cells in healthy and HIV-infected individuals. Best fits of the percentage of labeled DNA in naive and memory CD4+ and CD8+ T cells of 5 healthy volunteers (open symbols, grey curves) and 4 untreated chronic HIV-1 infected individuals (closed symbols, black curves). The curves show the best fit of the two-compartment mixed effect model to the full experimental dataset, including the long-term follow-up points whenever available. Label enrichment in the DNA of the different cell populations was scaled between 0 and 100% by normalizing for the estimated maximum percentage labeled DNA obtained in granulocytes (see Material and Methods).

for kinetic heterogeneity in the naive T-cell pool (p=0.09, see Material and Methods), *i.e.* the labeling kinetics of the naive T-cell pool could perfectly be described by a model in which all naive T cells had the same rate of turnover (fig. 1). The fits confirmed the very low rate of turnover of naive T cells that we previously reported (see Table 2), while they also described the late data points (fig. 1), strengthening our conclusion that naive T cells in healthy adults undergo very little turnover, and do not contain a substantial pool of short-lived recent thymic emigrants (RTE) (22). The labeling kinetics of the CD4+ and CD8+ memory T-cell populations, in contrast, were significantly better described when the model allowed for heterogeneity in turnover rates of memory T cells (p=0.03) (27). Summarizing, naive T cells in healthy adults are long-lived (with expected life spans of 5.6 and 8.8 years for CD4+ and CD8+ T cells, respectively, see Table 2) and form a kinetically homogeneous population, while memory T cells have a shorter expected life span (0.45 and 0.33 years for CD4+ and CD8+ T cells, respectively, see Table 2) and are kinetically heterogeneous.

CD4+ and CD8+ T-cell turnover in treatment-naive HIV-infected individuals. After 9 weeks of D$_2$O administration, T cells from treatment-naive HIV-infected patients reached significantly

Table 2. Average per capita turnover rates (p day^{-1}) of the T-cell subsets of healthy individuals

	A	*B*	*C*	*D*	*E*	median[a]
Naive CD4$^+$	0.0011 (0.0008-0.0015)[b]	0.0005 (0.0003-0.0008)	0.0003 (0.0002-0.0005)	0.0004 (0.0002-0.0006)	0.0006 (0.0003-0.0008)	**0.0005**
Naive CD8$^+$	0.0006 (0.0004-0.0009)	0.0002 (0.0001-0.0004)	0.0001 (0.0000-0.0004)	0.0003 (0.0002-0.0005)	0.0004 (0.0003-0.0006)	**0.0003**
Memory CD4$^+$	0.0141 (0.0105-0.0289)	0.0079 (0.0062-0.0153)	0.0035 (0.0025-0.0103)	0.0020 (0.0014-0.0081)	0.0061 (0.0048-0.0098)	**0.0061**
Memory CD8$^+$	0.0108 (0.0035-0.0213)	0.0084 (0.0055-0.0181)	0.0110 (0.0057-0.0280)	0.0064 (0.0026-0.0280)	0.0048 (0.0028-0.0133)	**0.0084**

[a]Median values of the 5 healthy individuals
[b]95%-confidence intervals (given in parentheses) were determined by a bootstrap method

higher labeling levels (of about 5-20% for naive CD4$^+$ and CD8$^+$ T cells, and 30-50% for memory CD4$^+$ and CD8$^+$ T cells, respectively) compared to healthy individuals. In order to follow the fate of the newly produced T cells in HIV infection, we also measured the percentage of labeled DNA within each T-cell population during the subsequent 16 weeks after label cessation (fig. 1). The average turnover rates of naive CD4$^+$ and CD8$^+$ T cells in treatment-naive HIV patients were ~0.16% and 0.37% of the naive CD4$^+$ and CD8$^+$ T-cell pool per day, corresponding to expected average life spans of 618 and 271 days, respectively, which is 3 and 12 times shorter than in healthy volunteers (Table 3 and fig. 2A). The average turnover rates of memory CD4$^+$ and CD8$^+$ T cells were 1.9% and 2.3% of the memory CD4$^+$ or CD8$^+$ T-cell pool per day, corresponding to expected life spans of 53 and 43 days, respectively, i.e. 3 times shorter than in uninfected individuals (Table 3 and fig. 2B). Although average *per capita* T-cell turnover rates of all T-cell subsets were increased in HIV infection, *total* naive CD4$^+$ T-cell production rates, expressed in cells per day, were not (fig. 2C), which is a direct consequence of the strongly reduced naive CD4$^+$ T-cell counts in the blood of the untreated HIV-infected individuals included in this study (p=0.016, Table 1). Total memory CD4$^+$ T-cell production was similar in HIV-infected and healthy individuals (fig. 3D). Total naive and memory CD8$^+$ T-cell production were significantly increased during HIV infection (p=0.049 and p=0.032, fig. 3C,D), even though naive CD8$^+$ T-cell counts were significantly decreased in untreated HIV-infected individuals (p=0.016, Table 1).

The labeling data of the HIV-infected individuals turned out to be significantly better described by a model that allowed for kinetic heterogeneity, not only for memory CD4$^+$ and CD8$^+$ but also for naive CD8$^+$ T cells (p-values<0.01). The fit to the naive CD4$^+$ T-cell labeling data did not improve significantly when a second sub-population was added to the model (see the 95% CI of α, which crosses 0 in fig. 3). The fit to the CD8$^+$ T-cell labeling data of HIV-1 infected

Table 3. Average per capita turnover rates (p day⁻¹) of the T-cell subsets of HIV-1 infected individuals

|	*A*	*B*	*C*	*D*	median[a]
Naive CD4⁺	0.0023 (0.0015-0.0033)[b]	0.0024 (0.0016-0.0034)	0.0010 (0.0005-0.0016)	0.0006 (0.0005-0.0008)	**0.0016**
Naive CD8⁺	0.0017 (0.0009-0.0031)	0.0038 (0.0031-0.0048)	0.0036 (0.0024-0.0054)	0.0039 (0.0027-0.0061)	**0.0037**
Memory CD4⁺	0.0190 (0.0139-0.0290)	0.0186 (0.0150-0.0245)	0.0291 (0.0148-0.1208)	0.0096 (0.0076-0.0142)	**0.0188**
Memory CD8⁺	0.0124 (0.0081-0.0319)	0.0140 (0.0103-0.0426)	0.0328 (0.0194-0.1055)	0.0344 (0.0256-0.0508)	**0.0234**

[a]Median values of the 4 HIV infected individuals
[b]95%-confidence intervals (given in parentheses) were determined by a bootstrap method
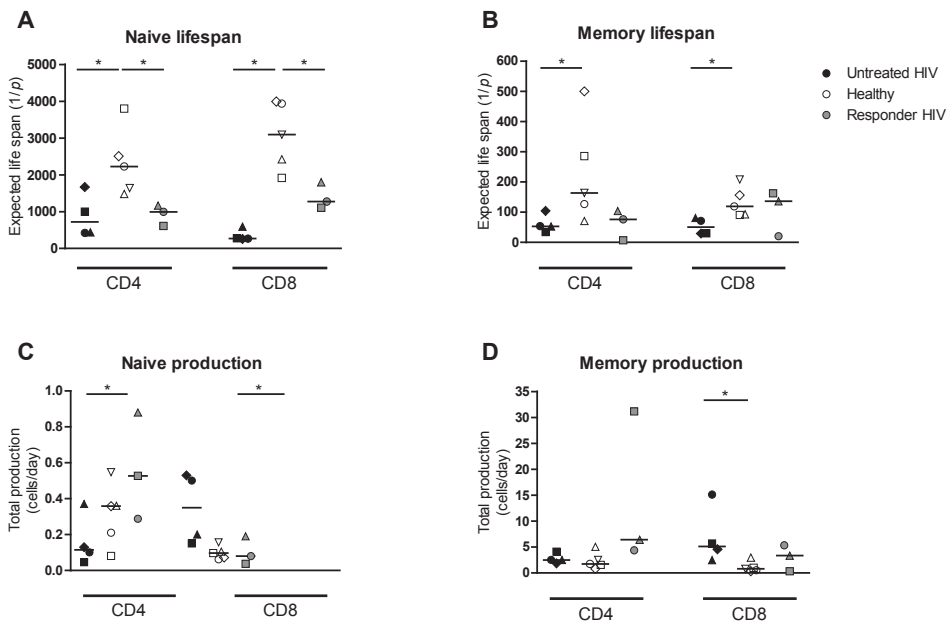
Figure 2. Estimated T-cell life spans and total daily production in healthy and HIV-infected individuals. Estimated life spans of A) naive and B) memory CD4⁺ and CD8⁺ T cells in untreated HIV-infected (closed symbols), healthy (open symbols) and cART-treated HIV-infected individuals, calculated from the average T-cell turnover rate (p) resulting from fitting a two-compartment model to the data. Total daily production (expressed in cells per day) of C) naive and D) memory CD4⁺ and CD8⁺ T cells in HIV-infected (closed symbols) and healthy (open symbols) individuals, calculated by multiplying the estimated average T-cell turnover rate (p), based on the two-compartment model) with the number of T cells in the population under investigation.

individuals, however, did improve significantly when a second sub-population was added. The fast sub-population contained about 10-20% of the naive CD8⁺T cells, with an average lifespan of 36 days. The memory CD4⁺ and CD8⁺ T-cell pools of both healthy and HIV-1 infected individuals
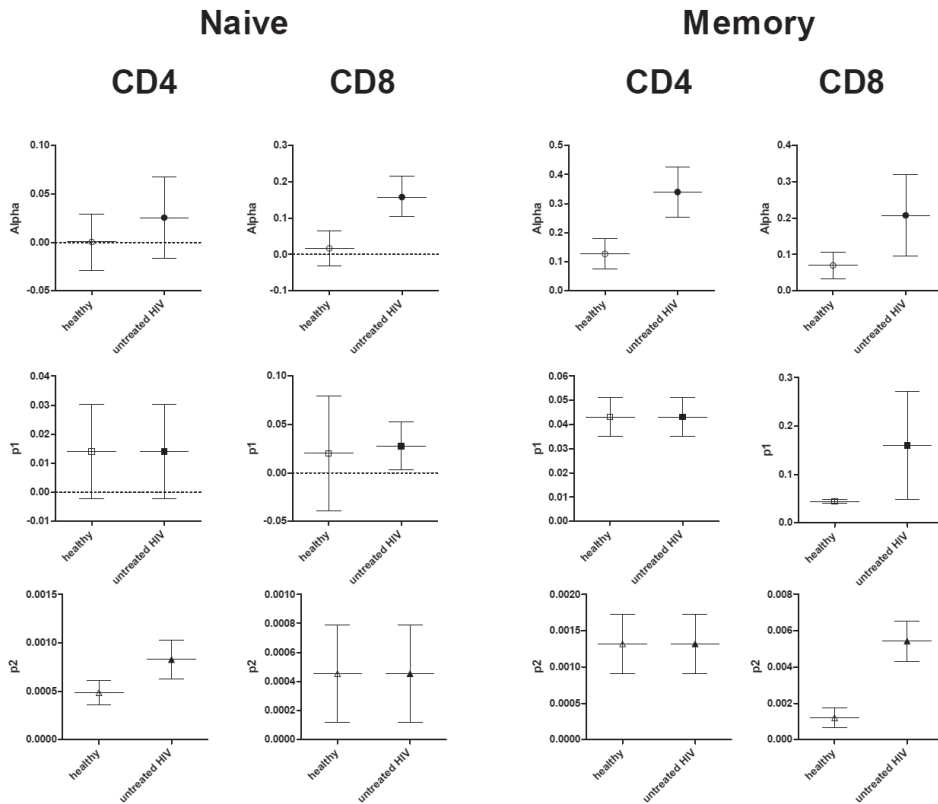
Naive

CD4   CD8

Memory

CD4   CD8

Figure 3. 95% confidence intervals on the individual parameters of the model. Parameter results of the best fit of the model with two kinetically different sub-populations to the data, where α is the size of the fast sub-population, p_1 its turnover rate and p_2 the turnover rate of the slower sub-population. Whenever the 95%CI on α crosses 0, adding a second sub-population to the model did not significantly improve the fit to the data.

(fig. 3) showed clear signs of kinetic heterogeneity (95%CI of α never crosses 0). In the memory CD4^{+} T-cell pool, the size α of the fast sub-population was significantly larger in HIV-1 infection, while in the memory CD8^{+} T-cell pool both the size α of the fast sub-population and the turnover rates p_1 and p_2 of the two sub-populations were higher than in healthy volunteers.

CD4^{+} and CD8^{+} T-cell turnover in immunological responders. We also studied whether cART could restore the increased rates of T-cell turnover in HIV-infected individuals (Table 4). To this end, we included HIV-1 infected individuals on cART with successfully suppressed viral loads who also responded well in terms of T-cell reconstitution. Deuterium labeling curves of the different T-cell populations in these individuals turned out to be close to those of healthy controls (fig. 4). The average turnover rates of memory CD4^{+} and CD8^{+} T cells in cART-treated HIV-infected individuals were similar to those of healthy individuals (fig. 2B). Only naive T-cell lifespans were still significantly shorter than in healthy volunteers (p=0.036, fig. 2A), although

Table 4. Average per capita turnover rates (p day^{-1}) of the T-cell subsets of cART-treated HIV-1 infected individuals

	IR1[a]	*IR2*	*IR3*	median[b]
Naive CD4$^+$	0.0006 (0.0001- 0.0007)[c]	0.0013 (0.0009- 0.0029)	0.0079 (0.0012- 0.0835)	**0.0013**
Naive CD8$^+$	0.00024 (0.0000- 0.0003)	0.0023 (0.0006- 0.0014)	0.0022 (0.0009- 0.0015)	**0.0023**
Memory CD4$^+$	0.0096 (0.0057- 0.0145)	0.0131 (0.0073- 0.1159)	0.1466 (0.0064- 0.2136)	**0.0131**
Memory CD8$^+$	0.0015 (0.0026- 0.1275)	0.0013 (0.0020- 0.1148)	0.0018 (0.0042- 0.1536)	**0.0015**

[a]IR = immunological responder
[b]Median values of 4 HIV infected individuals
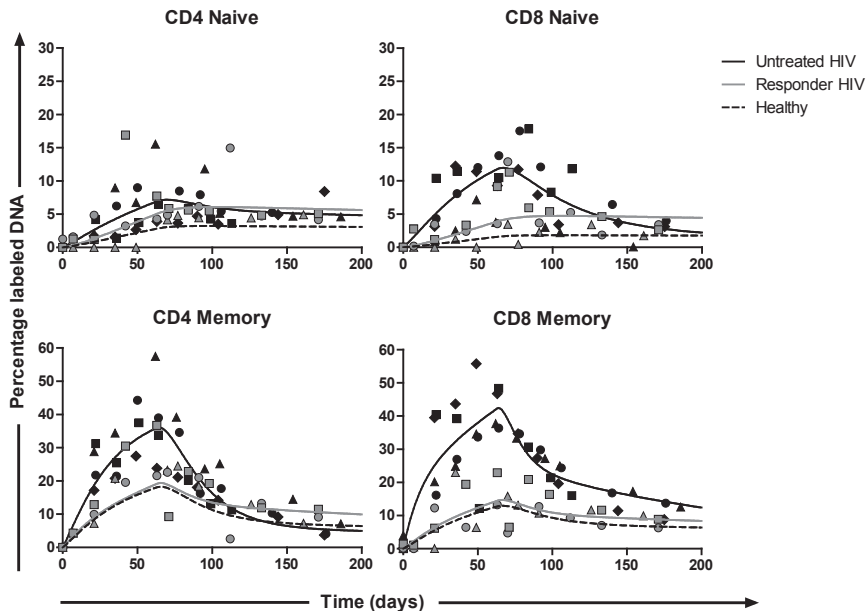[c]95%-confidence intervals (given in parentheses) were determined by a bootstrap method

Figure 4. ²H enrichment of naive and memory T cells of treated and untreated HIV-infected individuals. Best fits of the percentage of labeled DNA in naive and memory CD4$^+$ and CD8$^+$ T cells of 4 untreated HIV-infected individuals (black symbols and curves) and 3 cART-treated individuals with a good virological and immunological response to treatment (grey symbols and curves). For reference, the best fit through the data from healthy volunteers (fig. 1) is plotted as a dashed curve. The curves show the best fit of the mixed effect two-compartment model to the experimental data. Label enrichment in the DNA of the different cell populations was scaled between 0 and 100% by normalizing for the estimated maximum percentage labeled DNA obtained in granulocytes (see Material and Methods).

they were longer than in untreated HIV-infected individuals. Total naive and memory T-cell production was not significantly different between healthy and cART-treated individuals (fig. 2C,D).

DISCUSSION

Long-term administration of D_2O and follow-up of labeled T cells after label cessation enabled us to reliably quantify expected life spans and total daily T-cell production rates of naive and memory CD4$^+$ and CD8$^+$ T cells in healthy and HIV-infected individuals. Our data show that the average T-cell life span of naive CD4$^+$ and memory CD4$^+$ and CD8$^+$ T cells are 3-fold shortened during untreated, chronic HIV infection, and that naive CD8$^+$ T cells live up to 12-fold shorter during chronic HIV infection. Successful cART tends to normalize memory T-cell turnover rates, while naive T-cell turnover rates remain increased, albeit less than in untreated chronic HIV infection. Our analyses also point at qualitative changes in the kinetics of the naive T-cell pool of HIV-infected individuals. Whereas in healthy individuals, naive T cells form a kinetically homogeneous pool of cells that are extremely long-lived, upon HIV infection a significant subset of naive T cells acquires a high rate of turnover. During the entire follow-up period, naive T-cell numbers nevertheless stayed relatively constant in all HIV-infected individuals, because naive T cells with short expected life spans were produced at high rates.

The increased naive T-cell turnover rates in untreated HIV-1 infection that we found are in contrast to recent observations by Zhang et al. (2013) (23), who reported memory T-cell turnover rates to be significantly increased while naive T-cell turnover rates were hardly affected by HIV-1 infection. The reason for this discrepancy remains unclear, but factors that are likely to be involved include i) the different phenotypic markers used to define naive T cells, and ii) the higher sensitivity of a 9-weeks labeling protocol compared to a 1-day labeling protocol to pick up differences in turnover rates of populations with very slow turnover rates, such as naive T cells.

Elevated T-cell production rates in HIV-infected patients have been proposed to reflect either a homeostatic response to compensate for the progressive loss of CD4$^+$ T cells (28;29) or to be driven by immune activation (24). It has previously been shown that HIV-infected patients suffering from AIDS have increased levels of IL-7 production in lymphoid tissue (30), and that naive T cells can divide in response to IL-7 while retaining the naive phenotype (31;32), suggesting that homeostatic T-cell proliferation may occur in HIV infection. In line with this, a recent study based on *in vivo* BrdU labeling found that naive CD4$^+$ T-cell turnover rates in HIV patients correlated significantly with CD4$^+$ T-cell counts, but not with HIV viral load (33). However, the observation that HAART strongly decreases the percentage of Ki67-expressing CD4$^+$ T cells long before CD4$^+$ T-cell numbers have recovered to normal values suggests that increased T-cell production rates in HIV infection are driven by the effects of the virus, rather than by a homeostatic response to low CD4$^+$ T-cell numbers (34). We therefore tend to interpret the at least 3-fold higher T-lymphocyte turnover rates in HIV-infected individuals that we reported here as a direct immune stimulatory effect of the virus.

Our data suggest that 10-20% of the CD8$^+$ naive T-cell pool acquires a significantly increased turnover rate during HIV infection, and that the average lifespan of the latter cells

is about 36 days. This relatively high percentage of naive cells with rapid turnover suggests that the increased turnover is not merely due to an antigen-specific response to HIV. Both the acute, drastic loss of memory CD4⁺ T cells from the gastro-intestinal tract which causes translocation of microbial products from the gut into the blood of HIV-infected individuals (35), and the direct activation of Toll like receptors by HIV (36;37) may be drivers of the observed activation of the naive T-cell pool during HIV infection. It is important to realize, however, that the interpretation of the sizes a_i and turnover rates p_i of the sub-populations delivered by the model may not be straightforward. The uncertainty on the latter parameters tends to be larger than on the average turnover rate p, because of the strong correlation between the size of a subpopulation and its turnover rate (27). In fact, the subpopulations used in the model need not reflect phenotypically different subsets, and an alternative interpretation for the kinetic heterogeneity of T-cell pools that is found in HIV infection is that cells transiently have different turnover rates, e.g. resting cells and cells that have recently been produced or activated may have different life expectancies (27).The role of the thymus in the altered dynamics of naive T cells during HIV-1 infection is still debated (11;24;28;38). Using mathematical modeling it has been shown that the observed relatively rapid dilution of the average T-cell receptor excision circle (TREC) content of naive T cells in HIV-infected individuals (38) cannot be explained by changes in thymic output alone (24) if naive T cells are long-lived. Our long-term follow-up of D_2O-labeled individuals demonstrates that under healthy circumstances naive CD4⁺ and CD8⁺ T cells are indeed very long lived, with expected life spans as long as 5.6 and 8.8 years, respectively. An alternative explanation for the rapid dilution of TRECs in HIV infection that has been proposed is that the naive T-cell pool may comprise a sub-population of short-lived RTE, as has been suggested in mice (39;40). Through the effects on this RTE population, the average TREC content of naive T cells may be rapidly affected when thymic output is blocked (28). Our D_2O labeling data from healthy volunteers show, however, that human naive T cells form a kinetically homogeneous population of long-lived cells, arguing against the presence of a substantial RTE population with rapid kinetics in healthy adults (see Vrisekoop (22)).

TREC dilution in HIV infection is therefore presumably caused by the state of chronic immune activation induced by the virus (24). Our data show that naive and memory *per capita* turnover rates in HIV infection are significantly increased. This result is perfectly consistent with the increased levels of Ki67 expression that have been observed in T cells during HIV infection. The current results are more direct, however, because Ki67 expression may be high due to cell cycle arrest in HIV infection (17). We also show that the increased turnover in the naive T-cell population during HIV infection is probably caused by a sub-population of naive T cells with relatively high production and loss rates. Apparently these cells retain the CD45RA⁺CD27⁺ phenotype of naive T cells, and thereby explain the observed dilution of the naive T-cell TREC content during HIV infection.

Summarizing, mathematical modeling of long-term *in vivo* labeling in humans shows that the average life span of both naive and memory CD4⁺ and CD8⁺ T cells decreases during untreated chronic HIV-1 infection. While the turnover of the memory T-cell populations nearly normalizes during effective treatment, the turnover of naive CD4⁺ and CD8⁺ T cells remains increased.

ACKNOWLEDGEMENTS

REFERENCE LIST

1. Choudhary SK, Vrisekoop N, Jansen CA, et al. Low immune activation despite high levels of pathogenic human immunodeficiency virus type 1 results in long-term asymptomatic disease. J Virol **2007 Aug**;81(16):8838-42.

2. Deeks SG, Kitchen CM, Liu L, et al. Immune activation set point during early HIV infection predicts subsequent CD4+ T-cell changes independent of viral load. Blood **2004 Aug 15**;104(4):942-7.

3. Giorgi JV, Hultin LE, McKeating JA, et al. Shorter survival in advanced human immunodeficiency virus type 1 infection is more closely associated with T lymphocyte activation than with plasma virus burden or virus chemokine coreceptor usage. J Infect Dis **1999 Apr**;179(4):859-70.

4. Hazenberg MD, Otto SA, van Benthem BH, et al. Persistent immune activation in HIV-1 infection is associated with progression to AIDS. AIDS **2003 Sep 5**;17(13):1881-8.

5. Silvestri G, Sodora DL, Koup RA, et al. Nonpathogenic SIV infection of sooty mangabeys is characterized by limited bystander immunopathology despite chronic high-level viremia. Immunity **2003 Mar**;18(3):441-52.

6. Ferguson NM, deWolf F, Ghani AC, et al. Antigen-driven CD4+ T cell and HIV-1 dynamics: residual viral replication under highly active antiretroviral therapy. Proc Natl Acad Sci U S A **1999 Dec 21**;96(26):15167-72.

7. Hellerstein M, Hanley MB, Cesar D, et al. Directly measured kinetics of circulating T lymphocytes in normal and HIV-1-infected humans. Nat Med **1999 Jan**;5(1):83-9.

8. Kovacs JA, Lempicki RA, Sidorov IA, et al. Identification of dynamically distinct subpopulations of T lymphocytes that are differentially affected by HIV. J Exp Med **2001 Dec 17**;194(12):1731-41.

9. Kovacs JA, Lempicki RA, Sidorov IA, et al. Induction of prolonged survival of CD4+ T lymphocytes by intermittent IL-2 therapy in HIV-infected patients. J Clin Invest **2005 Aug**;115(8):2139-48.

10. Lempicki RA, Kovacs JA, Baseler MW, et al. Impact of HIV-1 infection and highly active antiretroviral therapy on the kinetics of CD4+ and CD8+ T cell turnover in HIV-infected patients. Proc Natl Acad Sci U S A **2000 Dec 5**;97(25):13778-83.

11. McCune JM, Hanley MB, Cesar D, et al. Factors influencing T-cell turnover in HIV-1-seropositive patients. J Clin Invest **2000 Mar**;105(5):R1-R8.

12. Mohri H, Perelson AS, Tung K, et al. Increased turnover of T lymphocytes in HIV-1 infection and its reduction by antiretroviral therapy. J Exp Med **2001 Nov 5**;194(9):1277-87.

13. Perelson AS, Essunger P, Ho DD. Dynamics of HIV-1 and CD4+ lymphocytes in vivo. AIDS **1997**;11 Suppl A:S17-S24.

14. Sachsenberg N, Perelson AS, Yerly S, et al. Turnover of CD4+ and CD8+ T lymphocytes in HIV-1 infection as measured by Ki-67 antigen. J Exp Med **1998 Apr 20**;187(8):1295-303.

15. Roederer M, Dubs JG, Anderson MT, Raju PA, Herzenberg LA, Herzenberg LA. CD8 naive T cell counts decrease progressively in HIV-infected adults. J Clin Invest **1995 May**;95(5):2061-6.

16. Hellerstein MK, Hoh RA, Hanley MB, et al. Subpopulations of long-lived and short-lived T cells in advanced HIV-1 infection. J Clin Invest **2003 Sep**;112(6):956-66.

17. Combadere B, Blanc C, Li T, et al. CD4+Ki67+ lymphocytes in HIV-infected patients are effector T cells accumulated in the G1 phase of the cell cycle. Eur J Immunol **2000 Dec**;30(12):3598-603.

18. Ladell K, Hellerstein MK, Cesar D, Busch R, Boban D, McCune JM. Central memory CD8+ T cells appear to have a shorter lifespan and reduced abundance as a function of HIV disease progression. J Immunol **2008 Jun 15**;180(12):7907-18.

19. Macallan DC, Asquith B, Irvine AJ, et al. Measurement and modeling of human T cell kinetics. Eur J Immunol **2003 Aug**;33(8):2316-26.

20. Macallan DC, Wallace D, Zhang Y, et al. Rapid turnover of effector-memory CD4(+) T cells in healthy humans. J Exp Med **2004 Jul 19**;200(2):255-60.

21. Ribeiro RM, Mohri H, Ho DD, Perelson AS. In vivo dynamics of T cell activation, proliferation, and death in HIV-1 infection: why are CD4+ but not CD8+ T cells depleted? Proc Natl Acad Sci U S A **2002 Nov 26**;99(24):15572-7.

22. Vrisekoop N, den B, I, de Boer AB, et al. Sparse production but preferential incorporation of recently produced naive T cells in the human peripheral pool. Proc Natl Acad Sci U S A **2008 Apr 22**;105(16):6115-20.

23. Zhang Y, De LC, Worth A, et al. Accelerated In Vivo Proliferation of Memory Phenotype CD4(+) T-cells in Human HIV-1 Infection Irrespective of Viral Chemokine Co-receptor Tropism. PLoS Pathog **2013 Apr**;9(4):e1003310.

24. Hazenberg MD, Stuart JW, Otto SA, et al. T-cell division in human immunodeficiency virus (HIV)-1 infection is mainly due to immune activation: a longitudinal analysis in patients before and during highly active antiretroviral therapy (HAART). Blood **2000 Jan 1**;95(1):249-55.

25. Previs SF, Des RC, Beylot M, David F, Brunengraber H. Assay of the 13C and 2H mass isotopomer distribution of phosphoenolpyruvate by gas chromatography/mass spectrometry. J Mass Spectrom **1996 Jun**;31(6):643-8.

26. Neese RA, Misell LM, Turner S, et al. Measurement in vivo of proliferation rates of slow turnover cells by 2H2O labeling of the deoxyribose moiety of DNA. Proc Natl Acad Sci U S A **2002 Nov 26**;99(24):15345-50.

27. Westera L, Drylewicz J, den B, I, et al. Closing the gap between T-cell life span estimates from stable isotope-labeling studies in mice and men. Blood **2013 Aug 14**.

28. Dion ML, Poulin JF, Bordi R, et al. HIV infection rapidly induces and maintains a substantial suppression of thymocyte proliferation. Immunity **2004 Dec**;21(6):757-68.

29. Ho DD, Neumann AU, Perelson AS, Chen W, Leonard JM, Markowitz M. Rapid turnover of plasma virions and CD4 lymphocytes in HIV-1 infection. Nature **1995 Jan 12**;373(6510):123-6.

30. Napolitano LA, Grant RM, Deeks SG, et al. Increased production of IL-7 accompanies HIV-1-mediated T-cell depletion: implications for T-cell homeostasis. Nat Med **2001 Jan**;7(1):73-9.

31. Soares MV, Borthwick NJ, Maini MK, Janossy G, Salmon M, Akbar AN. IL-7-dependent extrathymic expansion of CD45RA+ T cells enables preservation of a naive repertoire. J Immunol **1998 Dec 1**;161(11):5909-17.

32. Steffens CM, Managlia EZ, Landay A, Al-Harthi L. Interleukin-7-treated naive T cells can be productively infected by T-cell-adapted and primary isolates of human immunodeficiency virus 1. Blood **2002 May 1**;99(9):3310-8.

33. Srinivasula S, Lempicki RA, Adelsberger JW, et al. Differential effects of HIV viral load and CD4 count on proliferation of naive and memory CD4 and CD8 T lymphocytes. Blood **2011 Jul 14**;118(2):262-70.

34. Hazenberg MD, Hamann D, Schuitemaker H, Miedema F. T cell depletion in HIV-1 infection: how CD4+ T cells go out of stock. Nat Immunol **2000 Oct**;1(4):285-9.

35. Brenchley JM, Price DA, Schacker TW, et al. Microbial translocation is a cause of systemic immune activation in chronic HIV infection. Nat Med **2006 Dec**;12(12):1365-71.

36. Boasso A, Shearer GM. Chronic innate immune activation as a cause of HIV-1 immunopathogenesis. Clin Immunol **2008 Mar**;126(3):235-42.

37. Herbeuval JP, Boasso A, Grivel JC, et al. TNF-related apoptosis-inducing ligand (TRAIL) in HIV-1-infected patients and its in vitro production by antigen-presenting cells. Blood **2005 Mar 15**;105(6):2458-64.

38. Douek DC, McFarland RD, Keiser PH, et al. Changes in thymic function with age and during the treatment of HIV infection. Nature **1998 Dec 17**;396(6712):690-5.

39. Berzins SP, Boyd RL, Miller JF. The role of the thymus and recent thymic migrants in the maintenance of the adult peripheral lymphocyte pool. J Exp Med **1998 Jun 1**;187(11):1839-48.

40. Berzins SP, Godfrey DI, Miller JF, Boyd RL. A central role for thymic emigrants in peripheral T cell homeostasis. Proc Natl Acad Sci U S A **1999 Aug 17**;96(17):9787-91.

SUPPLEMENTAL INFORMATION
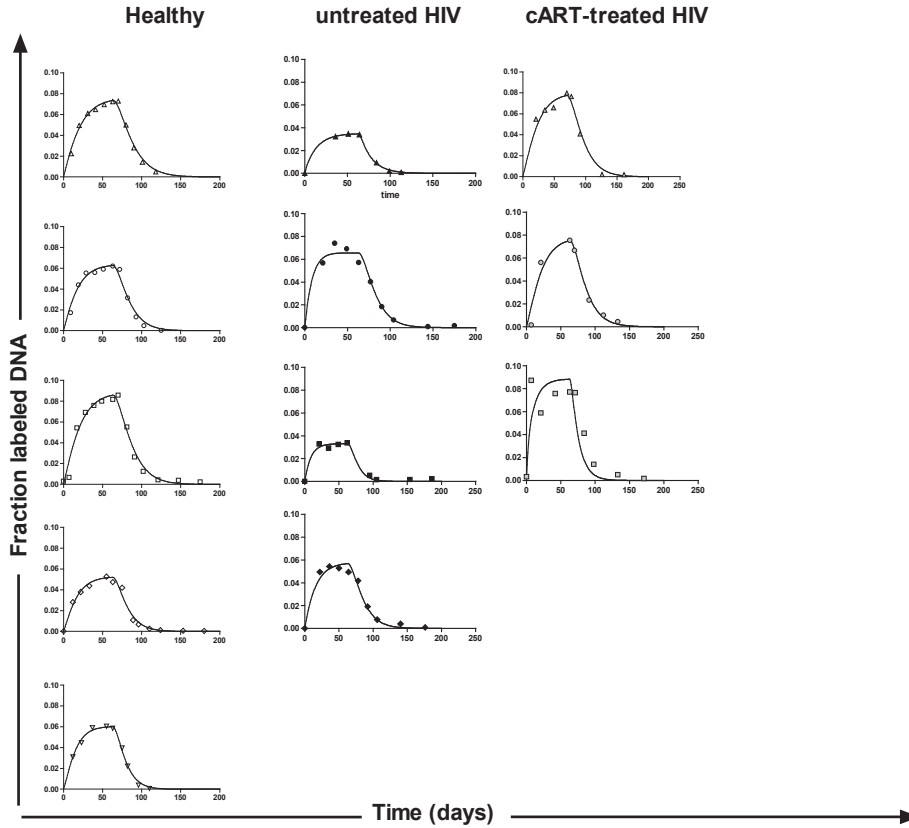
Supplemental Figure S1. ²H enrichment of granulocyte of healthy and HIV-infected individuals. The curves represent the best fits of the mathematical model to the experimental data (see Material and Methods).

Supplemental Figure S2. ²H enrichment in granulocytes of healthy individuals, and untreated and cART-treated HIV-infected individuals. The curves represent the best fits of the mathematical model to the experimental data (see Material and Methods).

2
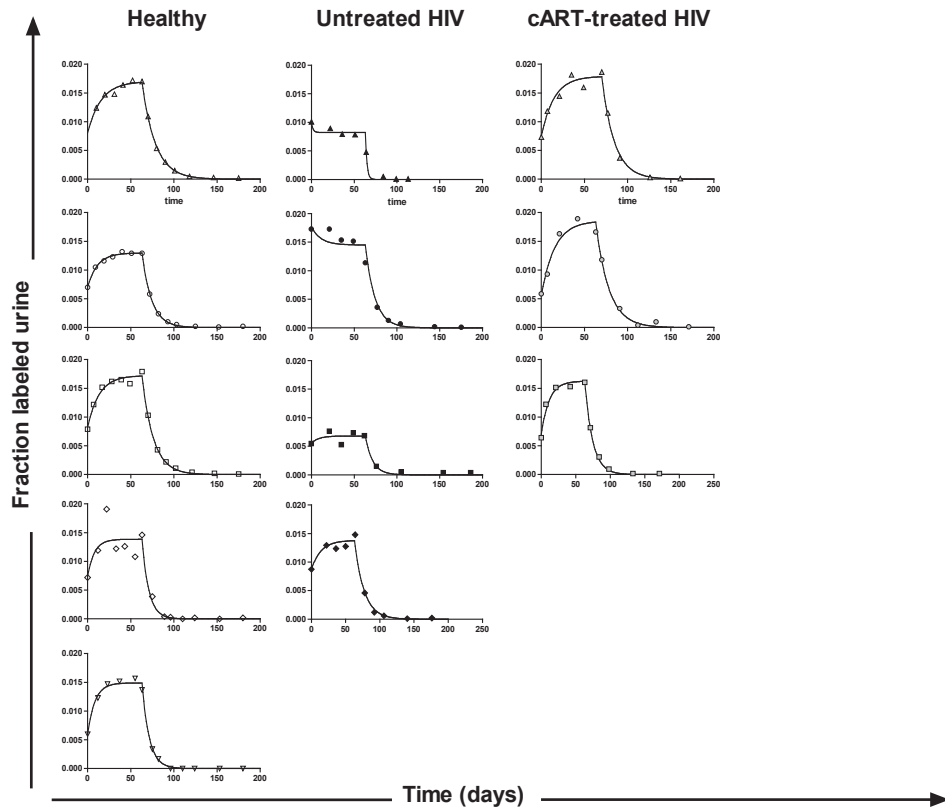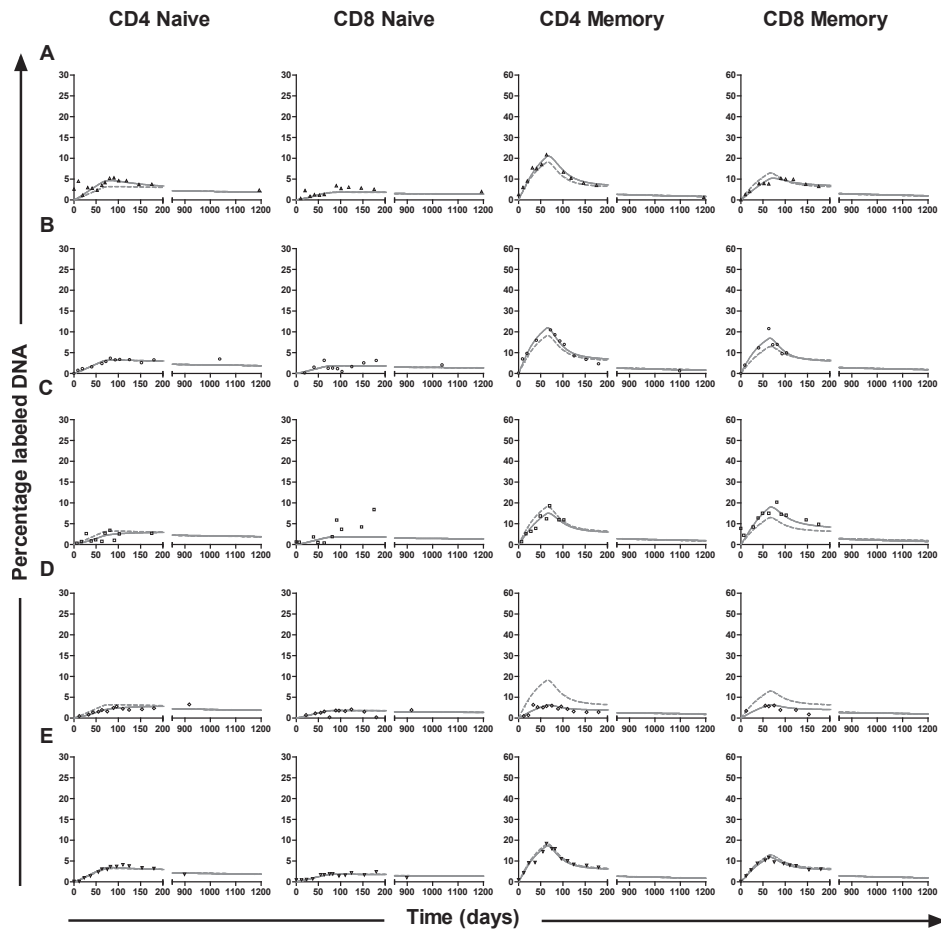
Supplemental Figure S3. ²H enrichment of naive and memory T cells of healthy individuals. Best fits of the percentage of labeled DNA in naive and memory CD4⁺ and CD8⁺ T cells of 5 healthy volunteers. The grey curves show the best fit of the multi-exponential model to the full experimental dataset, including the long-term follow-up points whenever available. For reference, the average labeling curves (derived from the complete group of healthy individuals) are plotted for each cell subset by the dashed grey curves. Label enrichment in the DNA of the different cell populations was scaled between 0 and 100% by normalizing for the estimated maximum percentage labeled DNA obtained in granulocytes (see Material and Methods).
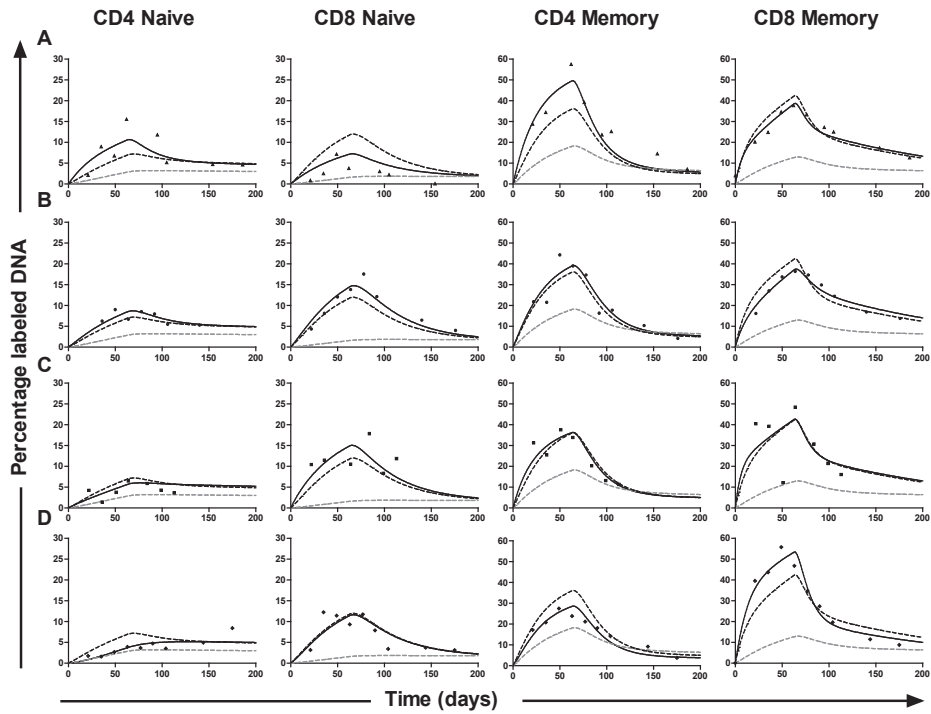
Supplemental Figure S4. ²H enrichment of naive and memory T cells of treatment-naive HIV-infected individuals. The percentage of labeled DNA in naive and memory CD4^{+} and CD8^{+} T cells of 4 treatment-naive HIV-infected individuals. The black curves show the best fit of the multi-exponential model to the experimental data. For reference, the average labeling curves of healthy (dashed grey curves) and HIV-infected (dashed black curves) individuals are plotted for each cell subset. Label enrichment in the DNA of the different cell populations was scaled between 0 and 100% by normalizing for the estimated maximum percentage labeled DNA obtained in granulocytes (see Material and Methods).

Supplemental Table S1. Parameter estimates of the urine enrichment curves of healthy volunteers, and untreated and cART-treated HIV-infected individuals.

	Healthy					Treatment-naive				cART-treated		
	A	B	C	D	E	A	B	C	D	IR1	IR2	IR3
f	0.0010	0.0011	0.0012	0.0017	0.0020	0.0007	0.0010	0.0009	0.0012	0.0178	0.0184	0.0165
δ	0.0610	0.0822	0.0705	0.1204	0.1338	0.1080	0.0735	0.1221	0.0811	0.0708	0.0647	0.0837
β	0.0086	0.0071	0.0082	0.0073	0.0059	0.0053	0.0087	0.0102	0.0178	0.0066	0.0062	0.0072

where f represents the fraction of ^2H_2O in the drinking water, δ is the turnover rate of body water per day, and β represents the baseline urine enrichment attained after the boost of label by the end of day 0.

Supplemental Table S2. Parameter estimates of the granulocyte enrichment curves of healthy volunteers, and untreated and cART-treated HIV-infected individuals.

	Healthy					Treatment-naive				cART-treated		
	A	B	C	D	E	A	B	C	D	IR1	IR2	IR3
pc	0.4105	0.4813	0.3729	0.3195	0.4237	0.5265	0.3391	0.5390	0.4174	0.3703	0.4116	1.5552
d	0.0938	0.1016	0.0751	0.0853	0.1052	0.0994	0.0790	0.1196	0.0937	0.0840	0.0922	0.2967

where d represents the loss rate of labeled granulocytes per day, p is the average production rate of granulocytes per day, and c the amplification factor.

CHAPTER

3

cART INTENSIFICATION WITH MARAVIROC DECREASES T-CELL TURNOVER IN HIV-1 IMMUNOLOGICAL NON RESPONDERS

Ellen Veel[1]*, Julia Drylewicz[1,3]*, Steven F.L. van Lelyveld[2]*,
Liset Westera[1], Sigrid Otto[1], Anita van Oort[1], J. Gaiser[1],
G. Spierenburg[1], Inge de Kroon[2], Andy I.M. Hoepelman[2],
José A.M. Borghans[1], Kiki Tesselaar[1]

[1]Laboratory for Translational Immunology, University Medical Center Utrecht
[2]Department of Internal Medicine and Infectious Diseases, University
Medical Center Utrecht
[3]Theoretical Biology and Bioinformatics, Department of Biology, Utrecht University

*These authors contributed equally

ABSTRACT

The CCR5 antagonist Maraviroc (MVC) has been implicated in optimizing CD4^{+} T-cell recovery in HIV-1 infected individuals with viral suppression but slow immune recovery during cART. In a double blinded placebo controlled MVC intensification study in this type of patients we performed *in vivo* labelling with deuterated water in a subset of the participants to determine the effect of MVC on T-cell turnover. We found that average naive and memory CD4^{+} and CD8^{+} T-cell turnover rates were lower in MVC treated individuals, compared with the placebo group. Furthermore, delta CCR5 expression during the duration of the study correlated significantly with the life span of memory T cells.

3

INTRODUCTION

Combination antiretroviral therapy (cART) is aimed at suppression of HIV replication and delay of disease progression. Successful cART, with viral load reduction to < 50 copies/ml not only stops CD4+ T-cell depletion, but generally allows for CD4+ T-cell recovery to near normal levels (1). Unfortunately not all patients with a successful virologic response show normalization of their CD4+ T-cell compartment. Pre-therapy CD4+ T-cell numbers are known to correlate with the increase in CD4+ T-cell numbers during cART (2) and patients who start cART with fewer than 350 CD4+ T cells per µl blood frequently fail to increase their CD4+ T-cell numbers during therapy, despite successful suppression of plasma HIV RNA (3-5). Other factors associated with a suboptimal immunologic response on cART are older age at start of cART, reduced thymic function, increased immune activation leading to increased lymphoid tissue fibrosis and T-cell apoptosis, and certain human genetic polymorphisms (5-10). Individuals who do not, or only very slowly, recover normal CD4+ T-cell numbers despite undetectable plasma HIV RNA are referred to as immunological non-responders. Seventeen to twenty-nine percent of all HIV infected individuals starting cART with less than 350 CD4+ T cells per µl blood have been reported to fall in this category (3;4).

One of the latest antiretroviral drug classes is formed by HIV entry inhibitors, including CCR5 antagonists. Currently, Maraviroc (MVC, Celsentry ®) is the only registered CCR5-antagonist for the treatment of antiretroviral treatment-naive (USA only) and ART-experienced HIV-1 infected patients (11). MVC selectively binds to the CCR5 co-receptor, thereby preventing HIV binding and inhibiting HIV-entry (12). Next to its proven *in vivo* virological properties, intensification of cART with MVC has been implicated in CD4+ T-cell recovery. In a study by Cooper et al., administration of a MVC containing regimen to treatment-naive R5 HIV-1 infected individuals led to a larger increase in CD4+ T-cell number than administration of an efavirenz containing regimen (13). Furthermore, a meta-regression analysis of clinical trials investigating CCR5-antagonists in antiretroviral treatment-experienced patients showed that the use of a CCR5-antagonist is associated with a significantly increased CD4+ T-cell gain (+30 cells/µL [95% CI, 19-42]) within 24 weeks after addition of the CCR5 antagonist to the treatment regimen (14). These findings are in line with a study showing that individuals with disease accelerating CCR5 genotypes and low CCL3L1 expression have impaired CD4+ T-cell reconstitution during cART (6). Significant CD4+ T-cell gain during MVC treatment intensification could, however, not be confirmed by more recent studies (15-17) and is therefore still under debate.

Several mechanisms have been proposed to explain a possible beneficial effect of MVC on CD4+ T-cell gain. Reduction of immune activation, either by lowering residual viral load or by a direct effect via the CCR5 molecule expressed on T cells, could alter T-cell turnover and recovery of peripheral T-cell numbers (18). In line with this, HIV-1 infection, which causes profound immune activation, increases the turnover of CCR5 expressing memory CD4+ T cells (19), suggesting that indeed reduction of T-cell activation could decrease turnover. Also, as has been suggested by others, redistribution of CCR5 expressing T cells could be involved (15;20-22). Treatment intensification with Maraviroc has been described not to increase CD8+ T-cell numbers in peripheral blood and to decrease CD8+ T cells in rectal tissue, which was suggested

to be compatible with a redistribution effect (15). Also, chemotaxis of PBMC from HIV infected individuals, measured directly *ex vivo*, has been shown to be reduced by approximately 60% after 6 months of MVC treatment (21). Furthermore, Reshef et al. (2012) showed that addition of MVC to the treatment regimen of allogeneic hematopoietic stem-cell transplanted individuals reduces the risk of visceral acute graft-versus-host disease, possibly by inhibition of lymphocyte trafficking (20).

We performed an in depth study among a subset of participants of the Maraviroc Immune Recovery Study (MIRS) (17), a double blinded study among immunological non-responders with viral suppression on cART, investigating the effect of MVC intensification on T-cell recovery. T-cell turnover rates of naive and memory CD4^{+} and CD8^{+} T cells were quantified using *in vivo* labeling with deuterated water in patients receiving placebo or MVC intensification. We observed reduced T-cell turnover rates of naive and memory CD4^{+} and CD8^{+} T cells during MVC intensification.

MATERIALS AND METHODS

Study population. Immunological non-responders were recruited from the 'MVC Immune Recovery Study' (MIRS), a multicenter, randomized, placebo-controlled study investigating the effect of MVC intensification of cART on CD4^{+} T-cell reconstitution in patients with a suboptimal immunological response, despite suppression of plasma HIV-RNA. Labeling with deuterated water (D_2O) was performed among patients visiting the University Medical Center Utrecht only. All subjects provided written informed consent. This study was approved by the Ethical Committee of the University Medical Center Utrecht, The Netherlands (ClinicalTrials.gov identifier: NCT00875368; EudraCT number 2008-003635-20).

Inclusion criteria were: age 18 years and older; either a CD4^{+} T-cell count <350 cells/µl while at least two years on cART, or CD4^{+} a T-cell count <200 cells/µl while at least one year on cART and successful viral suppression (plasma HIV-RNA < 50 copies/ml) for at least 6 months prior to inclusion. Exclusion criteria were: previous use of MVC; HIV-2 infection; cART regimen containing a combination of tenofovir and didanosine; active infection for which antimicrobial treatment was needed; acute hepatitis B or C; chronic hepatitis B or C for which treatment with (peg)interferon and/or ribavirin was needed; immunosuppressive medication; and, radiotherapy or chemotherapy in the 2 years prior to inclusion.

Included patients were randomized within the MIRS (17), to add MVC or placebo to their existing cART regimen for 48 weeks. All patients who participated in the MIRS at UMCU were asked to participate in the D_2O labelling study. The subgroup of patients that participated in the current study was representative of the total MIRS study in terms of CD4^{+} T-cell gain during the study. The MVC dose was 150-600 mg twice daily, depending on interactions with concurrent medication, as specified in the package insert. In case of virological failure (defined as two consecutive measurements of plasma HIV-1 RNA of 50 copies/ml or higher), participants had to discontinue the study medication. One individual discontinued the intake of D_2O after 5 weeks for personal reasons, but continued to follow the down labelling protocol; we did incorporate his data and took into account the shorter label intake in the analysis. All other participants followed the complete protocol.

Deuterium labeling protocol. Study subjects drank a bolus of 7.5 ml deuterated water per kg body water (60% of body weight) at the first day of the protocol, at which they also started using either MVC or the placebo (fig. 1). During the labeling period of 9 weeks, participants drank 1.25 ml deuterated water per kg body water daily. Blood (50 ml) and urine samples were collected at the indicated times (fig. 1) during the labeling period (5 times) and during 15 weeks after stop of label administration (5 times).

Flow cytometry and cell sorting. PBMC were obtained by Ficoll-Paque density gradient centrifugation from blood and either cryopreserved until further use or used directly. Absolute CD4$^+$ and CD8$^+$ T-cell numbers were determined by dual-platform flow cytometry, using TruCount tubes (BD Biosciences). Percentages of naive (CD27$^+$CD45RO$^-$) and memory (CD45RO$^+$) CD4$^+$ and CD8$^+$ T cells were assessed by flow cytometry. PBMC were incubated with monoclonal antibodies (mAb) to CD3 Pacific Blue, CD4 APC-Cy7 (eBioscience) and CD8 PE, CD45RO PE-Cy7 and CD27 APC (BD Biosciences). All experiments described above were analyzed on a FACS Canto II or FACS LSR II (BD Biosciences) with FACS Diva software (BD Biosciences).

To distinguish between naive (CD27$^+$CD45RO$^-$) and memory (CD45RO$^+$) CD4$^+$ and CD8$^+$ T-cell populations for our deuterium labeling study, PBMC were incubated with mAb to CD3 FITC, CD45RO-PE-Cy7 (BD Biosciences), CD27 APC, CD4 Pacific Blue (eBioscience) and CD8 V500 (Biolegend). The specified cell fractions were isolated by cell sorting on a FACSAria (BD PharMingen). Purity of the sorted cells was above 90% in the majority of the cases (84% of all samples analyzed).

TREC analysis. DNA was isolated using the QIAamp blood mini kit according to manufacturer's instructions (Qiagen). Signal joint (Sj) T-cell receptor excision circle (TREC) numbers were quantified using a real-time PCR method as previously described (23).
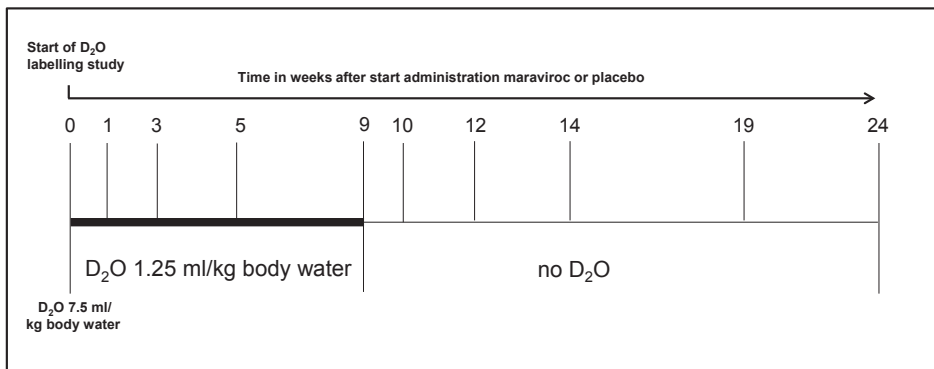

Figure 1. flow chart labeling protocol. The study-participants were subjected to the following study protocol; administration of either MVC or placebo started at day 0 and continued throughout the entire protocol. Blood (50 ml) and a urine sample were collected at the indicated time points; day 0, week 1, week 3, week 5, week 9, week 10, week 12, week 14, week 19 and week 24. The indicated amounts of deuterated water were administered to the participants from day 0 – week 9 of the protocol.

DNA isolation and measurement of deuterium enrichment. DNA isolation was performed using the QIAamp DNA blood mini kit (Qiagen) according to the manufacturer's instructions. Deuterium enrichment in urine was measured by gas chromatography/mass spectrometry (GC/MS), with modifications to published protocols (24). Deuterium enrichment in DNA isolated from granulocytes and sorted T-cell fractions was measured according to the GC/MS method described by Busch et al. with minor modifications (25). Briefly, DNA was enzymatically hydrolyzed into deoxyribonucleotides and derivatized to penta-fluoro-triacetate (PFTA) before injection (DB-17MS column, Agilent Technologies) into the gas chromatograph (7890A GC System, Agilent Technologies). PFTA was analyzed by negative chemical ionization mass spectrometry (5975C inert XL EI/CI MSD with Triple-Axis Detector, Agilent Technologies) measuring ions m/z 435 and m/z 436. Standards of known isotopic enrichments were used to control for varying sample concentrations (26;27).

Mathematical modeling of deuterated data. Following Vrisekoop et al. (28), the availability of deuterated water (D$_2$O) at any moment in time was calculated by fitting the following equations to the deuterium enrichment level in the urine of each individual:

$$U(t) = f\left(1 - e^{-\delta t}\right) + \beta e^{-\delta t} \text{ during label intake } (t \leq \tau) \qquad \text{(Equation 1a)}$$

and

$$U(t) = \left[f\left(1 - e^{-\delta \tau}\right) + \beta e^{-\delta \tau}\right] e^{-\delta(t-\tau)} \text{ after label intake } (t > \tau) \quad \text{(Equation 1b)}$$

where $U(t)$ represents the fraction of D$_2$O in urine at time t (in days), f is the fraction of D$_2$O in the drinking water, labelling was stopped at $t = \tau$ days, δ represents the turnover rate of body water per day, and β is the urine enrichment attained after the boost of label by the end of the first day of the protocol. Up- and down-labeling of the granulocyte population of each individual were analyzed as described previously (28), to estimate the maximum level of label intake that cells could possibly reach. The label enrichment data of all cell subsets were subsequently scaled by the granulocyte asymptote of each individual (28).

Mathematical models that allow for kinetic heterogeneity between cells of the cell population under investigation (29) were fitted to labeling data of the different T-cell subsets. Each kinetic sub-population i was modelled to contain a fraction α_i of cells with a turnover rate p_i. Assuming a steady state for each kinetic sub-population (i.e. constant cell numbers during the study, meaning that there is as much production as loss) the fraction of labelled DNA of each sub-population i was modelled by the following differential equation:

$$\frac{dL_i}{dt} = p_i c U(t) - p_i L_i \qquad \text{(Equation 2)}$$

where L_i represents the fraction of labelled DNA of sub-population i, c is an amplification factor that needs to be introduced because the adenosine deoxyribose moiety contains multiple

hydrogen atoms that can be replaced by deuterium (28). Basically, labelled adenosines in sub-population i are gained when a deuterium atom is incorporated with probability $cU(t)$ in the DNA of cells that replicate at rate p_i, and they are lost when cells of sub-population i are lost at rate p_i. For naive T cells this replication may occur both in the periphery and in the thymus. The corresponding analytical solutions are:

$$L_i(t) = \frac{c}{\delta - p_i} \left[\delta f (1 - e^{-p_i t}) - p_i f (1 - e^{-\delta t}) + \beta p_i (e^{-p_i t} - e^{-\delta t}) \right] \quad \text{(Equation 3a)}$$

during label intake ($t \leq \tau$), and

$$L_i(t) = \frac{c}{\delta - p_i} \left[\delta f (e^{-p_i (t-\tau)} - e^{-p_i t}) - p_i f (e^{-\delta (t-\tau)} - e^{-\delta t}) + \beta p_i (e^{-p_i t} - e^{-\delta t}) \right]$$

(Equation 3b)

after label intake ($t > \tau$).

The fraction of labelled DNA in the total T-cell population under investigation was subsequently derived from $L(t) = \sum \alpha_i L_i(t)$ and the average turnover rate p was calculated from $p = \sum \alpha_i p_i$.

Because all enrichment data were expressed as fractions, labelling data were arcsin(sqrt) transformed before fitting the model to the data.

Each parameter was modeled as the sum of a population (fixed) parameter (a) and a random effect (b_i) allowing each parameter to be different from one patient to another: $\theta_i = a + b_i + c * group$, where $group$=0 if the individual was in the placebo group and 1 otherwise. Each random effect was assumed to be normally distributed with a variance (σ_b^2) to be estimated: $b_i \sim N(0, \sigma_b^2)$. Hence, for each biological parameter, three parameters have to be estimated: one for the average value, one for the variance of the random effect and one for an additional effect of MVC. Parameters were estimated using the R package $nlme$ for random effect models (30).

Statistical analyses. Variables were compared using the Mann-Whitney test. Differences were considered statistically significant at p < 0.05. Correlations were calculated using Spearman's rank correlation coefficients. All statistical analyses were performed using the GraphPad Prism software (Graphpad Software, Inc.).

RESULTS

Study population and baseline characteristics. Seven patients of the randomized, placebo-controlled MIRS study were enrolled in the labeling study, of which at completion of the study 4 turned out to be in the MVC group and 3 in the placebo group. In terms of T-cell numbers, these patients were representative for the larger study group of patients in the MIRS study. Comparison of the patient characteristics and baseline immunological values (table 1) between the MVC and the placebo group showed no significant differences. All

Table 1. Patient characteristics and immunological baseline values

	Placebo			Maraviroc			
Subject	1042	1044	2026	1043	2041	2042	2076
Symbol	▲	●	■	Δ	○	□	◊
Age (years)	68.0	35.0	54.0	45.0	56.0	49.0	27.0
Sex	M	M	M	M	M	M	M
Duration ART	9.5	1.7	5.0	2.5	12.4	2.2	2.2
Nadir CD4+ T-cell number (cells/μl)*	4.0	1.0	153.0	47.0	86.0	33.0	56.0
CD4+ T-cell number Wk 0 (cells/μl)	180.0	90.0	267.0	176.0	264.0	312.0	286.0
% Naive CD4+ T-cells	5.0	48.0	25.7	40.7	47.1	27.6	44.9
% Memory CD4+ T-cells	94.9	51.5	73.4	17.0	47.9	63.4	54.6
% Naive CD8+ T-cells	5.3	60.9	34.7	71.5	21.5	35.9	37.5
% Memory CD8+ T-cells	76.7	38.3	54.3	16.8	49.9	20.3	43.8
% CD38+HLA-DR+ CD4+ T-cells	18.3	1.9	3.4	6.2	2.5	3.8	3.7
% CD38+HLA-DR+ CD8+ T-cells	29.0	2.1	5.0	5.3	12	3.3	8.1
% Ki67+ CD4+ T-cells	2.5	1.7	4.1	3.8	1.2	4.8	1.5
% Ki67+ CD8+ T-cells	1.6	0.5	2.5	1.6	0.8	1.8	1.5
% CD31+ naive CD4+ T-cells	50.0	84.5	61.2	70.3	35.4	36.4	73.2

* defined as the lowest CD4+ T-cell number (cells/μl) ever measured

participants were male and the average age, duration of ART and CD4+ T-cell numbers at the start of the study were similar in both groups. Nadir CD4+ T-cell numbers were lower than 200 cells/μl for all study participants. CD4+ and CD8+ T-cell numbers of participants in the labeling study remained relatively stable during this study as well as during the 48-week clinical trial (fig. S1).

TREC content remains stable in naive T cells. In order to investigate T-cell production and death, we analyzed Ki67 and CD38/HLA-DR expression and levels of AnnexinV. These markers reflect what is happening in T cells at a particular moment in time. We measured these markers at each study visit. None of the markers showed a significant change during the study in any of the T-cell subsets analyzed (data not shown). It is possible, however, that these markers were not sensitive enough to detect potential differences.

As a more accumulative marker, we measured the TREC content for both naive CD4+ and CD8+ T cells for each individual participating in the labeling study. The expected TREC content of naive CD4+ and CD8+ T-cell populations was calculated using the percentage of naive cells of each individual, as we measured the TREC content of total CD4+ and total CD8+ T cells. To this end, we divided the average TREC content of each T-cell population by the percentage of naive cells in that population, assuming that the average TREC content of a memory cell is negligible compared to that of a naive cell. We did not observe a significant change in TREC content for naive CD4+ and CD8+ T cells during the 48 weeks of the MIRS clinical trial in either treatment
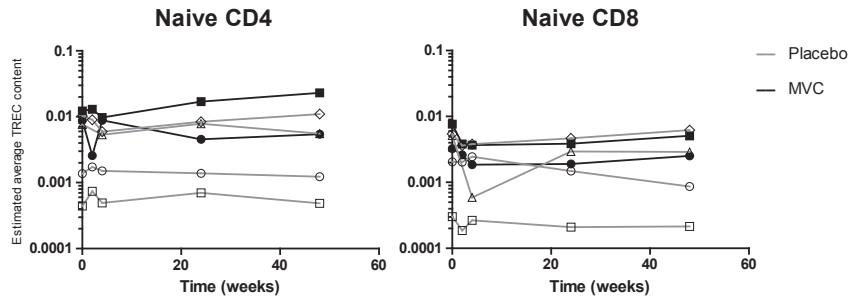
Figure 2. TREC content of naive CD4⁺ and CD8⁺ T cells. Calculated TREC content of naive CD4⁺ (left) and CD8⁺ (right) T cells plotted against time in the study protocol. The average TREC content of each T-cell population was divided by the percentage of naive cells in that population. Open symbols represent individuals in the MVC group and filled symbols represent individuals in the placebo group.

group (fig. 2). It could of course be that effects on both T-cell proliferation and T-cell death neutralize each other, which results in an unchanged TREC content.

Decreased turnover rate of T cells in immunological non-responders treated with MVC. Using *in vivo* labeling with deuterated water, we were able to investigate the effect of MVC on T-cell recovery in both patient groups with a much higher sensitivity.

The label incorporation and loss of all analyzed T-cell subsets was much faster in the placebo group compared to the MVC group (fig. 3), suggesting that MVC decreased the rate of T-cell turnover. Use of mixed effect models (see Materials and Methods), indeed showed that the average turnover rate of all T-cell subsets was significantly lower in the MVC treated group than in the placebo group (table 2 and fig. 4). Interestingly, the average T-cell turnover rate of MVC treated individuals did not significantly differ from that of healthy individuals, suggesting MVC treatment normalized T-cell turnover rates.

The median estimated average life spans of naive T cells in the placebo treated group were 262 and 348 days, for CD4⁺ and CD8⁺ T cells respectively. In the MVC group these were 4-6 fold longer, 1184 (p = 0.023) and 2407 (p = 0.014) days for CD4⁺ and CD8⁺ T cells respectively (table 2) and resembled the average life spans of these subsets in healthy individuals. The naive CD8⁺ T-cell turnover rate of one MVC treated participant was too low to accurately estimate the average life span of these cells. Although the results of this patient could not be included, this extremely low turnover rate reconfirms the very long life span of naive CD8⁺ T cells in MVC treated patients. Memory T cells in the placebo treated group had an average life span of 15 and 3 days, for CD4⁺ and CD8⁺ T cells, respectively. In comparison, in the MVC treated group, the average estimated life span of memory T cells was many fold higher, 55 and 79 days, for CD4⁺ and CD8⁺ T-cells resp. (p < 0.0001 for both CD4⁺ and CD8⁺ T cells), again resembling those of healthy individuals (fig. 4 and table 2).

In summary, contrary to other markers of T-cell production and death, T-cell turnover decreased significantly during MVC treatment intensification.
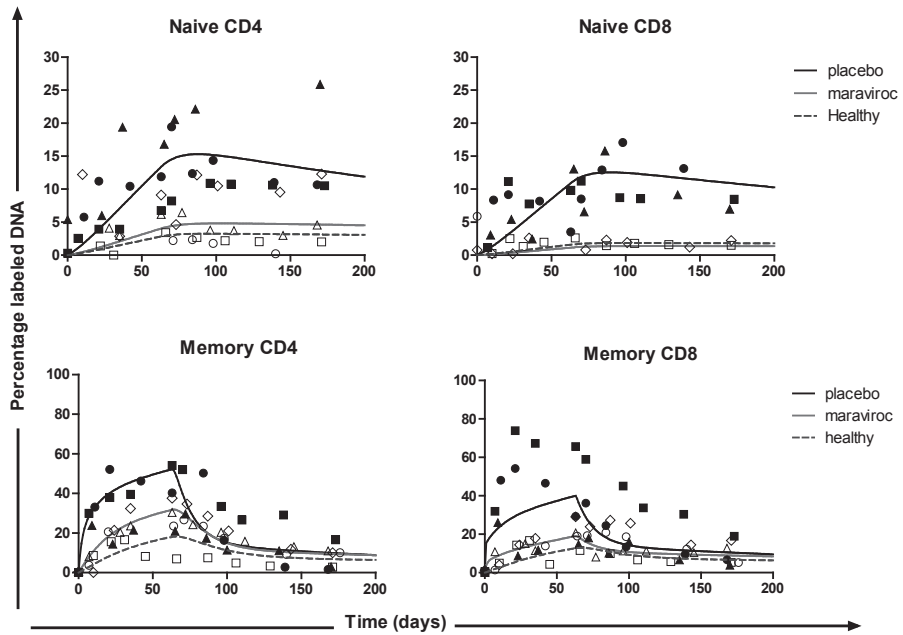
Figure 3. Average deuterium labeling curves of T-cell subsets in the MVC and the placebo group. A. DNA enrichment curves of naive CD4^{+} T cells (left graphs) and naive CD8^{+} T cells (right graphs) prepared with pooled data of the individuals of the placebo group (n=3, filled symbols, black line) and the MVC group (n=4, open symbols, grey line), compared with estimated curves of naive T cells of healthy individuals (dashed line). B. DNA enrichment curves of memory CD4^{+} T cells (left graphs) and memory CD8^{+} T cells (right graphs) prepared with pooled data of the individuals of the placebo group (n=3, filled symbols, black line) and the MVC group (n=4, open symbols, grey line), compared with enrichment curves of memory T cells of healthy individuals (dashed line).
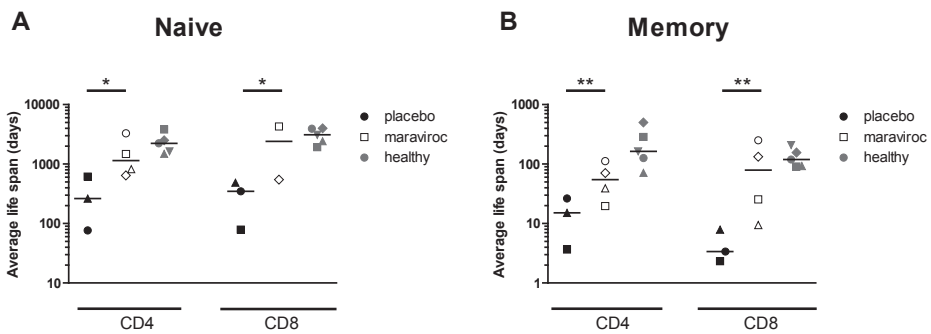

Figure 4. Estimated average life span of naive and memory T cells in the MVC group and the placebo group compared to healthy individuals. Estimated life span in days of naive (A) and memory (B) CD4^{+} T cells and CD8^{+} T cells of individuals in the placebo group (black filled symbols), the MVC group (open symbols) and healthy individuals (filled grey symbols. Statistical significance (* p < 0.05), (** p < 0.0001) was determined by the nonparametric Mann-Whitney U test for unpaired data.

Table 2. Estimated life spans of CD4^{+} and CD8^{+}, naive and memory T cells

	Naive		Memory	
	CD4	CD8	CD4	CD8
Placebo	262 [76;615]	348 [79;486]	15 [4;26]	3 [2;8]
Maraviroc	1148 [645;3282]	2407 [548;4266]	55 [19;112]	79 [9;250]
Healthy	2228 [1482;3803]	3095 [1920;3993]	164 [71;500]	119 [90;208]

The median estimated life span in days of CD4^{+} and CD8^{+}, naive and memory T cells in MVC treated individuals, individuals in the placebo group and healthy individuals. The range of the estimated life spans is indicated between brackets.

Delta CCR5 expression correlates with estimated life span in MVC treated individuals. MVC treatment intensification induces a change in CCR5 expression in memory T cells, particularly early after start of treatment (fig. S3). As MVC also affected the life span of memory T-cells substantially, we next investigated whether delta CCR5 expression is linked to the estimated average life span of memory T cells in MVC treated individuals. We therefore correlated the change in CCR5 expression between the first day of the treatment protocol and time point week 48 with the average estimated life span of memory T cells. Interestingly, we found a positive correlation between delta CCR5 expression and the estimated life spans in the MVC treated group (fig. 5). This correlation was significant for CD8^{+} memory T cells (R^2=0.9704, p = 0.015) and for memory CD4^{+} T cells there was a trend (R^2=0.8779). There was no correlation between delta CCR5 expression and average estimated life span in this group (data not shown).
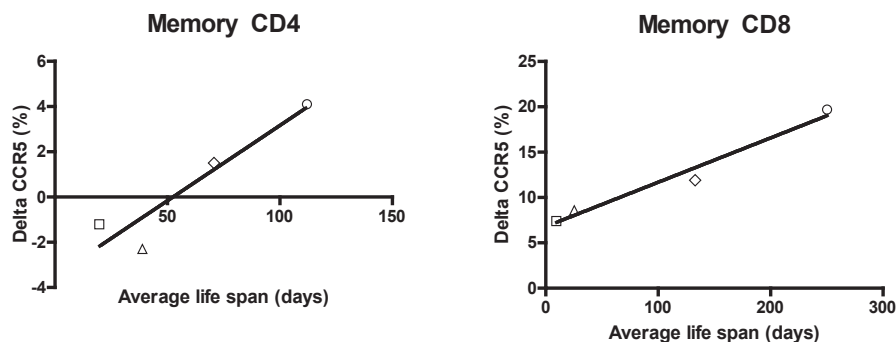

Figure 5. Correlations between delta CCR5 expression and estimated average estimated life span of CD4^{+} and CD8^{+} memory T cells in the MVC group. Delta CCR5 expression between day 0 and week 48 of the study protocol plotted against the estimated average life span of memory CD4^{+} and CD8^{+} T cells in MVC treated individuals.

DISCUSSION

We studied the effects of cART treatment intensification with MVC in immunological non-responders, focusing on T-cell kinetics. By using deuterium labeling we were able to show that T-cell turnover rates normalized in MVC treated individuals, as compared to placebo controls. These data suggest that MVC treatment decreases T-cell turnover and thereby results in longer life spans of T cells in treated HIV infected immunological non-responder patients.

MVC intensification has been suggested to influence T-cell dynamics by lowering residual viral load and immune activation. In the individuals participating in this study HIV-RNA was continuously suppressed (< 50 copies/ml) and no viral blips or reactivations were observed. An effect below the detection limit of 50 copies HIV-RNA per ml plasma in this study cannot be excluded, however two recent studies could not find a decrease of plasma HIV-RNA below 50 copies/ml after MVC intensification (15;31).

The reduced production rates that we found in the MVC treated group could mechanistically be explained by the fact that CCR5+ T cells of HIV-infected individuals have higher proliferation rates than CCR5- T cells of the same individuals (19). Blockade of CCR5 signalling by MVC may reduce turnover rates of CCR5+ T cells. In line with this, we observed the largest decrease in turnover in memory CD8+ T cells, which is also the subset that has the highest CCR5 expression, and would therefore experience the largest effect of CCR5 blockade. Furthermore, we observed a significant correlation between delta CCR5 expression during the MIRS clinical trial and estimated life span in memory T cells (fig. 5). This means the larger the effect on CCR5 expression, the larger the effect of CCR5 blockade by MVC.

CCR5 has been described to be involved in the activation of T cells. Contento et al. showed recruitment of CCR5 to the immunological synapse during the interaction of T cells and antigen presenting cells and induction of a second activation signal by CCR5, next to TCR triggering, in T cells *in vitro* (32). Furthermore, CCR5 density on HLA-DR+CD4+ T cells has been reported to be positively correlated with the percentage of CD38 expressing CD8+ T cells and HLA-DR expressing CD4+ T cells in HIV infected individuals, independent of HIV viral load (18). Given the above, blockade of CCR5 signaling by MVC may reduce T-cell activation and thereby decrease T-cell turnover, resulting in a longer estimated T-cell life span. However, conflicting results have been published regarding the effects of MVC intensification on T-cell activation (15;16;33). Hunt et al. described more CD8+ T cell activation and a lower decline in CD4+ T-cell activation after 24 weeks of MVC treatment intensification (15), whereas Rusconi et al. reported diminished T-cell activation after treatment with MVC (16). Cuzin et al. reported decreased CD8+ T-cell activation after 24 weeks of treatment intensification with MVC, however, at week 36 of this clinical trial, 7 weeks after cessation of MVC treatment intensification, CD8+ T-cell activation was back to baseline level (33). In the present study, we did not observe a change in the expression of either activation markers CD38 and HLA-DR expression, or in proliferation marker Ki67, which is also frequently upregulated upon activation, in MVC treated individuals.

Diminished T-cell apoptosis, due to blockade of CCR5 signaling, may also explain the decreased turnover that we observed in the MVC treated group. It was previously shown that markers of apoptosis decreased during MVC treatment intensification and reversed after discontinuation of MVC (14). A role of CCR5 in the induction of apoptosis has previously been

described (34-38). CCR5 ligands were shown to induce cell death in certain CCR5 expressing cell types (35) and CCL5 aggregates, which form at high ligand concentrations, have been described to induce apoptosis in T-cell lines as well as in primary human T cells (37). In subjects with acute primary HIV infection, high levels of apoptosis were observed in T cells with increased expression of CCR5 (38). If CCR5 is indeed correlated with apoptosis levels, these might decrease in cells in which CCR5-signaling is blocked by MVC. This would in turn result in a lower turnover. Indeed, apoptosis levels (as measured by annexin-V expression) in total CD8^{+} T cells in our MIRS study were lower in the MVC arm compared to the placebo arm (17). However, in CD4^{+} T cells there was no difference in levels of Annexin-V expression between the placebo and the MVC group (17). Therefore, reduction of T-cell turnover in MVC treated individuals, could only partly be explained by decreased apoptosis through blockade of CCR5 signaling.

Despite the observed changes in T-cell turnover in naive and memory CD4^{+} T cells, we did not observe a significant increase in CD4^{+} T-cell numbers in either study group (fig. S1). The MIRS clinical trial only showed an increase in CD8^{+} T cells, the other T-cell subsets, however, remained stable in terms of numbers (17). Positive effects of MVC intensification on CD4^{+} T-cell gain and immune activation have been observed, but are still under debate due to inconsistency between studies (14;16;33).

The question remains why, despite decreased turnover (and increased life span), T-cell numbers do not increase in the MVC group. An altered balance between T-cell activation and apoptosis may alter dynamics but leave numbers unchanged. When both these processes are linked, MVC could reduce proliferation and cell death resulting in decreased turnover with no net change in T-cell numbers. PBMC of MVC treated individuals have been shown to substantially and significantly reduce ex vivo migration towards FMLP and Rantes (21). Therefore, a difference in T-cell distribution between tissue, blood and lymphoid organs may also play a role.

In conclusion, we demonstrate that T-cell turnover normalizes in MVC treated individuals. We hypothesize that this is a direct result of blocking CCR5, resulting in diminished T-cell proliferation and death rates, which in turn result in no net CD4^{+} T-cell gain. Based on decreased T-cell turnover upon MVC treatment intensification, MVC could be beneficial in the long run due to the creation of a more quiet steady state of the T-cell compartments. However, further studies are necessary to confirm our results and to investigate the clinical benefits.

REFERENCE LIST

1. Vrisekoop N, van GR, de Boer AB, et al. Restoration of the CD4 T cell compartment after long-term highly active antiretroviral therapy without phenotypical signs of accelerated immunological aging. J Immunol **2008 Jul 15**;181(2):1573-81.

2. Hunt PW, Deeks SG, Rodriguez B, et al. Continued CD4 cell count increases in HIV-infected adults experiencing 4 years of viral suppression on antiretroviral therapy. AIDS **2003 Sep 5**;17(13):1907-15.

3. Florence E, Lundgren J, Dreezen C, et al. Factors associated with a reduced CD4 lymphocyte count response to HAART despite full viral suppression in the EuroSIDA study. HIV Med **2003 Jul**;4(3):255-62.

4. Grabar S, Le M, V, Goujard C, et al. Clinical outcome of patients with HIV-1 infection according to immunologic and virologic response after 6 months of highly active antiretroviral therapy. Ann Intern Med **2000 Sep 19**;133(6):401-10.

5. van Lelyveld SF, Gras L, Kesselring A, et al. Long-term complications in patients with poor immunological recovery despite virological successful HAART in Dutch ATHENA cohort. AIDS **2012 Feb 20**;26(4):465-74.

6. Ahuja SK, Kulkarni H, Catano G, et al. CCL3L1-CCR5 genotype influences durability of immune recovery during antiretroviral therapy of HIV-1-infected individuals. Nat Med **2008 Apr**;14(4):413-20.

7. Corbeau P, Reynes J. Immune reconstitution under antiretroviral therapy: the new challenge in HIV-1 infection. Blood **2011 May 26**;117(21):5582-90.

8. Haas DW, Geraghty DE, Andersen J, et al. Immunogenetics of CD4 lymphocyte count recovery during antiretroviral therapy: An AIDS Clinical Trials Group study. J Infect Dis **2006 Oct 15**;194(8):1098-107.

9. Marchetti G, Gori A, Casabianca A, et al. Comparative analysis of T-cell turnover and homeostatic parameters in HIV-infected patients with discordant immune-virological responses to HAART. AIDS **2006 Aug 22**;20(13):1727-36.

10. Zeng M, Smith AJ, Wietgrefe SW, et al. Cumulative mechanisms of lymphoid tissue fibrosis and T cell depletion in HIV-1 and SIV infections. J Clin Invest **2011 Mar**;121(3):998-1008.

11. Gulick RM, Lalezari J, Goodrich J, et al. Maraviroc for previously treated patients with R5 HIV-1 infection. N Engl J Med **2008 Oct 2**;359(14):1429-41.

12. Chen LF, Hoy J, Lewin SR. Ten years of highly active antiretroviral therapy for HIV infection. Med J Aust **2007 Feb 5**;186(3):146-51.

13. Cooper DA, Heera J, Goodrich J, et al. Maraviroc versus efavirenz, both in combination with zidovudine-lamivudine, for the treatment of antiretroviral-naive subjects with CCR5-tropic HIV-1 infection. J Infect Dis **2010 Mar 15**;201(6):803-13.

14. Wilkin TJ, Ribaudo HR, Tenorio AR, Gulick RM. The relationship of CCR5 antagonists to CD4+ T-cell gain: a meta-regression of recent clinical trials in treatment-experienced HIV-infected patients. HIV Clin Trials **2010 Nov**;11(6):351-8.

15. Hunt PW, Shulman N, Hayes TL, et al. The immunologic effects of maraviroc intensification in treated HIV-infected individuals with incomplete CD4+ T cell recovery: a randomized trial. Blood **2013 Apr 15**.

16. Rusconi S, Adorni F, Vitiello P. Maraviroc (MVC) as Intensification Strategy in Immunological Non-responder HIV-infected Patients with Virologic Success on HAART. EACS, Belgrade, Abstract PS1/7 **2011 Oct 12**.

17. van Lelyveld SFL, Veel E, Drylewicz J, et al. Maraviroc Intensification in Patients with Suboptimal Immunological recovery Despite Virological Suppressive cART: a 48-week, Placebo-controlled Trial. Submitted **2013**.

18. Portales P, Psomas KC, Tuaillon E, et al. The intensity of immune activation is linked to the level of CCR5 expression in human immunodeficiency virus type 1-infected persons. Immunology **2012 Sep**;137(1):89-97.

19. Zhang Y, de LC, Worth A, et al. Accelerated In Vivo Proliferation of Memory Phenotype CD4(+) T-cells in Human HIV-1 Infection Irrespective of Viral Chemokine Co-receptor Tropism. PLoS Pathog **2013 Apr**;9(4):e1003310.

20. Reshef R, Luger SM, Hexner EO, et al. Blockade of lymphocyte chemotaxis in visceral graft-versus-host disease. N Engl J Med **2012 Jul 12**;367(2):135-45.

21. Rossi R, Lichtner M, Sauzullo I, et al. Downregulation of leukocyte migration after treatment with CCR5 antagonist maraviroc. J Acquir Immune Defic Syndr **2010 Aug**;54(5):e13-e14.

22. Rossi R, Lichtner M, De RA, et al. In vitro effect of anti-human immunodeficiency virus CCR5 antagonist maraviroc on chemotactic activity of monocytes, macrophages and dendritic cells. Clin Exp Immunol **2011 Nov**;166(2):184-90.

23. Hazenberg MD, Otto SA, Cohen Stuart JW, et al. Increased cell division but not thymic dysfunction rapidly affects the T-cell receptor excision circle content of the naive T cell population in HIV-1 infection. Nat Med **2000 Sep**;6(9):1036-42.

24. Van Kreel BK, Van d, V, Meers M, Wagenmakers T, Westerterp K, Coward A. Determination of total body water by a simple and rapid mass spectrometric method. J Mass Spectrom **1996 Jan**;31(1):108-11.

25. Busch R, Neese RA, Awada M, Hayes GM, Hellerstein MK. Measurement of cell proliferation by heavy water labeling. Nat Protoc **2007**;2(12):3045-57.

26. Patterson BW, Zhao G, Klein S. Improved accuracy and precision of gas chromatography/mass spectrometry measurements for metabolic tracers. Metabolism **1998 Jun**;47(6):706-12.

27. Westera L, Zhang Y, Tesselaar K, Borghans JA, Macallan DC. Quantitating lymphocyte homeostasis in vivo in humans using stable isotope tracers. Methods Mol Biol **2013**;979:107-31.

28. Vrisekoop N, den B, I, de Boer AB, et al. Sparse production but preferential incorporation of recently produced naive T cells in the human peripheral pool. Proc Natl Acad Sci U S A **2008 Apr 22**;105(16):6115-20.

29. Westera L, Drylewicz J, den B, I, et al. Closing the gap between T-cell life span estimates from stable isotope-labeling studies in mice and men. Blood **2013 Aug 14**.

30. Pinheiro J, Bates D, DebRoy S, Sarkar D, the R development Core Team. Linear and Nonlinear Mixeds Effect Models. R package version 3 1-109 **2013 Jan 1**.

31. Gutierrez C, Diaz L, Vallejo A, et al. Intensification of antiretroviral therapy with a CCR5 antagonist in patients with chronic HIV-1 infection: effect on T cells latently infected. PLoS One **2011**;6(12):e27864.

32. Contento RL, Molon B, Boularan C, et al. CXCR4-CCR5: a couple modulating T cell functions. Proc Natl Acad Sci U S A **2008 Jul 22**;105(29):10101-6.

33. Cuzin L, Trabelsi S, Delobel P, et al. Maraviroc intensification of stable antiviral therapy in HIV-1-infected patients with poor immune restoration: MARIMUNO-ANRS 145 study. J Acquir Immune Defic Syndr **2012 Sep 14**.

34. Algeciras-Schimnich A, Vlahakis SR, Villasis-Keever A, et al. CCR5 mediates Fas- and caspase-8 dependent apoptosis of both uninfected and HIV infected primary human CD4 T cells. AIDS **2002 Jul 26**;16(11):1467-78.

35. Cartier L, Dubois-Dauphin M, Hartley O, Irminger-Finger I, Krause KH. Chemokine-induced cell death in CCR5-expressing neuroblastoma cells. J Neuroimmunol **2003 Dec**;145(1-2):27-39.

36. Julia E, Edo MC, Horga A, Montalban X, Comabella M. Differential susceptibility to apoptosis of CD4+T cells expressing CCR5 and CXCR3 in patients with MS. Clin Immunol **2009 Dec**;133(3):364-74.

37. Murooka TT, Wong MM, Rahbar R, Majchrzak-Kita B, Proudfoot AE, Fish EN. CCL5-CCR5-mediated apoptosis in T cells: Requirement for glycosaminoglycan binding and CCL5 aggregation. J Biol Chem **2006 Sep 1**;281(35):25184-94.

38. Zaunders JJ, Moutouh-de PL, Kitada S, et al. Polyclonal proliferation and apoptosis of CCR5+ T lymphocytes during primary human immunodeficiency virus type 1 infection: regulation by interleukin (IL)-2, IL-15, and Bcl-2. J Infect Dis **2003 Jun 1**;187(11):1735-47.
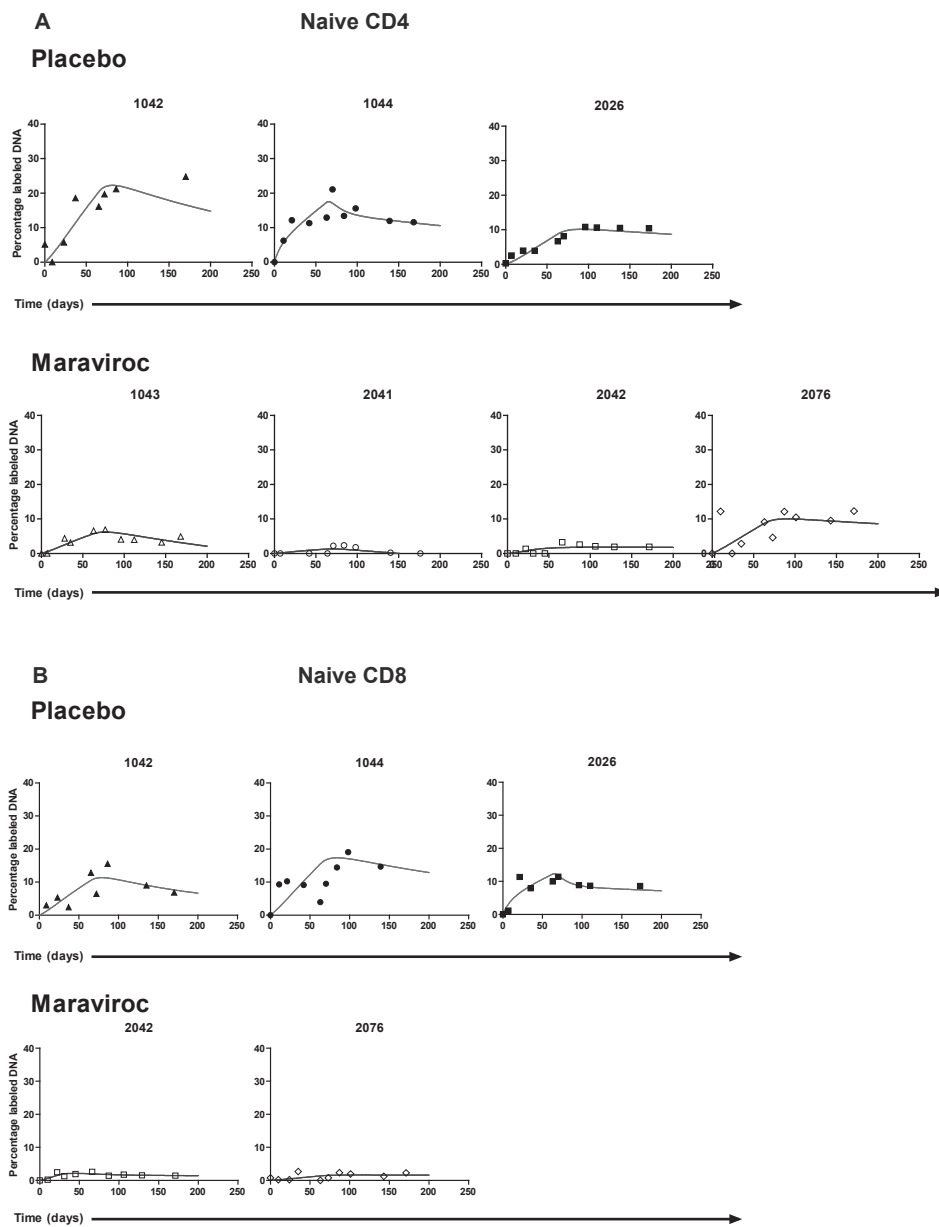
CD4

CD8
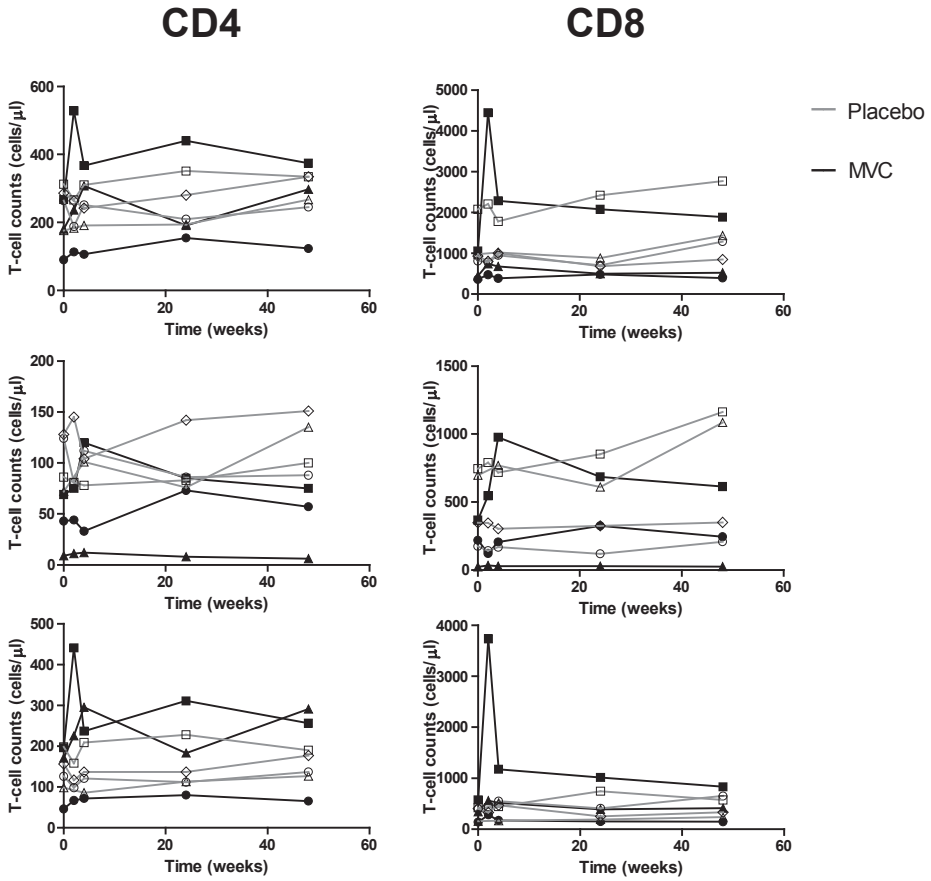
Supplemental Figure 1. CD4+ and CD8+ T-cell numbers during the study protocol. Total (A), naive (B) and memory (C) CD4+ T cells (left) and CD8+ T cells (right). Open symbols with a grey line represent individuals in the MVC group and filled symbols with a black line represent individuals in the placebo group.

Supplemental Figure 2. Individual deuterium labeling curves of T-cell subsets in individuals in the MVC and the placebo group. DNA enrichment curves of naive CD4+ T cells (A) and naive CD8+ T cells (B), memory CD4+ T cells.
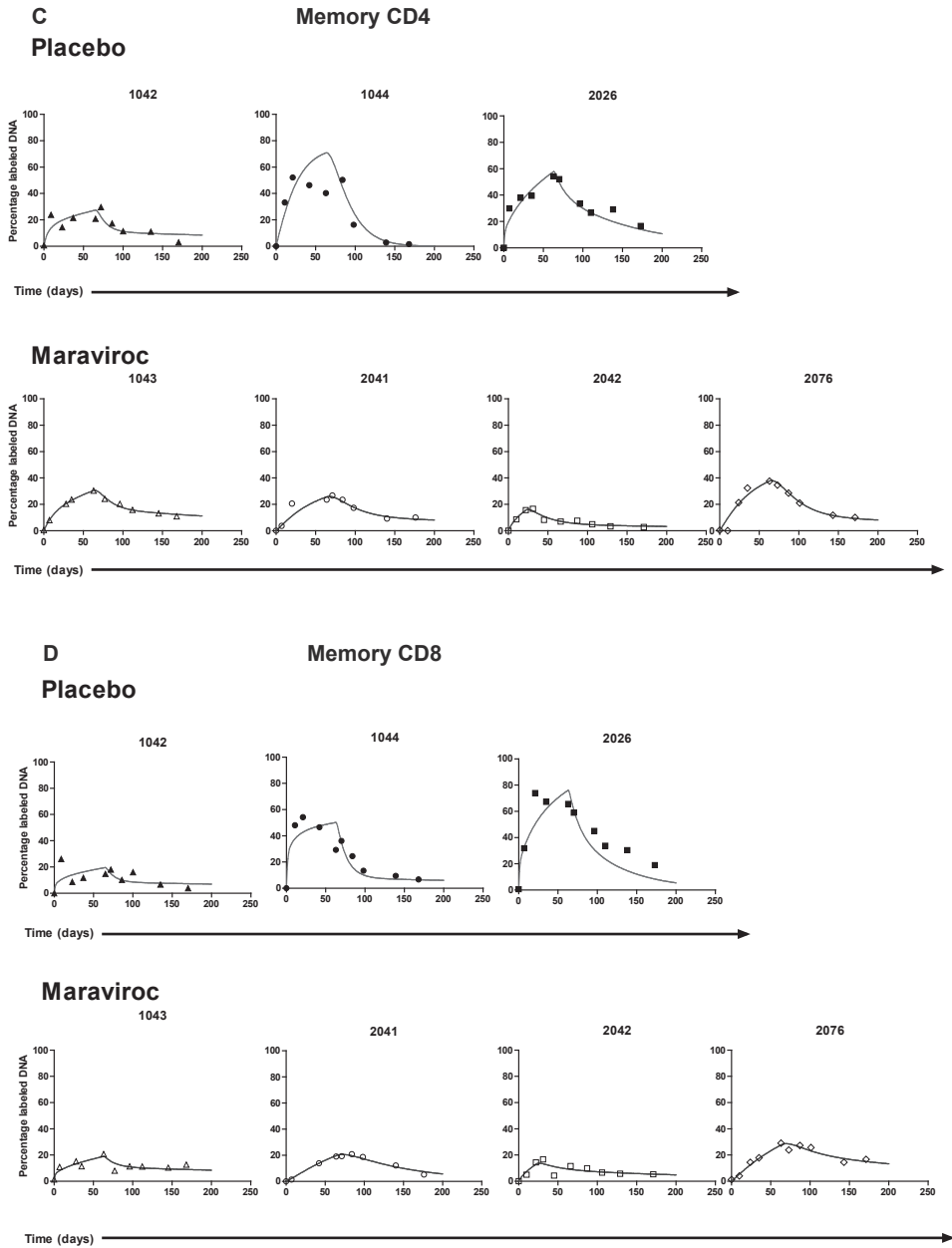
C   **Memory CD4**

Placebo

Maraviroc

D   **Memory CD8**

Placebo

Maraviroc

Supplemental Figure 2. Individual deuterium labeling curves of T-cell subsets in individuals in the MVC and the placebo group (*continued*). (C) and memory CD8^{+} T cells (D) of individual patients in the MVC and the placebo group. The upper graphs represent individuals in the placebo group and the lower graphs represent individuals in the MVC group.
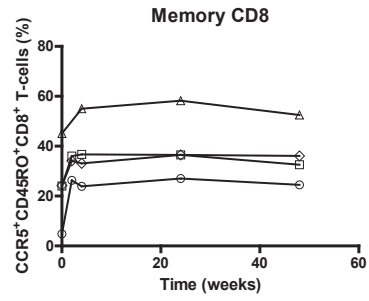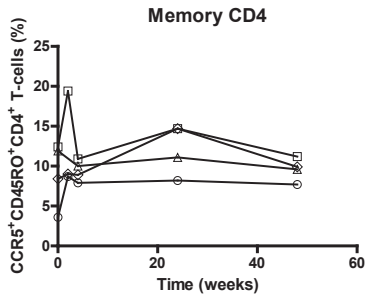
Supplemental Figure 3. CCR5 expression in the MVC group during the study protocol. Memory CD4^{+} T cells (left) and memory CD8^{+} T cells (right) in individuals in the MVC group.

CHAPTER 4

MARAVIROC INTENSIFICATION
IN PATIENTS WITH SUBOPTIMAL
IMMUNOLOGICAL RECOVERY DESPITE
VIROLOGICAL SUPPRESSIVE cART:
A 48-WEEK, PLACEBO-CONTROLLED TRIAL

Steven F.L. van Lelyveld[1], Ellen Veel[2*], Julia Drylewicz[2*],
Sigrid Otto[2], Clemens Richter[4], Robin Soetekouw[5],
Jan M. Prins[6], Kees Brinkman[7], Jan Willem Mulder[8],
Frank Kroon[9], Annemarie M.J. Wensing[1], Monique Nijhuis[3],
José A.M. Borghans[2], Kiki Tesselaar[2], Andy I.M. Hoepelman[1],
and the MIRS study group

Departments of [1]Internal Medicine & Infectious Diseases, [2]Immunology and [3]Medical
Microbiology, Virology, University Medical Center Utrecht, Utrecht; [4]Department
of Internal Medicine, Rijnstate Hospital, Arnhem; [5]Department of Internal Medicine,
Kennemer Gasthuis, Haarlem;[6]Department of Internal Medicine, Division of
Infectious Diseases, Center for Infection and Immunity, Academic Medical Center,
University of Amsterdam, Amsterdam;[7]Department of Internal Medicine, Onze
Lieve Vrouwe Gasthuis, Amsterdam;[8]Department of Internal Medicine, Slotervaart
Hospital, Amsterdam, and [9]Department of Infectious Diseases, Leiden University
Medical Center, Leiden, The Netherlands.

* These authors contributed equally

ABSTRACT

Background. Conflicting results of the effects of cART intensification with the CCR5-antagonist maraviroc (MVC) on CD4^{+} T cell reconstitution and residual immune activation have been reported for patients with suboptimal immunological recovery and successful viral suppression. We performed a 48-week, double-blind, placebo-controlled trial to determine if treatment intensification with MVC increases CD4^{+} T cell counts and reduces immune activation in these so called immunological non-responder patients.

Methods. Major inclusion criteria were: 1.CD4^{+} T cell count <350 cells/μL while at least two years on cART or CD4^{+} T cell count <200 cells/μL while at least one year on cART and 2. viral suppression for at least the previous 6 months. HIV-infected patients were randomized to add MVC (42 patients) or placebo (43 patients) to their existing cART regimen for 48 weeks.

Primary outcome was the change in CD4^{+} T cell count. Changes in CD4^{+} T cell counts and other parameters were modeled using mixed effects models.

Results. Patient characteristics and baseline values were not significantly different between the MVC and placebo arms. According to modelled slopes during 48 weeks of intensification the increase in CD4^{+} T cell count was +14.9 cells/μL (95% confidence interval (CI) [0.5; 29.3]) in the placebo arm versus +23.2 cells/μL (95% CI [7.8; 38.5]) in the MVC arm (p between arms = 0.48). Naive CD4^{+} T cell numbers increased significantly in both arms, while memory CD4^{+} T cell numbers did not change, and again there was no significant difference between both arms. MVC intensification increased the percentage of CCR5^{+} CD4^{+} and CD8^{+} T cells. Moreover, MVC intensification decreased both CD8^{+} and CD4^{+} T cell apoptosis levels and counteracted the decrease in memory CD8^{+} T cell numbers and the decrease in the percentage of the thymus proximal CD31^{+} naive CD4^{+} T cells that were observed in the placebo arm. No significant differences in the expression of markers for CD4^{+} and CD8^{+} T cell activation, proliferation and microbial translocation were found between the arms.

Conclusions. After 48 weeks of treatment intensification CD4^{+} T-cell reconstitution did not differ between the MVC and placebo arm. MVC intensification increased the percentage of CCR5 expressing T cells, and decreased T cell apoptosis levels. No differences between T cell activation levels were found between the arms.

ClinicalTrials.gov identifier: NCT00875368.

INTRODUCTION

Treatment of HIV-infection with combination antiretroviral therapy (cART) suppresses viral replication, leading to recovery of CD4$^+$ T cells. Unfortunately, 9-29% of the patients treated with cART experience a suboptimal immunological response, i.e. failure to restore CD4$^+$ T cell counts despite successful virological suppression (1–6).Several studies have shown a worse long term clinical outcome in terms of death, AIDS and non-AIDS defining diseases in these patients (1, 2, 4, 7).

The CCR5-antagonist maraviroc (MVC) was registered in 2008 for the treatment of antiretroviral treatment-naive (USA only) and -experienced HIV-1 infected patients (8). Next to its established efficacy in suppressing plasma HIV-RNA, there has been much interest in the potential immunological effects of CCR5 antagonists. Molecular studies have shown the CCR5 pathway can influence T cell trafficking, activation and apoptosis (9–11). In line with these observations, genetic studies have shown that the CCL3L1-CCR5 genotype influences the degree of CD4$^+$ T cell reconstitution during cART (12), and it was therefore postulated that manipulation of this pathway might enhance CD4$^+$ T cell recovery. Indeed, MVC containing regimens have been shown to lead to a larger increase in CD4$^+$ T cell counts than efavirenz containing regimens in treatment-naive HIV-1 patients (13). A meta-regression analysis of clinical trials investigating the effects of CCR5-antagonists in antiretroviral treatment-experienced patients showed that the use of a CCR5-antagonist was associated with a significant additional increase in CD4$^+$ T cell counts of +30 [95% confidence interval (CI), 19-42] cells/µL in 24 weeks, independent of virologic suppression (14).

In light of these findings studies were performed investigating whether intensification of cART in patients with a suboptimal immunological response despite adequate virologic control would result in an increased rate of CD4$^+$ T cell reconstitution, which might be of clinical benefit for these patients (15–17). At present only one placebo-controlled study has been published (18).

We performed the 'Maraviroc Immune Recovery Study (MIRS), a 48-week, double-blind, placebo-controlled trial to study the effect of MVC intensification of cART on CD4$^+$ T cell recovery in HIV-1 patients.

MATERIAL AND METHODS

Subjects. HIV-infected patients were recruited from 10 HIV treatment centers (4 University Medical Centers and 6 Teaching Hospitals) in the Netherlands. All subjects provided written informed consent. This study was approved by the Ethical Committee of the University Medical Center Utrecht, The Netherlands (ClinicalTrials.gov identifier: NCT00875368; EudraCT number 2008-003635-20).

Inclusion criteria were: age 18 years and older; a CD4$^+$ T cell count <350 cells/µL while at least two years on cART, or a CD4$^+$ T cell count <200 cells/µL while at least one year on cART; viral suppression (plasma HIV-RNA < 50 copies/ml) for at least 6 months prior to inclusion. Exclusion criteria were: previous use of MVC; HIV-2 infection; cART regimen containing a combination of tenofovir and didanosine; active infection treated with antimicrobial therapy; acute hepatitis

B or C infection; chronic hepatitis-B or C infection treated with (peg)interferon and/or ribavirine; immunosuppressive medication; and, radiotherapy or chemotherapy in the previous 2 years.

Study procedures. Included patients were randomized to add MVC or placebo to their existing cART regimen for 48 weeks. The MVC dose was 150-600 mg twice daily, depending on interactions with concurrent medication, as specified in the package insert. In case of virological failure (defined as two consecutive plasma HIV-1 RNA measurements of 50 copies/mL or higher), participants had to discontinue study medication. Subjects were seen for screening at baseline, and at weeks 2, 4, 8, 12, 24, 36 and 48 of their study participation. At all visits, patients were questioned for side effects and other complaints, physical examination (if indicated) was conducted, and EDTA- and heparin-plasma was drawn. Adherence to study drug was assessed at every visit by self-report, and at week 4, 12, 24, 36 and 48 by pill count.

Virologic Analyses. Plasma HIV-RNA was measured in the participating sites using standard commercial assays with a lower limit of detection (LLD) of 20-40 copies/mL.

Immunologic Analyses. Absolute CD4$^+$ T cell counts were assessed by flow cytometry at the local-site laboratory at each visit. Peripheral blood mononuclear cells (PBMCs) were isolated from whole blood via density gradient centrifugation, cryopreserved and stored. Total cell numbers and subsets (i.e. naive (CD27$^+$ CD45RO$^-$), memory (CD45RO$^+$) and effector (CD27$^-$CD45RO$^-$)), and the expression of markers for activation (%CD38$^+$/HLA-DR$^+$), proliferation (%Ki-67$^+$), and apoptosis (% annexin-V$^+$) were determined for CD3$^+$CD4$^+$ and CD3$^+$CD8$^+$ T cells. For CD4$^+$ T cells, we measured the expression of CD31$^+$ within the naive T-cell population as an indication of thymic T cell production. Soluble CD14 in plasma was assessed as a measure of monocyte activation.

T cell analysis was performed on thawed material by flow cytometry as described previously (19). Flow cytometry was performed using a FACS LSR II (BD Biosciences) and FACS Diva software (BD Biosciences). Lymphocytes were gated based on forward and side scatter and subsets were identified based on the expression of a combination of molecules (indicated above). The concentration of soluble CD14 was assessed on heparin plasma using a commercial ELISA kit (Gen-Probe Diaclone SAS).

Sample size calculation. To achieve a statistical power of 90% to detect a 30% difference in increase in CD4$^+$ T cell count, 62 patients in each group were required (alpha=0.05 and beta=0.10). We therefore planned to enrol 130 patients (65 in each group), in order to account for potential losses to follow-up, early treatment discontinuations or slow inclusion.

Statistical analyses. Primary outcome was the change in absolute CD4$^+$ T cell count. Analysis of the primary endpoint was done by an intention-to-treat (ITT) procedure, defined as the analysis of CD4$^+$ T cell counts of every patient from the moment study medication was started until the end of the planned study period. In case of premature discontinuation of the study, CD4$^+$ T cell counts of these patients after discontinuation until week 48 were included for ITT analysis.

Continuous variables were compared using a Student's t-test or a Mann-Whitney test, while for categorical variables a Chi-square or Fisher's exact test was used. Differences were considered statistically significant at p < 0.05.

Changes in biological markers were studied using linear mixed effects models. Trends in the evolution of markers were fitted using one or two slopes depending on the best fit (defined by Akaike criteria, the lower the better). The time taken for the slope to change was determined for all patients by a likelihood profile. To achieve normality and homoscedasticity of measurement error distributions, the fourth-root of markers was used instead of the natural markers when necessary. All statistical analyses were performed with SAS software (version 9.2, SAS institute Inc.).

p_m, p_p, denote p values of change over time (start to week 48) within the maraviroc and placebo arm respectively and the p_a denotes the p of the comparison between the arms.

RESULTS

Study population. Between February 2009 and February 2011 one hundred and four patients were screened for eligibility (figure 1), of these 7 declined to participate, 10 failed to meet the inclusion criteria and 2 were excluded for other reasons. Of the 85 included patients one patient was mistakenly treated with MVC instead of placebo during the entire study, therefore a modified intention-to-treat analysis was performed for the primary endpoint.

During the study, one patient deceased (in the placebo arm), and 5 patients discontinued the study medication because of side effects (n=3), no effect on CD4$^+$ T cell count (n=1) or other reasons (n=1). Seventy-nine patients completed the full study period.
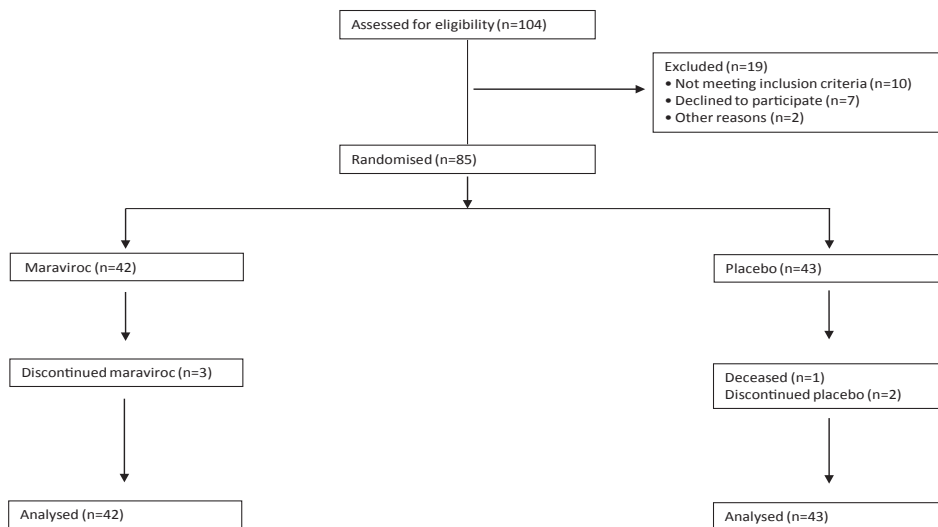

Figure 1. Study flow chart. One hundred and four patients were screened, of whom 85 were included in the study. One patient died (in the placebo arm) whereas 5 patients prematurely discontinued the study, 79 patients finished the complete study protocol. Viral load was measured during the entire study period, none of the study participants experienced virological failure.

Safety. The study medication was well tolerated. During the total study duration 16 serious adverse events were registered in 12 study participants, 7 in the placebo and 9 in the MVC arm (p_a = 0.55). In two cases the study medication could not be ruled out as a causative factor. One participant reported gastro-intestinal side effects and discontinued the study medication during week 17. However, stool cultures later pointed out that she had suffered a gastro-enteritis caused by *Giardia Lamblia* infection, and she recovered completely after treatment. In the other participant, plasma gamma-glutamyl transpeptidase (γGT), which was already elevated at the start of the study (800 U/L, >10 times upper limit of normal (ULN), temporarily increased to 1607 U/L. The latter study participant was known to have a large alcohol intake. Liver biopsy showed signs of steatotic hepatitis. It was therefore decided to continue his study medication, and after he decreased his alcohol intake the γGT returned to pre-study levels. One study participant in the placebo arm deceased during the study. The reason of his death remains unknown, and was classified as natural death by the coroner.

Baseline characteristics. The median age of the patients was 49 years (interquartile range (IQR) 43-57), 5 (6%) were women, and the median overall baseline CD4+ T cell count was 237 (IQR 180-286) cells/µL. The median duration of cART was 5.1 (IQR 9.9-3.2) years prior to study participation; the median overall nadir CD4+ T cell count was 40 (IQR 10-86) cells/µL. Clinical and immunological baseline characteristics did not differ significantly between the study arms, except for baseline effector CD8+ T cell counts, which were significantly higher in the MVC arm (table 1).

Changes in CD4+and CD8+ T cell counts and subsets. Linear mixed effect model analysis showed significant increases of 14.9 CD4+ T cells/µL (95% CI [0.5;29.3]) in the placebo arm versus 23.2 CD4+ T cells/µL (95% CI [7.8;38.5]) in the MVC arm over the treatment period. These increases were not significantly different between both arms (p_a = 0.48; figure 2 and 3). Naive CD4+ T cell counts (figure 3) increased similarly in the placebo and the MVC arm (p_m=0.98): with
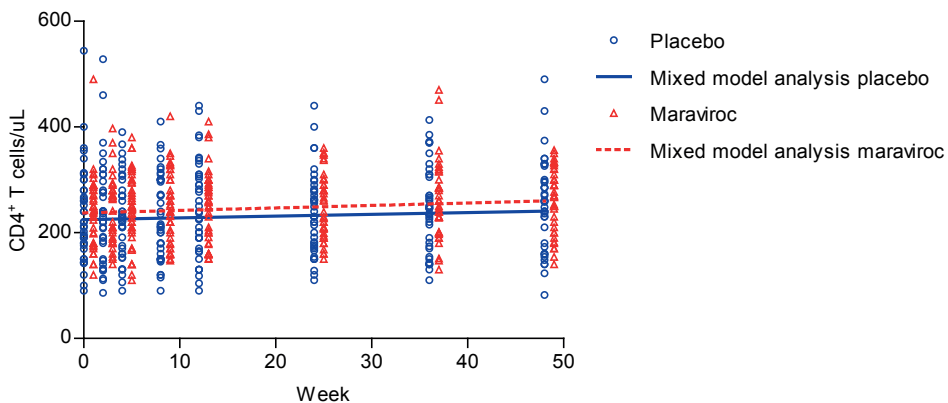

Figure 2. Change in CD4+ T cell counts during 48 weeks of intensification of cART with maraviroc or placebo. The open dots (placebo arm) and triangles (maraviroc arm) represents all CD4+ T cell measurements from the participants at the subsequent study visits.

Table 1. Clinical and immunological baseline characteristics.

	Total	Placebo	Maraviroc	P-value[b]
N	85	43	42	
Age (years)	49 (43-57)	51 (43-60)	48 (41-54)	0.08
Male sex[a] (%)	80 (94)	42 (98)	38 (90)	0.16
Duration cART	5.1 (9.9-3.2)	5.0 (3.2-9.4)	5.8 (3.0-12.4)	0.49
Years with undetectable VL	3.5 (2.2-.7)	4.0 (2.2-7.7)	3.3 (2.1-5.5)	0.59
Previous CDC-C events[a]	48 (56.5)	26 (60.5)	22 (52.4)	0.45
Nadir CD4+ T cell count (cells/µL)	40 (10-86)	30 (10-80)	44 (10-90)	0.71
CD4+ T cells (cells/µL)	237 (180-286)	220 (176-300)	240 (180-286)	0.61
Naive CD4+ T cells (cells/µL)	49 (28-73)	45 (21-74)	50 (33-73)	0.38
Memory CD4+ T cells (cells/µL)	169 (133-211)	172 (119-221)	166 (134-208)	1.00
Effector CD4+ T cells (cells/µL)	3 (2-13)	3 (1-16)	5 (2-12)	0.41
CD8+ T cells (cells/µL)	837 (597-1210)	765 (503-1107)	951 (706-1210)	0.11
Naive CD8+ T cells (cells/µL)	151 (95-213)	141 (62-262)	152 (117-183)	0.55
Memory CD8+ T cells (cells/µL)	424 (221-653)	361 (210-584)	437 (310-653)	0.75
Effector CD8+ T cells (cells/µL)	179 (75-385)	147 (54-259)	285 (97-495)	0.03

Baseline clinical and immunological characteristics of the study participants. All values are given as median (interquartile range), unless indicated otherwise. [a]Number of patients [N (%)].[b]P-value of maraviroc compared to placebo arm.

+10.9 cells/µL (95% CI [3.7;18.0]), in the placebo arm and +12.2 cells/µL (95% CI [4.0;20.5]) in the MVC arm. Neither memory nor effector CD4+ T cell counts changed significantly in either of the two arms during the study period.

For CD8+ T cells (figure 4), a significant decrease of 120.8 cells/µL (95% CI [-203.6;-38.1]) was observed in the placebo arm, whereas total CD8+ T-cell counts remained constant in the MVC arm (p_m = 0.50). Looking at the different CD8+ subsets, we found that neither naive nor effector CD8+ T cell counts changed significantly in either of the arms during the observation period. However, memory CD8+ T cell counts significantly decreased in the placebo arm (-120.2 cells/µL, 95% CI [-170.4;-70.0]), while in the MVC arm this subset did not change (p_m=0.33, figure 4).
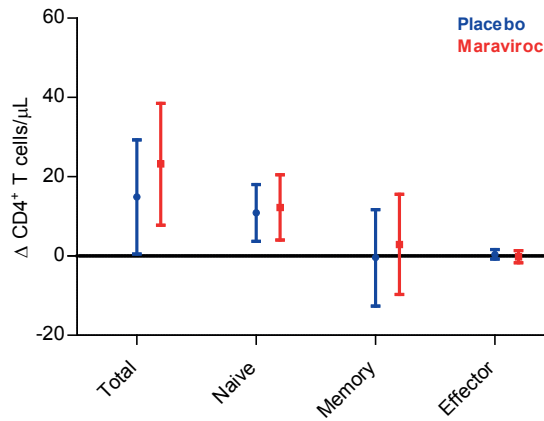
Figure 3. Change in CD4+ T-cell markers. Average change and ± 95% confidence intervals in total, naive, memory and effector CD4+ T cell counts in 48 weeks of maraviroc treatment intensification based on linear mixed effects models.

Figure 4. Change in CD8+ T-cell markers. Average change ± 95% confidence intervals in total, naive, memory and effector CD8+ T cell counts in 48 weeks of maraviroc treatment intensification based on linear mixed effects models. *Significant difference between the study arms.
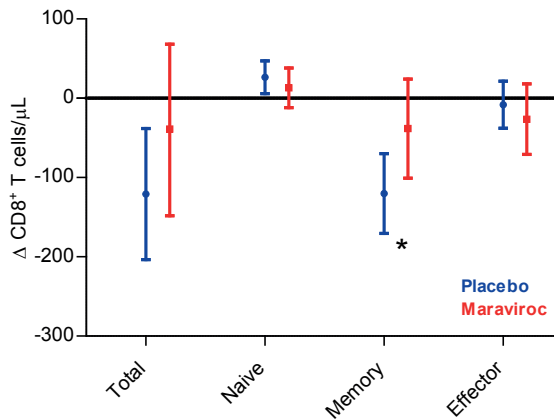
In summary, the only significant effect of MVC intensification on the sizes of the different T-cell populations that was observed when placebo-controlled was a constant number of memory CD8+ T cells during treatment.

Effects on T-cell characteristics. To investigate the effects of maraviroc intensification on cART on T-cell production, proliferation, activation and death, we performed an extended analysis of the effects on T cells in a subset of 67 patients that was not different from the study population in terms of baseline values and endpoints. The percentages of cells expressing

markers for proliferation (Ki67^{+}), activation (CD38^{+} HLA-DR^{+}) and apoptosis (Annexin-V^{+}) were measured for CD4^{+} and CD8^{+} T cells, as well as the percentage of naive CD4 cells expressing CD31^{+} as a thymic production marker and the level of soluble CD14 (sCD14) as a monocyte marker. At baseline, the expression or concentration of none of these markers differed significantly between the treatment arms (table 1).

The percentage of Ki67^{+} CD4^{+} and CD8^{+} T cells did not change significantly in either one of the arms (figure 5). The percentage of CD38^{+} HLA-DR^{+} CD4^{+} T cells decreased significantly by -1.4% (95% CI [-2.7;-0.2]) in the placebo arm, which was comparable (p_a = 0.57) to the -0.3% (95% CI [-1.6;-0.9]) decrease observed in the MVC arm (figure 5). Within the CD8^{+} T cell pool, the percentage of CD38^{+} HLA-DR^{+} cells remained constant in both arms (p_a = 0.59, figure 5).
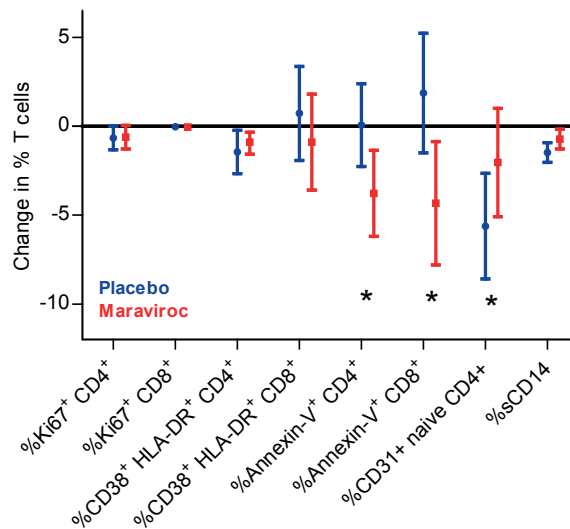
Figure 5. Change in expression of T-cell markers. Average change and ± 95% confidence intervals in expression of markers for T cell proliferation (%Ki67^{+}), activation (%CD38^{+}HLA-DR^{+}), apoptosis (Annexin-V^{+}), and thymus proximity (%CD31^{+} within the naive CD4^{+} T cell population) as well as soluble CD14 (sCD14 in ng/ml) levels in 48 weeks of maraviroc treatment intensification, based on linear mixed effects models. *Significant difference between the study arms.

With respect to T-cell apoptosis, the percentage of Annexin-V^{+} CD4^{+} T cells significantly decreased in the maraviroc arm (-3.8% 95% CI [-6.2;-1.3]), while it remained constant in the placebo arm (p_a = 0.96; figure 5). In the CD8^{+} T-cell pool, the percentage of Annexin-V^{+} T cells significantly decreased by 4.3% (95% CI [-7.8;-0.9]) in the MVC arm while it remained constant in the placebo arm (p_p = 0.27; figure 5).

Since CD31^{+} naive T cells are thought to be more proximal to the thymus than their CD31^{-} counterparts (20), we also followed the change in the percentage of CD31^{+} naive CD4^{+} T cells during treatment intensification. The percentage of CD31^{+} naïve CD4^{+} T cells decreased

significantly in the placebo arm (p_p=0.0002) by 5.6% (95% CI [-8.6;-2.6]) while it remained constant in the MVC arm (p_m = 0.19) (figure 5).

As a marker of bacterial translocation and monocyte activation, we measured plasma levels of sCD14. In both arms, the plasma concentration of sCD14 decreased significantly, however sCD14 levels tended to decrease less in the MVC arm: -1.5% (95% CI [-2.0;-0.9]) in the placebo arm versus -0.7% (95% CI [-1.3;-0.2]) in the MVC arm (p_a=0.06).

In summary, when placebo-controlled, the effects of MVC intensification on the different T-cell characteristics that we measured were that MVC intensification i) prevents the decrease of the percentage of CD31^{+} naive CD4^{+} T cells during treatment, and ii) decreased the percentage of apoptotic Annexin-V^{+} in CD4^{+} and CD8^{+} T cells.

CCR5^{+} and CXCR4^{+} expression. While no significant change in the percentage of CD4^{+} T cells expressing CCR5 was observed in the placebo arm (p_p=0.95, figure 6), a significant increase of 2.3% (95% CI [0.3;4.2]) was observed in the MVC arm. This increase was mainly observed during the first two weeks of treatment (+0.93% per week, 95%CI=[0.24;1.63]; p_m=0.009). Likewise, the percentage of CCR5 expressing CD8^{+} T cells did not change significantly in the placebo arm (p_p=0.93, figure 6), while it did increase significantly in the MVC arm by 4.5% (95% CI [0.9;8.1]). We observed a similar decline in both arms (p_a=0.98) for the percentage CXCR4^{+} CD4^{+} T cells (figure 6): in the placebo arm -10.3% (95% CI [-16.8;-3.9]) and in the MVC arm -10.2% (95% CI [-16.7;-3.7]). The percentage of CXCR4^{+} CD8^{+} T cells significantly decreased in both arms (p_a=0.80): in the placebo arm with -10.0% (95% CI [-17.0;-2.9]) and in the MVC arm with -11.3% (95% CI [-18.3;4.2]).
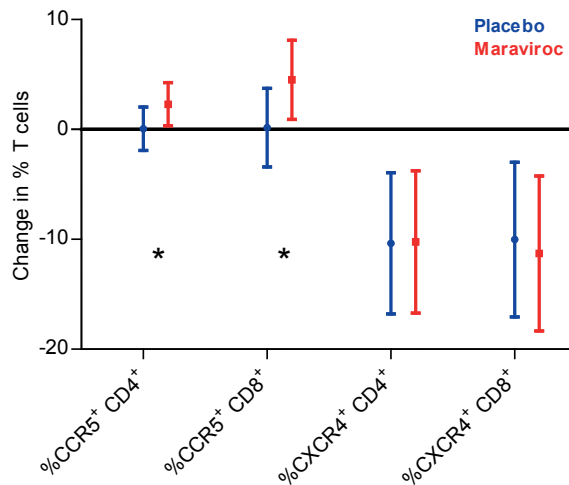

Figure 6. **Change in CXCR4 and CCR5 expression.** Average change and ± 95% Confidence Intervals in the percentage of CCR5^{+} and CXCR4^{+} T-cells in 48 weeks of maraviroc treatment intensification, based on linear mixed effects models. *Significant difference between the study arms.

Table 2.

	Total	Placebo	Maraviroc	P-value[a]
N	67	34	33	
CD38+ CD4+ T cells (%)	3.1 (2.3-4.4)	3.1 (2.2-4.0)	3.1 (2.5-4.5)	0.78
CD38+ CD8+ T cells (%)	5.0 (2.8-8.1)	5.8 (2.8-10.2)	4.9 (3.0-7.1)	0.55
Ki67+ CD4+ T cells (%)	3.3 (2.0-4.3)	3.4 (2.2-4.3)	3.2 (1.9-4.2)	0.52
Ki67+ CD8+ T cells (%)	1.0 (0.7-1.6)	1.0 (0.7-1.9)	1.2 (0.8-1.6)	0.69
CD31+ naive CD4+ T cells (%)	56.3 (41.8-66.6)	57.7 (44.9-64.6)	54.1 (40.7-66.6)	0.81
Annexin-V+ CD4+ T cells (%)	20.4 (14.2-27.4)	19.0 (13.1-26.1)	20.7 (15.4-28.2)	0.39
Annexin-V+ CD8+ T cells (%)	34.5 (20.3-47.6)	33.7 (14.3-46.1)	35.7 (26.7-51.3)	0.27
CCR5+ CD4+ T cells (%)	4.7 (1.8-9.1)	5.0 (2.1-7.2)	4.3 (18-12.0)	0.69
CCR5+ CD8+ T cells (%)	12.9 (7.0-21.9)	14.1 (7.4-21.9)	11.5 (6.0-15.5)	0.41
CXCR4+ CD4+ T cells (%)	42.2 (27.3-62.1)	42.2 (28.0-65.0)	45.7 (24.9-61.6)	0.89
CXCR4+ CD8+ T cells(%)	34.5 (16.1-62.3)	32.6 (17.2-58.4)	36.3 (14.1-63.5)	0.83
sCD14 (µg/L)[b]	5.8 (4.9-10.0)	7.9 (5.7-9.5)	7.2 (5.8-10.3)	0.98

Baseline T-cell characteristics and soluble CD14 (sCD14) levels of the study participants. All values are given as median (interquartile range). [a]P-value of maraviroc compared to placebo arm. [b]N=80 (41 placebo, 39 MVC).

DISCUSSION

In this randomized, placebo-controlled trial, we investigated the effect of MVC intensification on CD4+ T-cell recovery in patients with a suboptimal immunological response despite viral suppression. No significant effect on CD4+ T-cell gain in 48 weeks of MVC intensification of cART was observed. MVC intensification did, however, influence the immune system: it increased CCR5 expression on CD4+ and CD8+ T cells and decreased T-cell apoptosis levels. Moreover it reduced the loss of CD8+ memory T cells and counteract the decrease in CD31+ naive CD4+ T cells. Possible clinical implications of these differences are not yet clear but might be directly related to interference with the physiological rather than the patho-physiologicol role of CCR5.

Besides the fact that the CCR5 receptor is a co-receptor for HIV-1 (21, 22) this receptor has also been shown to directly influence T cells. Binding of chemokines to CCR5 stimulates T-cell migration, co-stimulates T-cell activation (9, 10) and modulates apoptosis (23). Effects of MVC on the immune system and in particular immune activation could thus act via further

suppression of residual low level viral replication, via direct manipulation of T cells or a synergistic combination of both mechanisms. To our knowledge five other MVC intensification studies in immunological non-responders have been published in peer-reviewed journals (15–18, 24, 25), of these only one was placebo-controlled (18). In this 24 week placebo-controlled trial Hunt and colleagues included 45 patients with a median baseline CD4+ T cell count of »200 CD4 cells/μL. In agreement with our results they observed a modest increase in CD4+ T cells in both arms (placebo 17 (95% CI 17-127; p = 0.008), versus 17 (95% CI, 17 -28; p = 0.004) cells/μL in the MVC arm) and an increase of CCR5 expression in the maraviroc arm.

In contrast CD8+ T-cell counts increased by a mean 187 cells/μL over 24 weeks in the MVC arm (95% CI, 10-164 cells/μL; p_m = 0.026), while no change was observed in the placebo arm. CD4+ and CD8+ T-cell activation (CD38+HLA-DR+) was determined in peripheral blood as well as gut mucosa and increased especially in the gut mucosa as compared to no change in the placebo arm. Although the study population included in our trial seemed comparable to the one of Hunt and colleagues in terms of CD4+ T-cell count, age and sex, the average time on cART before start of intensification was 2-3 fold longer and base line levels of CD4+ and CD8+ T-cell activation were 2-3 fold lower in our study population. The differences in cART duration and levels of immune activation might be related since longitudinal data has shown that T cell activation under cART reduces over time, despite the fact that even after long term cART immune activation levels are still increased compared to healthy control. Why immune activation is differently effected by maraviroc intensification in these different baseline situations remains unclear. Hunt et al suggested that blocking of the CCR5 co-receptor would lead to an increased production of chemokines, leading to an increase in T-cell activation via other pathways.

In French (MARIMUNO-ANRS 145 Study (17)) and U.S. (ACTG A5256 (16)) open label single arm studies modest increases in CD4+ T-cell counts were found during MVC intensification. However since we and Hunt found comparable increase in the placebo arm, this increase does not seem to be the result of MVC intensification but is most likely the normal average CD4+ T-cell increase occurring in these types of treated HIV-1 patient. Thus, emphasizing the need for placebo-controlled studies. The increased expression of CCR5 in the CD4+ and CD8+ T-cell populations during treatment with a CCR5 receptor antagonist, is in line with the MVC-induced CCR5 up-regulation on T cells *in vitro* (26) and might be the consequence of disruption of the CCL5-CCR5 interaction. This interaction has been shown to result in internalisation of the CCR5 receptor and to inversely correlate with CCR5 expression on the T-cell surface.

We observed a decrease in the level of expression of the apoptosis marker AnnexinV on CD4+ and CD8+ T cells in the MVC arm, whereas no change was observed in the placebo arm (figure 5). In the single-arm open-label study of Wilkin et al (16) the authors observed an increase in the percentage of anti-apoptotic marker BCL-2 expressing CD4+ and CD8+ T cells and a decrease in the percentage of the apoptosis marker caspase3 expressing CD4+ and CD8+ T cells, consistent with reduced levels of apoptosis in T cells. Modulation of apoptosis by crosslinking of CCR5 has previously been described (23, 27–29). CCR5 ligands were shown to induce cell death in certain CCR5 expressing cell types (28) and CCL5 aggregates, which form at high ligand concentrations, have been described to induce apoptosis in T-cell lines as well as in primary human T-cells in a CCR5-dependent manner (23). These observations are

supported by the notion that susceptibility to activation-induced cell death (30) (AICD) and Fas-mediated apoptosis was selectively increased in CD4$^+$CCR5$^+$T cells compared to CD4$^+$CCR5$^-$ and CD4$^+$CXCR3$^{-/+}$T cells in humans (29). In subjects with acute primary HIV infection, high levels of apoptosis were observed in T-cells with increased expression levels of CCR5 (30) and interaction of CCR5 and 'R5 tropic' env was described to activate the Fas pathway and caspase-8 as well as triggering of FasL production in HIV infected primary human CD4$^+$ T cells (27). If CCR5 indeed is important in the induction of apoptosis, the apoptosis levels might decrease in cells in which CCR5 activation is blocked by MVC. In our study, none of the study participants experienced virological failure and since other studies also did not find an effect of MVC intensification on residual plasma HIV-RNA (17, 18), we think that the observed effects on T cells apoptosis are the consequence of a direct blockade of CCR5 signalling on T cells and not an indirect effect of changes in plasma HIV-RNA by MVC intensification.

Several studies show a worse long term clinical outcome in terms of death, AIDS and non-AIDS defining diseases, in patients with a suboptimal immunological response on cART (1, 2, 4, 7, 31). Since suppression of HIV-1 replication by cART is the only therapy currently available for increasing CD4$^+$ T-cell counts, there is a need for immunomodulating therapies for this particular group of patients. Next to MVC treatment intensification studies, trials with interleukin (IL)-2 and IL-7 have been performed. Subcutaneous recombinant IL-2 treatment in combination with antiretroviral therapy resulted in a substantial and sustained increase in CD4$^+$ T-cell counts, however this treatment did not translate into an effect on clinical endpoints (opportunistic disease or death from any cause) and had substantial toxicity (32). A recently published phase I/IIa trial investigating the effect subcutaneous recombinant IL-7 therapy on T cell recovery in antiretroviral treated patients with a suboptimal immunological response showed promising results in terms of CD4$^+$ T-cell count increase and toxicity, but larger trials with clinical endpoints are needed to establish its clinical utility(33). In addition, it will be interesting to investigate whether IL-7 therapy will affect levels of T cell activation, apoptosis and plasma HIV-RNA in patients with as suboptimal immunological response on cART.

In conclusion, the data of this study do not support MVC intensification of cART in patients with a suboptimal immunological response in order to restore CD4$^+$ T-cell counts. However, since we did observe an increase in CCR5$^+$ T cells and a decrease in T-cell apoptosis levels in the MVC arm, further (placebo-controlled) studies are needed to investigate whether these findings have any clinical consequences.

ACKNOWLEDGEMENTS

- *Maasstadziekenhuis, Rotterdam:* Dr. J. Hollander, mrs. E. Smit.
- *Onze Lieve Vrouwe Gasthuis, Amsterdam:* Prof. Dr. K. Brinkman, mrs. L. Schrijnders-Gudde.
- *Rijnstate Hospital, Arnhem:* Dr. C. Richter, mrs. G. ter Beest, mrs. P. van Bentem, drs. N. Langebeek.
- *Sint Elisabeth Ziekenhuis, Tilburg:* Dr. M. van Kasteren, mrs. M. Kuipers.
- *University Medical Center Utrecht, Utrecht:* Prof. Dr. A.I.M. Hoepelman, drs. S.F.L. van Lelyveld, mrs. I. de Kroon, Dr. J. Borghans, Dr. J. Drylewicz, mrs. S. Otto, Dr. K. Tesselaar, drs. E. Veel, drs. J. Symons, Dr. M. Nijhuis, Dr. A.M.J. Wensing.

FUNDING/FINANCIAL SUPPORT

REFERENCE LIST

1. Grabar S, Pradier C, Le Corfec E, Lancar R, Allavena C, et al. **2000.** Factors associated with clinical and virological failure in patients receiving a triple therapy including a protease inhibitor. *AIDS*. 14(2):141–49

2. Dronda F, Moreno S, Moreno A, Casado JL, Pérez-Elías MJ, Antela A. **2002.** Long-term outcomes among antiretroviral-naive human immunodeficiency virus-infected patients with small increases in cd4+ cell counts after successful virologic suppression. *Clin. Infect. Dis.* 35(8):1005–9

3. Florence E, Lundgren J, Dreezen C, Fisher M, Kirk O, et al. **2003.** Factors associated with a reduced cd4 lymphocyte count response to haart despite full viral suppression in the eurosida study. *HIV Med.* 4(3):255–62

4. Moore DM, Harris R, Lima V, Hogg B, May M, et al. **2009.** Effect of baseline cd4 cell counts on the clinical significance of short-term immunologic response to antiretroviral therapy in individuals with virologic suppression. *J. Acquir. Immune Defic. Syndr.* 52(3):357–63

5. Tan R, Westfall AO, Willig JH, Mugavero MJ, Saag MS, et al. **2008.** Clinical outcome of hiv-infected antiretroviral-naive patients with discordant immunologic and virologic responses to highly active antiretroviral therapy. *J. Acquir. Immune Defic. Syndr.* 47(5):553–58

6. Kelley CF, Kitchen CMR, Hunt PW, Rodriguez B, Hecht FM, et al. **2009.** Incomplete peripheral cd4+ cell count restoration in hiv-infected patients receiving long-term antiretroviral treatment. *Clin. Infect. Dis.* 48(6):787–94

7. Baker J V, Peng G, Rapkin J, Krason D, Reilly C, et al. **2008.** Poor initial cd4+ recovery with antiretroviral therapy prolongs immune depletion and increases risk for aids and non-aids diseases. *J. Acquir. Immune Defic. Syndr.* 48(5):541–46

8. Gulick RM, Lalezari J, Goodrich J, Clumeck N, DeJesus E, et al. **2008.** Maraviroc for previously treated patients with r5 hiv-1 infection. *N. Engl. J. Med.* 359(14):1429–41

9. Camargo JF, Quinones MP, Mummidi S, Srinivas S, Gaitan AA, et al. **2009.** Ccr5 expression levels influence nfat translocation, il-2 production, and subsequent signaling events during t lymphocyte activation. *J. Immunol.* 182(1):171–82

10. Portales P, Psomas KC, Tuaillon E, Mura T, Vendrell J-P, et al. **2012.** The intensity of immune activation is linked to the level of ccr5 expression in human immunodeficiency virus type 1-infected persons. *Immunology*. 137(1):89–97

11. Reshef R, Luger SM, Hexner EO, Loren AW, Frey N V, et al. **2012.** Blockade of lymphocyte chemotaxis in visceral graft-versus-host disease. *N. Engl. J. Med.* 367(2):135–45

12. Ahuja SK, Kulkarni H, Catano G, Agan BK, Camargo JF, et al. **2008.** Ccl3l1-ccr5 genotype influences durability of immune recovery during antiretroviral therapy of hiv-1-infected individuals. *Nat. Med.* 14(4):413–20

13. Cooper DA, Heera J, Goodrich J, Tawadrous M, Saag M, et al. **2010.** Maraviroc versus efavirenz, both in combination with zidovudine-lamivudine, for the treatment of antiretroviral-

naive subjects with ccr5-tropic hiv-1 infection. *J. Infect. Dis.* 201(6):803–13

14. Wilkin TJ, Ribaudo HR, Tenorio AR, Gulick RM. **2010.** The relationship of ccr5 antagonists to cd4+ t-cell gain: a meta-regression of recent clinical trials in treatment-experienced hiv-infected patients. *HIV Clin. Trials.* 11(6):351–58

15. Stepanyuk O, Chiang TS, Dever LL, Paez SL, Smith SM, et al. **2009.** Impact of adding marviroc to antireroviral regimens in patients with full viral suppression but impaired cd4 recovery. *AIDS*, pp. 1911–22

16. Wilkin TJ, Lalama CM, McKinnon J, Gandhi RT, Lin N, et al. **2012.** A pilot trial of adding maraviroc to suppressive antiretroviral therapy for suboptimal cd4+ t-cell recovery despite sustained virologic suppression: actg a5256. *J. Infect. Dis.* 206:

17. Cuzin L, Trabelsi S, Delobel P, Barbuat C, Reynes J, et al. **2012.** Maraviroc intensification of stable antiviral therapy in hiv-1-infected patients with poor immune restoration: marimuno-anrs 145 study. *J. Acquir. Immune Defic. Syndr.* 61(5):557–64

18. Hunt PW, Shulman NS, Hayes TL, Dahl V, Somsouk M, et al. **2013.** The immunologic effects of maraviroc intensification in treated hiv-infected individuals with incomplete cd41 t-cell recovery : a randomized trial, pp. 4635–46

19. Bloemers BLP, Bont L, de Weger R a, Otto S a, Borghans J a, Tesselaar K. **2011.** Decreased thymic output accounts for decreased naive t cell numbers in children with down syndrome. *J. Immunol.* 186(7):4500–4507

20. Kohler S, Thiel A. **2009.** Life after the thymus: cd31+ and cd31- human naive cd4+ t-cell subsets. *Blood.* 113(4):769–74

21. Berson JF, Long D, Doranz BJ, Rucker J, Jirik FR, Doms RW. **1996.** A seven-transmembrane domain receptor involved in fusion and entry of t-cell-tropic human immunodeficiency virus type 1 strains. *J. Virol.* 70(9):6288–95

22. Deng H, Liu R, Ellmeier W, Choe S, Unutmaz D, et al. **1996.** Identification of a major co-receptor for primary isolates of hiv-1. *Nature.* 381(6584):661–66

23. Murooka TT, Wong MM, Rahbar R, Majchrzak-Kita B, Proudfoot AEI, Fish EN. **2006.** Ccl5-ccr5-mediated apoptosis in T cells: requirement for glycosaminoglycan binding and ccl5 aggregation. *J. Biol. Chem.* 281(35):25184–94

24. Gutiérrez C, Díaz L, Vallejo A, Hernández-Novoa B, Abad M, et al. **2011.** Intensification of antiretroviral therapy with a ccr5 antagonist in patients with chronic hiv-1 infection: effect on T cells latently infected. *PLoS One.* 6(12):e27864

25. Mavigner M, Delobel P, Cazabat M, Dubois M, L'faqihi-Olive F-E, et al. **2009.** Hiv-1 residual viremia correlates with persistent t-cell activation in poor immunological responders to combination antiretroviral therapy. *PLoS One.* 4(10):e7658

26. Arberas H, Guardo a C, Bargalló ME, Maleno MJ, Calvo M, et al. **2012.** In vitro effects of the ccr5 inhibitor maraviroc on human t cell function. *J. Antimicrob. Chemother.*, pp. 1–10

27. Algeciras-Schimnich A, Vlahakis SR, Villasis-Keever A, Gomez T, Heppelmann CJ, et al. **2002.** Ccr5 mediates fas- and caspase-8 dependent apoptosis of both uninfected and hiv infected primary human cd4 T cells. *AIDS.* 16(11):1467–78

28. Cartier L, Dubois-Dauphin M, Hartley O, Irminger-Finger I, Krause K-H. **2003.** Chemokine-induced cell death in ccr5-expressing neuroblastoma cells. *J. Neuroimmunol.* 145(1-2):27–39

29. Julià E, Edo MC, Horga A, Montalban X, Comabella M. **2009.** Differential susceptibility to apoptosis of cd4+T cells expressing ccr5 and cxcr3 in patients with ms. *Clin. Immunol.* 133(3):364–74

30. Zaunders JJ, Parseval M De, Kitada S, Reed JC, Rought S, et al. **2003.** Polyclonal proliferation and apoptosis of ccr5 + t lymphocytes during primary human immunodeficiency virus type 1 infection : regulation by interleukin (il)– 2, il-15, and bcl-2. 187(II):1735–48

31. Van Lelyveld SFL, Wensing AMJ, Hoepelman AIM. **2012.** The motivate trials: maraviroc therapy in antiretroviral treatment-experienced hiv-1-infected patients. *Expert Rev. Anti. Infect. Ther.* 10(11):1241–47

32. Abrams D, Lévy Y, Losso MH, Babiker A, Collins G, et al. **2009.** Interleukin-2 therapy in patients with hiv infection. *N. Engl. J. Med.* 361(16):1548–59

33. Lévy Y, Sereti I, Tambussi G, Routy JP, Lelièvre JD, et al. **2012.** Effects of recombinant human interleukin 7 on t-cell recovery and thymic output in hiv-infected patients receiving antiretroviral therapy: results of a phase i/iia randomized, placebo-controlled, multicenter study. *Clin. Infect. Dis.* 55(2):291–300

CHAPTER 5

PERSISTENT DISTURBANCES OF THE
MEMORY CD8^{+} T-CELL COMPARTMENT
AFTER SUCCESSFUL LONG-TERM cART

Ellen Veel[1], Tania Mudrikova[2], Rogier van Gent[1], Sigrid A. Otto[1],
Annemarie M.J. Wensing[3], Andy I.M. Hoepelman[2], José A.M.
Borghans[1], Kiki Tesselaar[1]

[1]Laboratory for Translational Immunology, University Medical Center Utrecht
[2]Department of Internal Medicine and Infectious Diseases,
University Medical Center Utrecht
[3]Department of Virology, University Medical Center Utrecht

ABSTRACT

HIV infection leads to a progressive decline in naive and memory CD4^{+} as well as naive CD8^{+} T-cell numbers. In contrast, the CD8^{+} T-cell memory and effector compartments expand during untreated HIV infection. We have previously shown that, during long-term successful cART, the CD4^{+} T-cell compartment reconstitutes to a normal size and composition. Here, we investigated whether the CD8^{+} T-cell compartment is similarly normalizing during long-term cART in patients with undetectable HIV RNA load.

In contrast to the CD4^{+} T-cell compartment, the CD8^{+} T-cell compartment did not normalize, when compared to healthy controls. Naive CD8^{+} T-cell numbers increased to healthy levels but the numbers of memory and effector CD8^{+} T cells remained elevated. Longitudinal analysis showed that, despite these elevated CD8^{+} T-cell numbers, cART resulted in a loss of memory CD8^{+} T cells, mainly during the first year of cART. The failure of memory CD8^{+} T-cell numbers to decline during later stages of cART was not related to residual HIV replication, nor to decreased levels of apoptosis of CD8^{+} T cells. In conclusion, the CD8^{+} T-cell compartment was rejuvenated by long-term cART, but elevated numbers of memory and effector CD8^{+} T cells were still observed

5

CD8^{+} T-CELL EXPANSION AFTER LONG-TERM cART

INTRODUCTION

Infection with human immunodeficiency virus (HIV) leads to substantial changes in T-cell characteristics and competence (1). Next to infection of T cells by HIV, the chronic activation state of the immune system and impairment of thymic production play an important role in the induction of these changes (2;3). There is a relative abundance of highly differentiated T cells, characterized by a reduced capacity to proliferate, short telomere length (4) and changes in cytokine secretion capacity (1). A progressive decline in CD4$^+$ as well as naive CD8$^+$ T-cell numbers and an increase in memory and effector CD8$^+$ T-cell numbers occurs.

Interestingly, similar changes are also observed during healthy aging (4;6;7). Immunosenescence during aging is thought to be the result of multiple rounds of activation, which an individual experiences, throughout a lifetime and is most apparent in individuals infected with persistent viruses, especially cytomegalovirus (CMV). During HIV infection, this aging process is thought to be accelerated due to the hyper immune activation that is associated with the persistent nature of this infection (2).

Effects of combination antiretroviral therapy (cART) on the dynamics of CD4$^+$ T cells have been studied extensively. Accelerated aging of the CD4$^+$ T-cell compartment is reversible in the majority of cases when HIV viral replication is low (8). We have previously shown that treatment with cART enables the CD4$^+$ T-cell compartment to fully reconstitute (8). CD4$^+$ T-cell numbers increase gradually during the first years of cART to eventually reach a plateau, which is comparable with healthy, age matched, individuals. The time that is needed for the CD4$^+$ T-cell compartment to fully reconstitute depends on the CD4$^+$ T-cell number at the start of cART (8). The CD4$^+$ T-cell compartment thus seems able to recover very well from HIV inflicted damage (8).

The behavior of the CD8$^+$ T-cell compartment during cART, especially long-term, is less well understood. In the first month of cART, absolute CD8$^+$ T-cell numbers in blood, both naive and memory, have been shown to increase significantly (9;10). This sudden increase is thought to be due to redistribution of CD8$^+$ T cells, that were located in the tissues, to the blood. Based on T-cell Receptor Excision Circle (TREC) and T-cell receptor (TCR) repertoire analysis, a role of thymic production during this early period after the start of cART has been suggested (11;12). Hence, there seems to be a trend towards normalization of the CD8$^+$ T-cell pool during cART, but extensive longitudinal analyses after long-term cART have so far not been performed.

In the present study, we determined numbers and characteristics of naive, memory and effector CD8$^+$ T cells in long-term cART treated HIV-1 infected individuals with undetectable virus load and good CD4$^+$ T-cell recovery, to address to what extent and how the CD8$^+$ T-cell compartment restores. We conclude that after long-term cART the naive CD8$^+$ T-cell compartment normalizes but memory and effector CD8$^+$ T-cell numbers remained elevated.

MATERIALS AND METHODS

Study population. Thirty HIV-1 infected individuals of 18 years of age or older, who were under follow up in the Department of Infectious Diseases of the University Medical Center Utrecht (UMCU Utrecht, The Netherlands) were included for cross-sectional analyses. At the moment

of the inclusion, they were treated with cART for at least five years, during which they had undetectable HIV RNA plasma levels (<50 copies per ml) with no more than two isolated viral blips of HIV RNA (number of copies between 50 and 400 per ml) which were followed by undetectable levels during the subsequent measurement (within three months). Participants had to have CD4$^+$ T-cell numbers above 500 per microliter blood and express HLA-A2 and/or HLA-B8 alleles.

To discriminate between short term redistribution and long-term restoration, thirteen HIV-1 infected individuals from the UMCU were included in a longitudinal analysis. They were 18 years or older and treated with cART for at least seven years, with undetectable HIV RNA plasma levels (<50 copies per ml), and CD4$^+$ T-cell numbers above 400 per ul blood. In this group a maximum of three viral blips above 50 copies/ml was allowed. Thirty healthy individuals older than 18 years served as control group This study was approved by the Medical Ethical Committee of the UMC Utrecht and written informed consent was obtained from all study participants in agreement with the Declaration of Helsinki (version: 59th WMA General Assembly, Seoul, October 2008).

Flow cytometry. PBMC were obtained by Ficoll-Paque density gradient centrifugation from heparinized blood and were cryopreserved until further use. Absolute CD4$^+$ and CD8$^+$ T-cell counts were determined by dual-platform flow cytometry. Naive (CD27$^+$CD45RO$^-$), central memory (CD27$^+$CD45RO$^+$), effector memory (CD27$^-$CD45RO$^+$) and effector (CD27$^-$CD45RO$^-$) CD8$^+$ T cells were assessed by flow cytometry. All experiments were performed on cryopreserved cells that were thawed shortly before the experiment. To identify the different CD8$^+$ T-cell subsets, cells were incubated with mAb to CD3 FITC (Biolegend) or CD3 eFluor450 (eBioscience), CD8 Amcyan (BD biosciences) or CD8 V500 (BD Biosciences), CD27 APC or APC-AF750 (eBioscience) and CD45RO-PE-Cy7 (BD biosciences). Within the subsets, characteristics of the cells were determined following standard staining protocols using CD28 FITC (BD Biosciences) and CD57 APC (Biolegend) for the level of senescence, Bcl-2 PE (BD biosciences) for apoptosis sensitivity, AnnexinV PE and 7AAD (BD biosciences) for the level of apoptosis, Ki67 FITC (Dako) as a proliferation marker, CD38 PE (Invitrogen) and HLA-DR FITC (eBioscience) as activation markers and tetramers to identify antigen-specific cells. For detection of HIV-specific CD8$^+$ T cells the following tetramers were used: FLKEKGGL, EiYKRWII and SLYNTVATL, which were prepared as previously described (13). All experiments were analyzed on a FACS Canto II of FACS LSR II (BD Biosciences) with FACS Diva software.

TREC analysis. To measure the average TREC content of CD8$^+$ T cells, the indicated subsets were purified from thawed PBMC by magnetic bead separation using the MiniMACS multisort kit according to the manufacturer's instructions (Miltenyi Biotec). DNA was isolated using the Nucleospin Blood QuickPure kit according to the manufacturer's instructions (Machery-Nagel). Signal joint TREC numbers were quantified using real-time PCR as described previously (8).

Analysis of CMV serostatus. Analysis of CMV serostatus was performed with the Cytomegalovirus IgG ELISA kit (IBL international) according to the manufacturer's instructions, using heparinized plasma.

Statistical analysis. In our cross-sectional analysis, Wilcoxon rank sum tests were used to compare the results obtained in the group of HIV infected individuals during long-term cART to those of healthy individuals. Wilcoxon matched-pairs signed rank tests were used for the comparisons in the longitudinal data. Differences with *p*-value <0.05 were regarded statistically significant.

RESULTS

Patient characteristics. To investigate the effect of long-term successful cART we studied 30 HIV-1 infected individuals that had undetectable viral load for at least 5 years and a CD4$^+$ T-cell count of >500 cells/μl at time of the inclusion (mean CD4$^+$ T-cell count 668 /μl blood). Four out of 30 individuals experienced occasional appearances of HIV RNA in plasma in the five years preceding the study. The mean time on cART was 14 years (range 8-12). Values were compared to values in healthy, aged matched, controls. The mean age of the healthy donors was years (range 28 – 62), and of the HIV infected individuals 52 years (range 36 – 71).

Absolute CD8$^+$ T-cell numbers remain elevated after long-term cART. To determine whether CD8$^+$ T-cell numbers and the subset distribution within the CD8$^+$ T-cell compartment had normalized after long-term cART, we compared the CD8$^+$ T-cell numbers of HIV infected individuals to CD8$^+$ T-cell numbers of healthy individuals (fig. 1A). In contrast to what was previously observed for CD4$^+$ T-cell numbers (8), total CD8$^+$ T-cell numbers had not normalized after long-term cART, but instead remained significantly elevated (635 vs 342 CD4$^+$ T cells per μl blood in HIV-infected and healthy individuals, respectively, (fig. 1A)). Based on the expression of the markers CD27 and CD45RO we next distinguished between naive (CD27$^+$CD45RO$^-$), memory (CD27$^+$CD45RO$^+$), effector memory (CD27$^-$CD45RO$^+$) and effector (CD27$^-$CD45RO$^-$) CD8$^+$ T cells. Naive CD8$^+$ T-cell numbers of HIV infected individuals after long-term cART (mean number of cells 179/μl blood) had normalized to levels comparable to healthy individuals
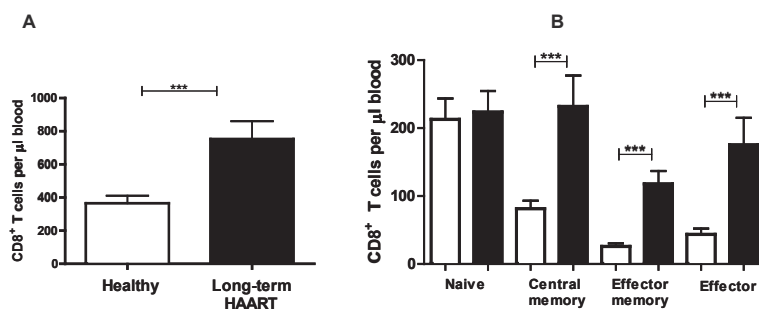
Figure 1. CD8$^+$ T-cell numbers during long-term cART. (*A*) Total CD8$^+$ T-cell numbers and (B) naive (CD27$^+$CD45RO$^-$), central memory (CD27$^+$CD45RO$^+$), effector memory (CD27$^-$CD45RO$^+$) and effector CD8$^+$ T cells (CD27$^-$CD45RO$^+$) CD8$^+$ T-cell numbers of 30 HIV-infected individuals after long-term HAART were compared to age-matched healthy controls. Data are shown as mean + SEM and considered significantly different *p* <0.05.

(mean 163 cells/μl blood) (fig. 1B). In contrast, memory-, as well as effector CD8^{+} T-cell numbers remained more than two-fold increased, compared to healthy individuals (fig. 1B). Complete normalization of the CD8^{+} T-cell compartment was thus not achieved after >5 years of cART.

Expanded memory CD8^{+} T-cell pools did contract during cART. Since CD8^{+} central memory-, effector memory- and effector T-cell numbers had not normalized after long-term successful cART we studied whether these pools had been stably maintained or whether in fact, during the course of cART, they had (slowly) decreased. To this end we measured absolute CD8^{+} T-cell numbers longitudinally in thirteen patients. These patients had CD4^{+} T-cell numbers above 400 per μl blood. Two participants had one, one participant had two and one participant had three occasional appearances of plasma HIV RNA above 50 copies/ml. Total CD8^{+} T-cell numbers were high before cART and stayed stable during long-term cART. Despite these constant total CD8^{+} T-cell numbers, there were substantial changes in the subset composition of the CD8^{+} T-cell pool. Naive CD8^{+} T-cell numbers, which were low at the start of cART, increased over time to levels which were not significantly different from age-matched control values (fig. 2). In contrast, central memory and effector memory CD8^{+} T-cell numbers decreased during long-term cART, but remained significantly elevated compared to age-matched control values. Effector CD8^{+} T-cell numbers, which were elevated at the start of cART, even increased during long-term cART.

We next investigated whether the observed decrease in memory CD8^{+} T-cell numbers during long-term cART occurred mainly during the first period of cART, or whether it was more gradual. We analyzed CD8^{+} T-cell numbers at start, 1 year after start of cART and after long-term
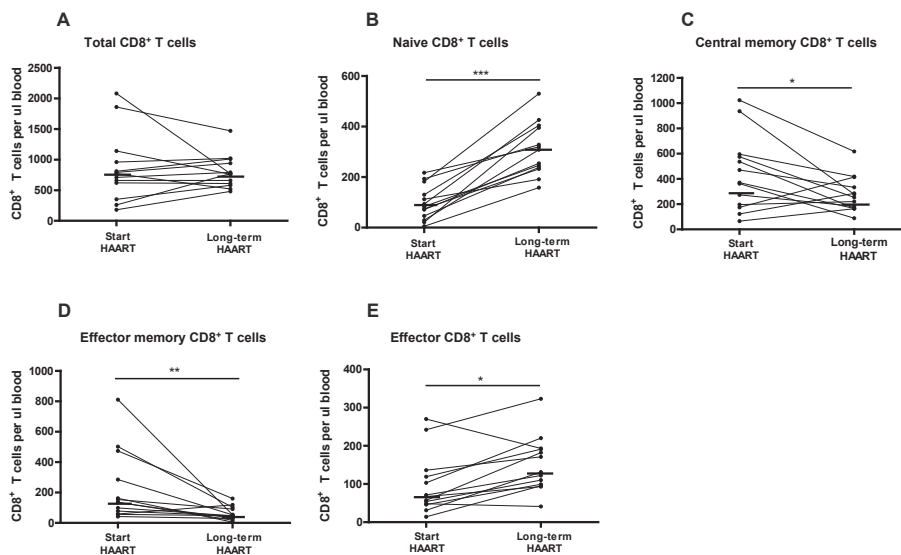

Figure 2. Longitudinal follow-up of absolute CD8^{+} T-cell numbers. Total (A), naive (B), central memory (C), effector memory (D) and effector (E) CD8^{+} T cells were analyzed longitudinally in 13 HIV infected individuals at the start of cART and after long-term cART. Horizontal lines depict the median of the subsets. Data were considered significantly different at p <0.05
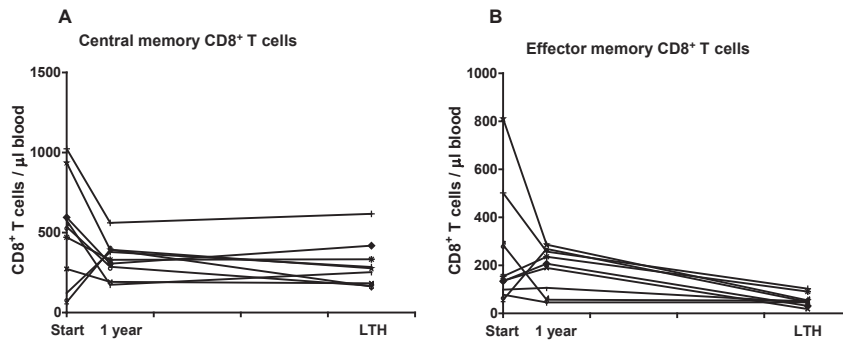
Figure 3. Longitudinal follow-up of absolute CD8+ T-cell numbers. Central memory (A) and effector memory (B) CD8+ T-cell numbers were analyzed longitudinally, including a 1 year time point in 9 HIV infected individuals after long-term cART.

cART in nine HIV-infected participants (fig. 3). The largest decrease in memory CD8+ T-cell numbers was observed during the first year of cART, both for central- and effector memory CD8+ T cells, particularly for individuals who started cART with very high memory CD8+ T-cell numbers (fig. 3A+B). After the first year, changes in memory CD8+ T-cell numbers were more subtle. Apparently, reduction of sizeable HIV replication has a fast and large impact on memory CD8+ T-cell numbers.

CD8+ T cells of HIV infected individuals have normal activation and apoptosis levels after long-term cART. Residual activation and an increased fraction of senescent T cells upon cART have been reported for the CD4+ T-cell compartment. If these features also occur for CD8+ T cells, this could explain why memory CD8+ T-cell numbers, after the first years of cART decrease very slowly. To investigate whether memory CD8+ T cells have increased levels of activation despite years of cART we analyzed the expression of activation markers HLA-DR and CD38. HLA-DR and CD38 expression on CD8+ T cells was not increased in HIV infected individuals after long-term cART (fig. 4A), nor was it increased when naive, memory or effector CD8+ T cells were analyzed separately (data not shown). We next analyzed the expression of Ki67, a proliferation marker which is frequently up-regulated upon T-cell activation. We did not find elevated levels of Ki67 expression in total CD8+ T cells (fig. 4B) or any of the individual subsets (data not shown) compared to healthy individuals. Since we found no indications that CD8+ T-cell numbers during long-term cART were maintained through activation, we next studied whether CD8+ T cells had become senescent and more resistant to apoptosis. We studied senescence with markers for terminal differentiation (CD28) and senescence (CD57). Naive and central memory CD8+ T cells in HIV infected individuals after long-term cART had no increased fraction of senescent cells (fig. 4C). Effector memory and effector CD8+ T cells had a more senescent phenotype, expressing less CD28 and more CD57 (fig. 4C). This, however, did not lead to apoptosis resistance (fig. 4D,E): we tested the level of AnnexinV binding and the expression of the anti-apoptotic molecule BCl-2, but these markers did not differ between HIV infected individuals after cART and healthy individuals in any of the CD8+ T-cell subsets (fig. 4D and data not shown).
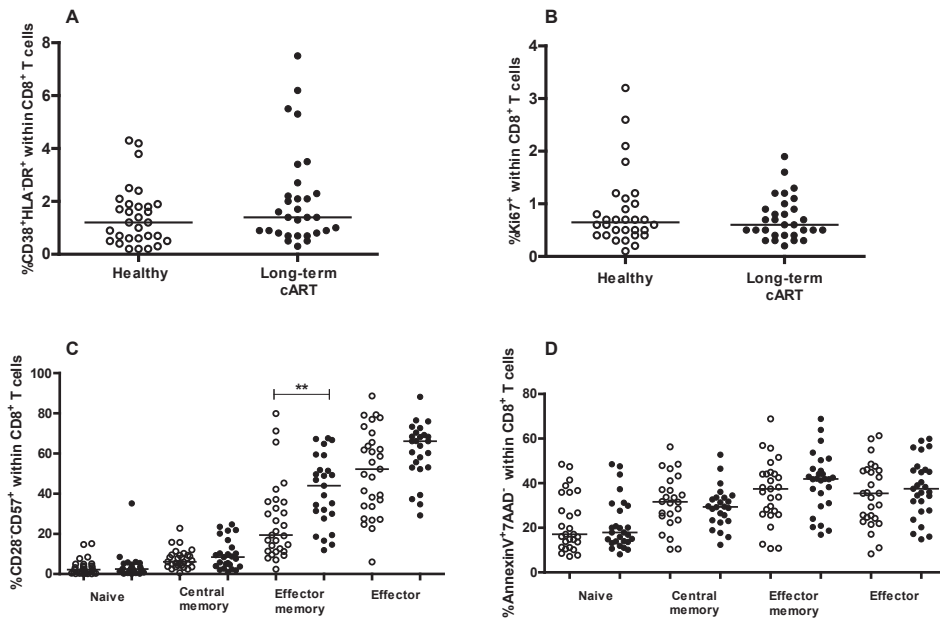
Figure 4. CD8⁺ T-cell characteristics during long-term cART. (A) The percentage of activated, (measured with CD38 and HLA-DR), (B) proliferating (measured with Ki67), (C) terminally differentiated, (CD28⁺CD57⁻) and (D) apoptotic (AnnexinV⁺7AAD⁻) cells in HIV infected individuals after long-term cART were compared to age-matched healthy controls. Horizontal lines depict the median value.

Therefore, increased levels of memory and effector CD8⁺ T cells in HIV infected individuals after long-term cART cannot be explained by maintenance through activation or by senescence and resistance to apoptosis.

Low level HIV replication does not maintain high CD8⁺ T-cell numbers. All individuals on long-term cART that were included in this study had HIV RNA plasma loads below 50 copies/ml. We could, however, not exclude that replication of HIV below 50 copies/ml maintains the CD8⁺ T-cell pool after long-term cART. HIV replication is strongly correlated with an increase in and maintenance of (at least) HIV specific CD8⁺ T cells (13-16). We therefore tested whether viral replication below the commonly used detection limit of 50 HIV RNA copies/ml plasma correlated with the number of CD8⁺ T cells after long-term cART. We found residual replication of HIV in a considerable number of HIV infected individuals, (fig. 5A). However, individuals that experienced low level HIV replication did not have significantly higher total CD8⁺ T-cell numbers than individuals that did not. Also, when we analyzing the memory subsets, central memory CD8⁺ T-cell numbers did not correlate with the number of HIV RNA copies. Individuals who did not experience low level HIV replication tended to have lower effector memory CD8⁺ T-cell numbers than individuals who did, although this was not statistically significant (fig. 5A).

Additionally, we studied whether there were still HIV specific CD8⁺ T cells present and whether their relative contribution correlated with the absolute central memory and
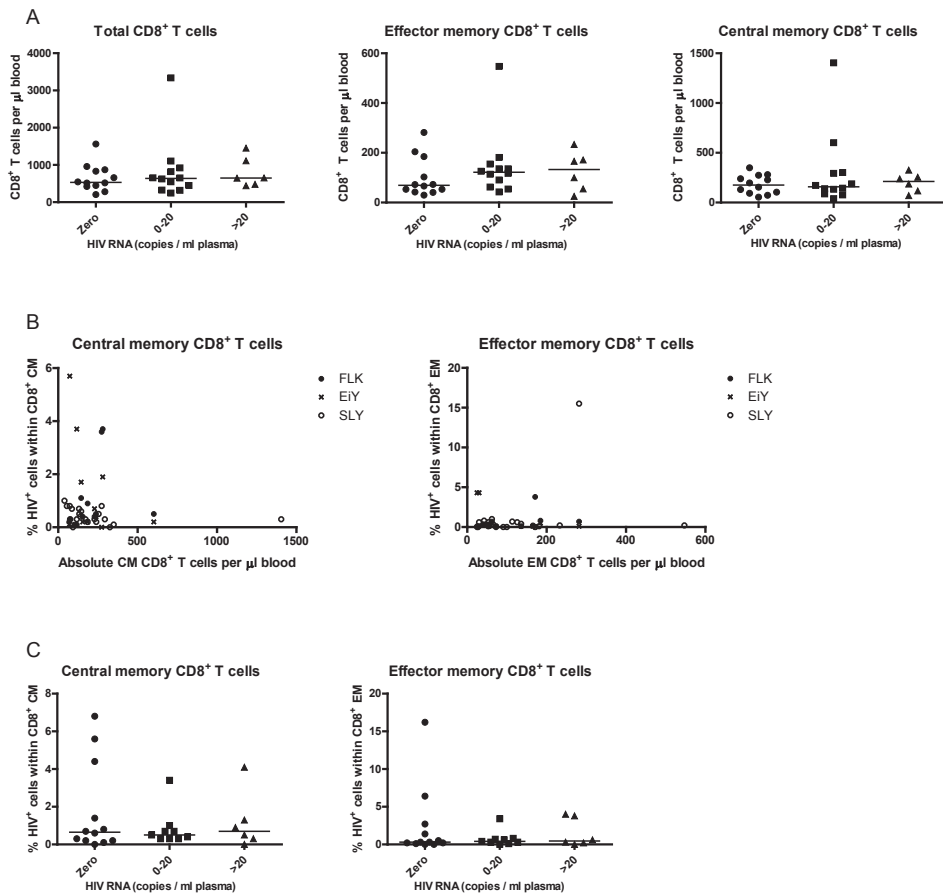
Figure 5. Low level HIV viremia. A. The number of CD8^{+} T cells in HIV infected individuals after long-term cART that were grouped according to the number of RNA copies per ml plasma. B. Percentage of CD8^{+} T cells specific for HIV tetramers FLK, EIY or SLY depicted against total number of central memory CD8^{+} T cells per μl blood. C. The number of HIV specific central memory and effector memory CD8^{+} T cells in HIV infected individuals, that were grouped according to the number of RNA copies per ml plasma, after long-term cART. Horizontal lines depict the median value.

effector memory CD8^{+} T-cell numbers (fig. 5B). We used HLA-A2 and HLA-B8 tetramers of the immunodominant HIV-1 peptides FLKEKGGL, EIYKRWII and SLYNTVATL, respectively, and measured the fractions of tetramer binding cells in HLA-A2 and/or HLA-B8 expressing individuals. We did not find a correlation between the presence of HIV specific CD8^{+} T cells and the absolute CD8^{+} T-cell number for central memory cells or effector memory cells, nor had individuals that experienced residual HIV replication have a larger fraction of HIV specific central memory or effector memory CD8^{+} T cells (fig. 5C). Combined, these results do not implicate residual replication of HIV as the primary driving force behind the expansions in the memory and effector CD8^{+} T-cell subsets.
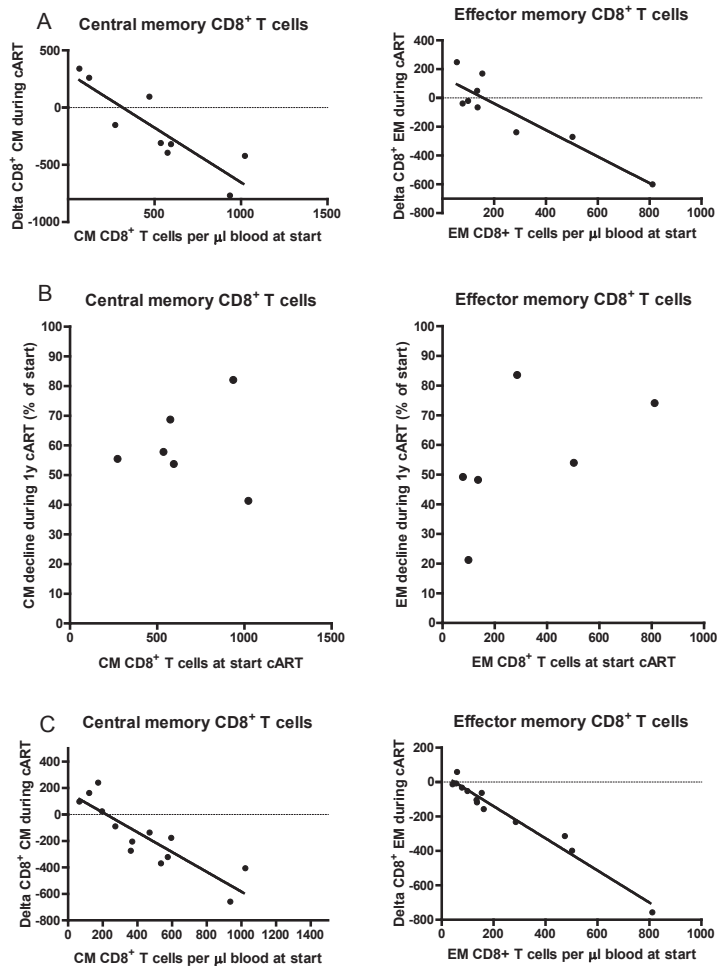
Figure 6. Correlation between absolute and relative change in cell numbers and cell numbers at start of cART. A. Absolute changes of central (r^2 = 0.6565) and effector memory (r^2 = 0.7741) CD8+ T cells after 1 year of cART were correlated to the numbers of these cells at start of treatment. B. Relative changes of central and effector memory CD8+ T cells after 1 year of cART were correlated to the numbers of these cells at start of treatment. C. Absolute changes of central (r^2 = 0.7685) and effector memory (r^2 = 0.9643) CD8+ T cells after long-term cART were correlated to the numbers of these cells at start of treatment. Linear regression lines are shown if $p<0.05$.

CMV has been described as the viral determinant of CD8+ T-cell expansion during healthy aging (17). We therefore aimed to test whether there was a correlation between CMV serostatus and CD8+ T-cell numbers after long-term cART. 28 out of the 30 patients in our study had detectable anti-CMV IgG (results not shown). Since the prevalence of CMV was nearly 100% in our HIV infected study population, we could not analyze the influence of CMV in this study.

Memory CD8⁺ T-cell number at the start of cART determines the decrease in memory CD8⁺ T cells during cART. We next studied whether in individuals that start cART with the highest CD8⁺ T-cell numbers also have the largest decrease in CD8⁺ T cells during cART. Indeed, absolute central memory CD8⁺ T-cell numbers at the start of cART correlated strongly with the absolute decrease in central memory CD8⁺ T cells during the first year of cART (fig. 6A). This correlation was even more apparent for effector memory CD8⁺ T-cell numbers (fig. 6A). Interestingly, this is not due to a fixed proportion of cells that is lost during the first year, since the relative decrease is not the same for all individuals (fig. 6B). During long-term cART the same pattern was observed (fig. 6C).

DISCUSSION

In untreated HIV-1 infected individuals, CD8⁺ T-cell numbers are substantially altered compared to healthy individuals. Naive CD8⁺ T-cell numbers are strongly decreased and non-naive cell populations are more than two-fold expanded. Whether CD8⁺ T-cell numbers normalize during long-term cART has not been investigated in depth. We show that, in contrast to CD4⁺ T-cell numbers, which normalize during long-term cART (8), absolute CD8⁺ T-cell numbers remain elevated after long-term immunological and virological successful antiretroviral treatment. An increase in naive CD8⁺ T-cell numbers to healthy levels and persisting expansion in the memory and effector compartments explain the elevated total CD8⁺ T-cell numbers.

Naive CD8⁺ T-cell numbers have been described to increase relatively fast during cART, but complete normalization is not achieved in a short period (<18 months (15)). We show that, after 5 years of anti-retroviral treatment, naive CD8⁺ T-cell numbers normalized to those of healthy individuals. In this respect the CD8⁺ T-cell compartment behaves similar to its CD4⁺ counterpart (8). For naive CD4⁺ T cells the increase in numbers is accompanied by normalization of the fraction of CD31 positive naive T cells that contain most TRECs (8). This indicates that the newly generated CD4⁺ T cells are produced, at least partially, by the thymus and TCR diversity would increase upon treatment. Recent thymic emigrants cannot be identified in the CD8⁺ T-cell subset by means of CD31 analyses, but TREC levels in this subset were investigated. In the present study, we did not observe normalization of the TREC content of CD8⁺ T cells after long-term cART (data not shown), but since we did not have access to longitudinal data we could not analyze the effect during cART. Others, however, reported an increase in TREC in naive CD8⁺ T cells early during cART (11), which suggests production by the thymus.

Decreases of memory CD8⁺ T-cell number during cART were very slow, our longitudinal analyses only showed a very modest decline in central and effector memory CD8⁺ T-cell numbers during long-term cART. Analysis after 1 year of cART showed that the largest decline occurred shortly after start of cART, which makes the long-term decline even slower.

To explain the slow nature of the memory cell decrease after the first year of cART, we studied whether the memory pool was maintained by activation upon long-term cART. Expression of CD38/HLA-DR and Ki67 is upregulated on CD8⁺ T cells in untreated HIV infection (18;19), gradually decreases after start of cART but remains elevated until at least until week 48 after start of cART (20;21). In the present study, we showed that the fractions of activated CD38⁺/HLA-DR⁺ and Ki67⁺CD8⁺ T cells were no longer elevated and 5 years of cART thus

suffices to normalize the activation levels of the CD8^{+} T-cell compartment. Recently Wittkop et al. (2012) reported on the activation status of CD8^{+} T cells after long-term cART (22). They showed a significantly increased activation within the CD8^{+} T-cell compartment after 5 years of cART. However, in contrast to our study, the study performed by Wittkop et al. was not restricted to immunological responders, which might explain the discrepancy and suggest that in immunological non-responders immune activation persists. Attenuated control of CMV could in this case be a driving factor since presence of CMV responses is related to the level of immune activation after long-term cART (23).

HIV infection has a large impact on the dynamics of the T-cell compartment. For CD4^{+} and CD8^{+} T cells, the fractions of proliferating and apoptotic cells are increased compared to healthy controls and the life span of the naive and memory CD4^{+} and CD8^{+} T cells is 3 to 10 fold decreased (24;25). Upon start of cART these, characteristics normalize to a large extend and in line with these changes, profound alterations in T-cell numbers were observed (21;25). To investigate the slow decay of memory CD8^{+} T cells after the first year of cART, we measured markers related to the dynamics of the CD8^{+} compartment and compared these to healthy controls. The only observed difference was an increase of the fraction of effector memory cells expressing the 'senescence' marker CD57. Although CD57 expression is widely used as a surrogate measure for senescent, replication incompetent, apoptosis resistant T cells, congruence of these characteristics is strong for terminally differentiated effector CD8^{+} T cells and it is not found for all CD57 expressing CD8^{+} memory T cells (26). Analysis of the fractions of Ki67 or annexinV positive cells showed no significant differences, which indicates no altered proliferation or apoptosis of effector memory cells compared to healthy controls. This suggest that, also after long-term cART, an increased fraction of CD57 expressing cells is not a true marker of senescence and is not associated with altered dynamics of effector memory cells.

Finally, we investigated the role of HIV replication in the increased memory numbers. The fast decline of CTL against HIV which occurs when HIV epitopes are replaced by mutational variants (14) suggests that continuous antigen recognition is necessary to maintain these cells and that there is an HIV specific component in the expansion of the CD8^{+} T-cell compartment during untreated infection. If so, the largest changes in cell numbers are expected shortly after start of cART and not in the longer run. Our longitudinal analyses indeed showed the largest decline in the first year after cART and only little decline in the following years. In these later periods we detected HIV specific CD8^{+} T cells and low level viremia in many patients, but no correlations between the fraction of HIV specific CD8^{+} T cells or residual replication with the decline of memory CD8^{+} T cells, suggesting that in this phase HIV does not play a substantial role in CD8^{+} T-cell maintenance.

Of the four CD8^{+} T-cell populations, the effector population was the only population of which the numbers were increased before start of cART and continued to increase during cART. Changes in the CD8^{+} T-cell compartment of HIV infected individuals are often compared to changes that occur during chronological aging and HIV infection has therefore been described as accelerated immunological aging. One characteristic of immunological aging is accumulation of highly differentiated effector T cells. This is observed in uninfected aging individuals (27), as well as untreated HIV infection (4). In accordance with the skewing of HIV specific CD8^{+}

T cells towards central memory status (1;28), we hardly found any HIV specific CD8⁺ T cells in the effector compartment when we stained with tetramers. Therefore, the cells that we find in the effector compartment are not likely HIV specific. Others have shown that HIV infected individuals on cART, with undetectable viral loads, have remarkably high CMV specific effector cell numbers (29). Levels of CMV specific effector cells in HIV infected individuals during cART are comparable to those in the very elderly, only they occur at much younger ages (29). Since the incidence of CMV in HIV infected individuals was nearly 100%, it is very plausible that infection with CMV is the driving force behind the increase in effector CD8⁺ T-cell numbers during cART, as it is in HIV uninfected individuals (17).

In summary, our results show that in immunological responders CD8⁺ T-cell numbers were not completely normalized during long-term successful cART. We found no evidence that the increased CD8⁺ T-cell numbers were explained by residual immune activation, HIV specific T cells or altered dynamic characteristics suggesting, that despite the increased numbers, at least CD8⁺ T-cell dynamics are normalized after long-tern successful viral suppression.

REFERENCE LIST

1. Appay V, Dunbar PR, Callan M, et al. Memory CD8+ T cells vary in differentiation phenotype in different persistent virus infections. Nat Med **2002 Apr**;8(4):379-85.

2. Hazenberg MD, Hamann D, Schuitemaker H, Miedema F. T cell depletion in HIV-1 infection: how CD4+ T cells go out of stock. Nat Immunol **2000 Oct**;1(4):285-9.

3. Roederer M, Dubs JG, Anderson MT, Raju PA, Herzenberg LA, Herzenberg LA. CD8 naive T cell counts decrease progressively in HIV-infected adults. J Clin Invest **1995 May**;95(5):2061-6.

4. Effros RB, Allsopp R, Chiu CP, et al. Shortened telomeres in the expanded CD28-CD8+ cell subset in HIV disease implicate replicative senescence in HIV pathogenesis. AIDS **1996 Jul**;10(8):F17-F22.

5. Appay V, Dunbar PR, Callan M, et al. Memory CD8+ T cells vary in differentiation phenotype in different persistent virus infections. Nat Med **2002 Apr**;8(4):379-85.

6. Czesnikiewicz-Guzik M, Lee WW, Cui D, et al. T cell subset-specific susceptibility to aging. Clin Immunol **2008 Apr**;127(1):107-18.

7. Fagnoni FF, Vescovini R, Mazzola M, et al. Expansion of cytotoxic CD8+. Immunology **1996 Aug**;88(4):501-7.

8. Vrisekoop N, van GR, de Boer AB, et al. Restoration of the CD4 T cell compartment after long-term highly active antiretroviral therapy without phenotypical signs of accelerated immunological aging. J Immunol **2008 Jul 15**;181(2):1573-81.

9. Autran B, Carcelain G, Li TS, et al. Positive effects of combined antiretroviral therapy on CD4+ T cell homeostasis and function in advanced HIV disease. Science **1997 Jul 4**;277(5322):112-6.

10. Pakker NG, Notermans DW, de Boer RJ, et al. Biphasic kinetics of peripheral blood T cells after triple combination therapy in HIV-1 infection: a composite of redistribution and proliferation. Nat Med **1998 Feb**;4(2):208-14.

11. Di MM, Sereti I, Matthews LT, et al. Naive T-cell dynamics in human immunodeficiency virus type 1 infection: effects of highly active antiretroviral therapy provide insights into the mechanisms of naive T-cell depletion. J Virol **2006 Mar**;80(6):2665-74.

12. Kostense S, Raaphorst FM, Joling J, et al. T cell expansions in lymph nodes and peripheral blood in HIV-1-infected individuals: effect of antiretroviral therapy. AIDS **2001 Jun 15**;15(9):1097-107.

13. Kostense S, Vandenberghe K, Joling J, et al. Persistent numbers of tetramer+ CD8(+) T cells, but loss of interferon-gamma+ HIV-specific T cells during progression to AIDS. Blood **2002 Apr 1**;99(7):2505-11.

14. Liu Y, McNevin JP, Holte S, McElrath MJ, Mullins JI. Dynamics of viral evolution and CTL responses in HIV-1 infection. PLoS One **2011**;6(1):e15639.

15. Pohling J, Zipperlen K, Hollett NA, Gallant ME, Grant MD. Human immunodeficiency virus type I-specific CD8+ T cell subset abnormalities in chronic infection persist through effective antiretroviral therapy. BMC Infect Dis **2010**;10:129.

16. Schellens IM, Pogany K, Westerlaken GH, et al. Immunological analysis of treatment interruption after early highly active antiretroviral therapy. Viral Immunol **2010 Dec**;23(6):609-18.

17. Chidrawar S, Khan N, Wei W, et al. Cytomegalovirus-seropositivity has a profound influence on the magnitude of major lymphoid subsets within healthy individuals. Clin Exp Immunol **2009 Mar**;155(3):423-32.

18. Gaines H, von Sydow MA, von Stedingk LV, et al. Immunological changes in primary HIV-1 infection. AIDS **1990 Oct**;4(10):995-9.

19. Prince HE, Kleinman S, Czaplicki C, John J, Williams AE. Interrelationships between serologic markers of immune activation and T lymphocyte subsets in HIV infection. J Acquir Immune Defic Syndr **1990**;3(5):525-30.

20. Cohen Stuart JW, Hazebergh MD, Hamann D, et al. The dominant source of CD4+ and CD8+ T-cell activation in HIV infection is antigenic stimulation. J Acquir Immune Defic Syndr **2000 Nov 1**;25(3):203-11.

21. Hazenberg MD, Stuart JW, Otto SA, et al. T-cell division in human immunodeficiency virus (HIV)-1 infection is mainly due to immune activation: a longitudinal analysis in patients before and during highly active antiretroviral therapy (HAART). Blood **2000 Jan 1**;95(1):249-55.

22. Wittkop L, Bitard J, Lazaro E, et al. Effect of cytomegalovirus-induced immune response, self antigen-induced immune response, and microbial translocation on chronic immune activation in successfully treated HIV type 1-infected patients: the ANRS CO3 Aquitaine Cohort. J Infect Dis **2013 Feb 15**;207(4):622-7.

23. Pedersen KK, Pedersen M, Gaardbo JC, et al. Persisting inflammation and chronic immune activation but intact cognitive function in HIV-infected patients after long-term treatment with combination antiretroviral therapy. J Acquir Immune Defic Syndr **2013 Jul 1**;63(3):272-9.

24. Douek DC, Betts MR, Hill BJ, et al. Evidence for increased T cell turnover and decreased thymic output in HIV infection. J Immunol **2001 Dec 1**;167(11):6663-8.

25. Vrisekoop N, Veel E, Van Gent R, Mugwagwa T, Drylewicz J, et al. Quantification of Naive and Memory T-cell Turnover During HIV-1 Infection. Thesis E M Veel **2013 Jan 1**;chapter 2.

26. Strioga M, Pasukoniene V, Characiejus D. CD8+. Immunology **2011 Sep**;134(1):17-32.

27. Effros RB. Loss of CD28 expression on T lymphocytes: a marker of replicative senescence. Dev Comp Immunol **1997 Nov**;21(6):471-8.

28. Champagne P, Ogg GS, King AS, et al. Skewed maturation of memory HIV-specific CD8 T lymphocytes. Nature **2001 Mar 1**;410(6824):106-11.

29. Naeger DM, Martin JN, Sinclair E, et al. Cytomegalovirus-specific T cells persist at very high levels during long-term antiretroviral treatment of HIV disease. PLoS One **2010**;5(1):e8886.

CHAPTER 6

DELINEATING THE NUMBERS OF THE CD8^{+} T-CELL COMPARTMENT: THE EFFECT OF AGE AND CMV SEROSTATUS

Ellen Veel[1], Rogier van Gent[1], Liset Westera[1], Beatrijs L. Bloemers[1], Sigrid A. Otto[1], Bram Ruijsink[1], Huib Rabouw[1], José A. M. Borghans[1], Kiki Tesselaar[1]

[1]Laboratory for Translational Immunology, University Medical Center Utrecht

ABSTRACT

Immunocompetence, or the lack thereof is linked to the absolute number of specific immune cells. It is generally accepted that blood CD8^{+} T-cell number depends on the CMV serostatus and age in healthy individuals, but despite this knowledge clinical studies often fail to include matched control groups. In this study, we measured absolute numbers of the 4 most used (naive, central memory, effector memory and effector) CD8^{+} T-cell subsets as defined by the commonly used markers CD27 and CD45RO and compared CMV seropositive and seronegative healthy individuals over age. We show significant differences in effector memory and effector CD8^{+} T-cell numbers between CMV seropositive and CMV seronegative individuals in both children and adults. When donors were stratified by age, significant differences were again detected in the effector memory and effector CD8^{+} T-cell subsets, remarkably with the largest differences at the youngest age.

Given the results of our study, we strongly recommend that CMV serostatus is taken into account when absolute CD8^{+} T-cell numbers are studied, particularly when effector memory and effector CD8^{+} T-cells are investigated in children under the age of 10.

6

EFFECT OF AGE AND CMV ON CD8^{+} T-CELL NUMBERS

INTRODUCTION

When reference groups of healthy donors are included in studies comparing absolute CD8^{+} T-cell numbers in humans, usually cytomegalovirus (CMV) serostatus is not taken into account. It is, however, known that CMV seroprevalence associates with altered CD8^{+} T-cell numbers (1-5). Depending on age, ethnicity, geographic location and socio-economic status, CMV seroprevalence has been shown to differ between subgroups of individuals (6).

In CMV seropositive (CMV+) adults and children, the relative subset distribution of the CD8^{+} T-cell compartment has been shown to be significantly different from that of CMV seronegative (CMV-) individuals (1). For instance, the percentage of naive CD8^{+} T cells in CMV+ individuals was shown to be decreased and the percentage of effector CD8^{+} T cells to be increased compared to CMV- adults (1). In terms of absolute numbers, terminally differentiated (CD28^{-}CD8^{+}) T cells, which are end stage effector cells, have been described to be significantly increased in CMV+ adults, whereas CD28^{+}CD8^{+} T-cell numbers were significantly decreased (4). In addition, it has been reported that absolute memory and effector CD8^{+} T-cell numbers were increased in CMV+ compared to CMV- adults (2). In healthy children, effector CD8^{+} T-cell numbers were significantly increased in CMV+ compared to CMV- individuals (3). Also, infants of 9 and 13 months of age have been shown to have elevated numbers of terminally differentiated CD8^{+} T cells (5).

An absolute and relative increase in effector CD8^{+} T cells has been described for healthy individuals during aging (7). Given the above, apparently these changes already occur in young individuals, if they are CMV+. The observed increase in effector CD8^{+} T-cell number during aging could thus be caused by an increase in CMV seroprevalence, actual changes to the CD8^{+} T-cell compartment of a combination of both.

Taken together, these data suggest that CMV may be a driving force in CD8^{+} T-cell differentiation.

In this paper, we investigate to what extent CMV and age alter the CD8^{+} T-cell compartment of healthy individuals in terms of absolute T-cell numbers, in order to determine to what extent these factors may interfere with the interpretation of study results.

MATERIALS AND METHODS

Study population. Whole EDTA-anticoagulated or sodium heparine anti-coagulated blood was obtained by venipuncture. A total of two hundred and eighty seven donors were included in the current study. Forty one adults were registered blood donors and were included within the Dutch Blood Bank. Forty eight adults were employees of the University Medical Center Utrecht (UMCU, Utrecht, The Netherlands) and were included within the UMCU. Individuals > 18 years of age where included in the adult group. CMV+ adults had a mean age of 48.3 years and CMV- adults had a mean age of 46.8 years. One hundred and fifty children were included within the UMCU. All children were admitted to the UMCU in order to undergo an elective urological, plastic, ophthalmologic, or general surgery. To minimize interference on immunologic parameters, blood was drawn prior to or directly after anesthesia was given. CMV+ children had a mean age of 7.18 years and CMV- children had a mean age 7.23 years. All participants were

considered healthy as they did not have any history of infectious diseases or hematological and immunological disorders or showed signs of acute infection at the time of venipuncture. This study was approved by the medical ethical committee of the UMCU and written informed consent was obtained from all study participants or their guardians in agreement with the Declaration of Helsinki (version: 59th WMA General Assembly, Seoul, October 2008).

Flow cytometry. Absolute CD4$^+$ and CD8$^+$ T-cell numbers were determined by dual-platform flow cytometry, using TruCount tubes (BD Biosciences) or were calculated by multiplying the percentage of the indicated subset as obtained by flow cytometry and absolute lymphocyte number as determined with a Cell-Dyn Sapphire hematology Analyzer (Abbott Diagnostics). PBMC were obtained by Ficoll-Paque density gradient centrifugation and were cryopreserved until further use. All experiments were performed on cryopreserved cells that were thawed shortly before the experiment. Naive (CD27$^+$CD45RO$^-$), central memory (CD27$^+$CD45RO$^+$), effector memory (CD27$^-$CD45RO$^+$) and effector (CD27$^-$CD45RO$^-$) CD8$^+$ T cells were assessed by flow cytometry. PBMC were incubated with mAb to CD8 PerCP-Cy5.5, CD8 APCCy7, CD8 V500, CD8 Amcyan, CD27 APC, CD27 APC-Cy7, CD45RO PE, CD45RO PE-Cy7 (BD Biosciences), CD27 APC, CD27 APC-AF750, CD3 eFluor450 (eBioscience), CD3 PerCP (Biolegend) or CD27 FITC (Sanquin). To measure T-cell proliferation, PBMC were stained intracellularly with Ki67 FITC (DakoCytomation) after fixation and permeabilization with Cytofix/ Cytoperm and PermWash according to the manufacturer's instructions (BD Biosciences). All experiments described above were analyzed on a FACS Canto II of FACS LSR II (BD Biosciences) with FACS Diva software (BD Biosciences).

Determination of CMV serostatus. Cytomegalovirus IgG class antibodies were qualitatively determined by ELISA in human plasma according to the manufacturer's instructions (IBL international GmbH).

Statistical analysis. Linear regression analyses was used to analyze CD8$^+$ T-cell change over age of CMV+ and CMV- individuals. Analysis of Covariance was used to determine whether the slopes of CD8$^+$ T-cell change over age in CMV+ and CMV- individuals were significantly different from each other. A F-test was used to determine whether the individual slopes were significantly different from zero. Nonparametric Mann-Whitney U tests for unpaired data were used to compare absolute CD8$^+$ T-cell numbers and both relative and absolute Ki67 expression on CD8$^+$ T-cells between CMV+ and CMV- children and adults. All statistical analyses were performed using the GraphPad Prism software (Graphpad Software, Inc.).

RESULTS

Absolute CD8$^+$ T-cell numbers in CMV+ compared to CMV- individuals. First, we determined whether there were significant differences in median absolute CD8$^+$ T-cell numbers between CMV+ and CMV- individuals. Absolute CD8$^+$ T-cell numbers of 287 healthy donors (age range 0.2 – 75 years) were measured. CMV serostatus of the donors was determined based on the presence of IgG antibodies against CMV antigens. CD27 and CD45RO were used to distinguish between naive (CD27$^+$CD45RO$^-$), central memory (CD27$^+$CD45RO$^+$), effector memory (CD27$^-$

CD45RO$^+$) and effector (CD27$^-$CD45RO$^-$) CD8$^+$ T cells. When we analyzed median absolute effector memory CD8$^+$ T-cell numbers we found elevated numbers in CMV+ individuals compared to CMV- individuals, in both children (CMV+: 44 cells/μl blood vs CMV-: 18 cells/μl blood) (P < 0.0001) and adults (CMV+: 42 cells/μl blood vs CMV-: 22 cells/μl blood) (P = 0.0065) (fig. 1C). Median absolute effector CD8$^+$ T-cell numbers were also significantly elevated in CMV+ individuals compared to CMV- individuals in both children (CMV+: 92 cells/μl blood vs CMV-: 48 cells/μl blood) (P < 0.0001) and adults (CMV+: 87 cells/μl blood vs CMV-: 15 cells/μl blood) (P < 0.0001) (fig. 1D). Medians of absolute naive and central memory CD8$^+$ numbers did not differ between CMV+ and CMV- individuals (fig. 1A,B), but as expected naive and memory numbers did differ between children and adults.

Changes in CD8$^+$ T-cell number in CMV+ and CMV- individuals over age. To further look into the effect of age we stratified our donors by age. When we did so, we found no significant difference in absolute total CD8$^+$ T-cell numbers between CMV+ and CMV- individuals in any of the age groups (table 1 and fig. 2). Naive CD8$^+$ T-cell numbers have been shown to decrease during healthy aging (8). In our data, we also observed a significant decrease in naive CD8$^+$
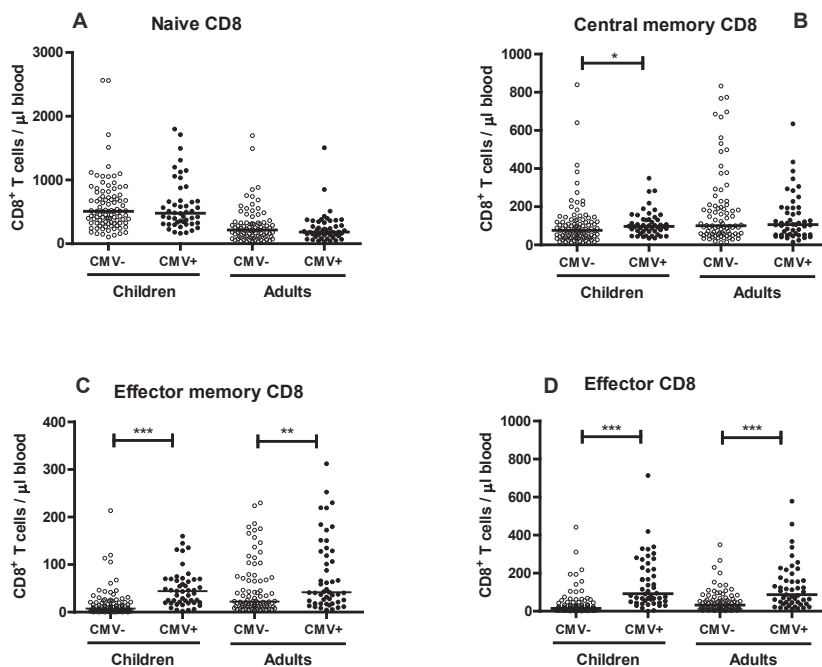
Figure 1. Absolute CD8$^+$ T-cell numbers in CMV seropositive and CMV seronegative individuals. (A) Absolute naive (CD27$^+$CD45RO$^-$), (B) central memory (CD27$^+$CD45RO$^+$), (C) effector memory (CD27$^-$CD45RO$^+$) and (D) effector (CD27$^-$CD45RO$^-$) CD8$^+$ T-cell numbers in CMV seropositive and CMV seronegative children and adults. Data are expressed as the mean number of cells per microliter in the peripheral blood. Statistical significance (*, p < 0.05; **, p < 0.01; ***, p < 0.001) was determined by the nonparametric Mann-Whitney U test for unpaired data.

Table 1. Absolute CD8+ T-cell numbers in CMV seropositive and CMV seronegative individuals stratified by age

Donor age (years)	Median age (years)	CMV status	Number of subjects	CD8 Total	CD8 Naive	CD8 Central Memory	CD8 Effector Memory	CD8 Effector
0-5	2.3	CMV+	21	1017	609	101*	48***	168***
	2.5	CMV-	38	827	679	60	6	15
5-10	8.2	CMV+	10	865	525	105	50**	82**
	6.5	CMV-	29	639	521	99	15	27
10-15	11.3	CMV+	13	618	347	83	55**	83**
	12.1	CMV-	19	480	382	80	7	9
15-20	15.8	CMV+	4	471	274	116	22	64*
	16.2	CMV-	10	410	276	54	6	10
20-35	25.5	CMV+	11	514	316	86	31	55*
	28	CMV-	25	363	230	88	18	18
35-50	43	CMV+	13	441	177	109	39	67
	43	CMV-	20	344	158	92	19	29
50-60	55	CMV+	19	553	195	163	77	115*
	54	CMV-	27	736	322	213	55	55
60+	61	CMV+	10	383	163	52	41	123
	67	CMV-	16	238	74	72	21	36

Data are expressed as the median number of cells per microliter in the peripheral blood. Statistical significance (*, $p < 0.05$; **, $p < 0.001$; ***, $p < 0.001$) was determined by the nonparametric Mann-Whitney U test for unpaired data.

T-cell numbers over age in CMV+ as well as CMV- individuals ($r2 = 0.1574$, $P = < 0.0001$) and ($r2 = 0.2299$, $P < 0.0001$) resp. (fig. 2A). We did not find a significant difference between CMV+ and CMV- individuals in any of the age groups (table 1) nor did the slopes of naive CD8+ T-cell decrease differ significantly between CMV+ and CMV- individuals ($p = 0.7473$)). Central memory CD8+ T-cell numbers increased significantly in both CMV+ and CMV- individuals ($r2 = 0.0894$, $P = < 0.0001$) and ($r2 = 0.0404$, P 0.0484) resp. (fig. 2B). Absolute central memory CD8+ T-cell numbers were only significantly elevated in CMV+ individuals in the youngest age group (0-5 years) (table 1), but the slopes of central memory CD8+ T-cell number decrease did not differ significantly between CMV+ and CMV- individuals ($p = 0.0944$). Effector memory CD8+ T-cell numbers increased significantly in CMV- individuals ($r2 = 0.1617$, $P < 0.0001$), but not in CMV+ individuals ($r2 = 0.0345$, $P = 0.0684$) resp. (fig. 2C). Effector memory CD8+ T-cell numbers were significantly elevated in CMV+ individuals in the age groups 0-5, 5-10 and 10-15 years of age (table 1). Surprisingly, there was no statistical difference between the slopes of effector memory CD8+ T-cell increase between CMV+ and CMV- individuals ($p = 0.284$). Effector CD8+ T-cell numbers increased significantly in CMV- individuals ($r2 = 0.0340$. $P = 0.0089$), but not in CMV+ individuals ($r2 = <0.0001$, $P = 0.9524$) (Fig. 2D). Effector CD8+ T-cell numbers were significantly elevated in all age groups except for 35-50 and 60+ years of age (table 1). Again,
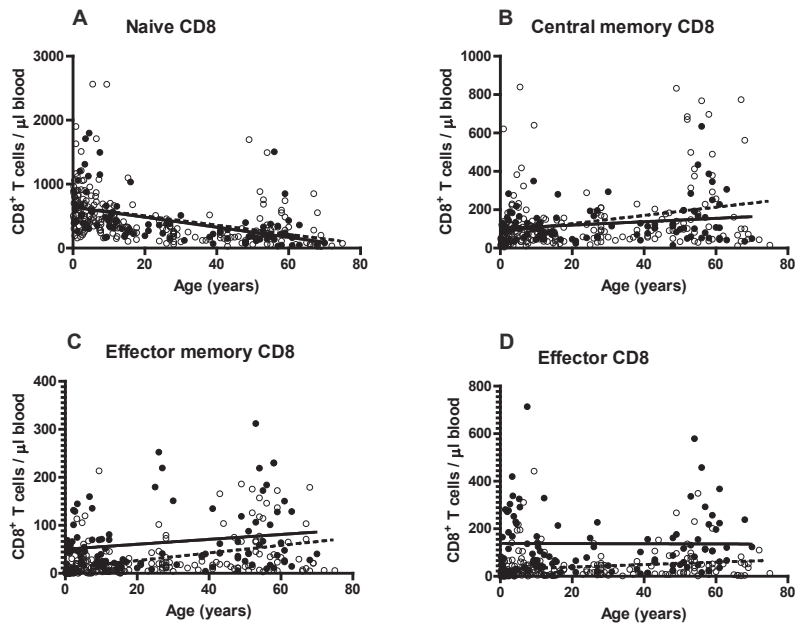
Figure 2. Absolute CD8+ T-cell numbers in CMV seropositive and CMV seronegative individuals plotted against age. (A) Absolute naive (CD27+CD45RO-), (B) central memory (CD27+CD45RO+), (C) effector memory (CD27-CD45RO+) and (D) effector (CD27-CD45RO-) CD8+ T-cell numbers in CMV seropositive and seronegative individuals plotted against age. Linear regression analyses was used to analyze CD8+ T-cell number change over age.

there was no significant difference between the slopes of CD8+ effector T-cell change between the two groups (P = 0.2668).

Remarkably, we observed that young children (< 5 years) that were CMV+ already had very high effector memory – and effector CD8+ T-cell numbers.

In conclusion, we did not find a difference between the slopes of CD8+ T-cell number change over age between CMV+ and CMV- individuals. Remarkably, in CMV+ individuals, effector memory and effector CD8+ T-cell numbers did not increase over age. In summary, the most significant differences in absolute CD8+ T-cell numbers between CMV+ and CMV- individuals were found in the effector memory and effector CD8+ T-cell compartments.

Ki-67 expression in effector memory and effector CD8+ T cells in CMV+ and CMV- individuals.
Since we found elevated numbers of effector memory and effector CD8+ T cells in CMV+ individuals compared to CMV- individuals we hypothesized that these might be maintained through continuous activation and proliferation. To investigate this, we measured the cell division marker Ki67. The levels of Ki67 expression in both effector memory and effector CD8+ T cells were not significantly different between CMV+ and CMV- individuals in both children and adults (fig. 3A,B). When we analyzed the absolute number of Ki67 expressing effector memory CD8+ T cells in blood we did not find a significant difference between CMV+ and CMV-
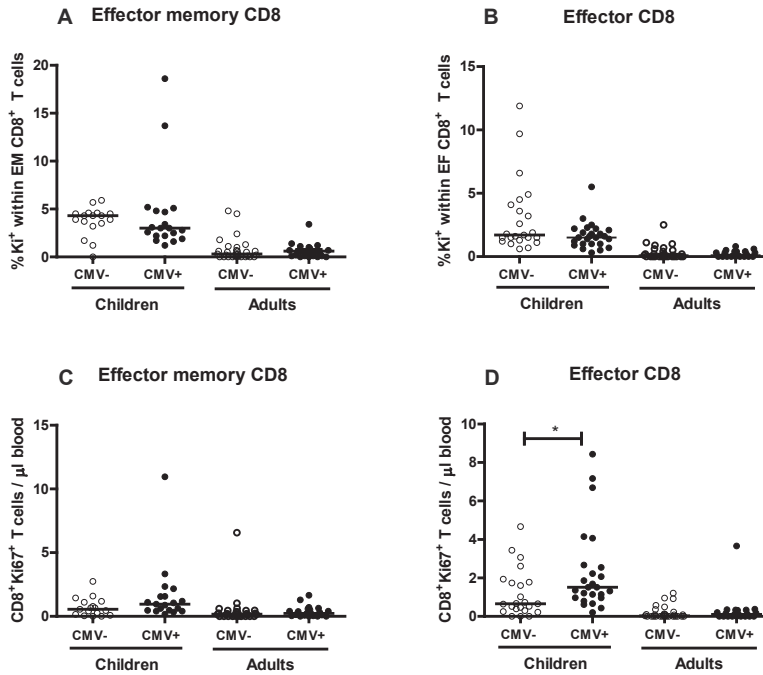
Figure 3. Ki-67 expression in effector memory and effector CD8$^+$ T cells in CMV seropositive and CMV seronegative individuals. (A) Absolute naive (CD27$^+$CD45RO$^-$), (B) central memory (CD27$^+$CD45RO$^+$), (C) effector memory (CD27$^-$CD45RO$^+$) and (D) effector (CD27$^-$CD45RO$^-$) CD8$^+$ T cells in CMV seropositive and CMV seronegative children and adults. Data are expressed as the median percentage ki67$^+$CD8$^+$ T cells within total CD8$^+$ T cells (A, B). Data are expressed as the median of the absolute number of Ki67$^+$CD8$^+$ T cells per microliter in the peripheral blood (C,D). Statistical significance (*, p < 0.05) was determined by the nonparametric Mann-Whitney U test for unpaired data.

individuals (fig. 3C). The absolute number of Ki67 expressing effector CD8$^+$ T cells in blood was significantly elevated in CMV+ children ((CMV+: 1.51 cells/μl blood vs CMV-: 0.65 cells/μl blood) (P = 0.0176), but not in adults (fig. 3D). In conclusion, high effector memory and effector CD8$^+$ T-cell numbers are most likely not maintained through activation.

DISCUSSION

In the present study, we compared median CD8$^+$ T-cell numbers between CMV+ and CMV- individuals. Significant differences were detected mainly in effector memory and effector CD8$^+$ T-cell numbers, which were elevated in CMV+ individuals compared to CMV- individuals, in both children and adults. When donors were stratified by age, in nearly all age groups, the most significant differences were again detected in the effector memory and effector CD8$^+$ T-cell subsets. Furthermore, we demonstrate that slope of absolute CD8$^+$ T-cell number change over age does not differ between CMV+ and CMV- individuals in any CD8$^+$ T-cell subsets.

Remarkably, young CMV+ children already have very high effector memory and effector CD8+ T-cell numbers and these do not increase significantly over age.

It has been reported that both age and CMV serostatus have a significant effect on absolute CD8+ T-cell numbers (2). We did not observe a difference in naive CD8+ T-cell numbers when comparing median absolute CD8+ T-cell numbers in CMV+ and CMV- individuals (fig. 1A). Remarkably, a difference in absolute naive CD8+ T-cell numbers between CMV+ and CMV- individuals has previously been described in adults (2). Chidrawar et al. (2009) reports a decrease in naive CD8+ T-cell numbers of 40% in all age groups. A difference between the present study and Chidrawar et al. (2009) that may possibly explain this discrepancy is the antibody panel used to distinguish between naive, central memory, effector memory and effector CD8+ T cells. Chidrawar et al. (2009) used LFA-1 and CD45RA to distinguish between the above mentioned subsets and in the present study, CD27 and CD45RO were used. Furthermore, it is unclear what the age distribution is within the three age groups (2). Since age has a significant effect on naive CD8+ T-cell numbers in this study, this is very relevant information. Almanzar et al. also reports fewer naive CD8+ T cells in CMV+ individuals, however, in this study only relative CD8+ T-cell numbers were compared (1). The lower percentage of naive CD8+ T cells could thus very well have resulted from the relative increase in memory and effector CD8+ T cells (Fig. 1, (1;2)). In children, lower naive CD8+ T-cell numbers in CMV+ individuals were never reported. Our data suggest there is no difference between naive CD8+ T-cell numbers of CMV+ and CMV- individuals. This observation is strengthened by the fact that we do not find a different slope for naive CD8+ T-cell number decline between CMV+ and CMV- individuals.

We did find a significant difference in effector memory and effector CD8+ T-cell numbers between CMV+ and CMV- individuals in both children and adults (fig. 1C,D). This has also been reported in previous publications (2;3;9). This expansion could, for a large part, be comprised of CMV specific cells, since CD8+ T cells specific for either the major immediate early 1 protein (EI-1) or the structural phosphoprotein pp65 have been described to occupy up to 8% of the total CD8+ T-cell pool in adults (10;11). Furthermore, with combined analyses of the responses against IE-1, pp65 and nonstructural phosphoprotein pp50 it has been shown that up to 45% of total CD8+ T cells may be CMV specific in the elderly (12). We observed a larger expansion of effector CD8+ T-cell numbers, compared with effector memory CD8+ T-cell numbers. This is in line with previously published data that describe CMV specific CD8+ T cells to reside mainly in the effector CD8+ T-cell pool and to a lesser extent in the effector memory subset (13). Interestingly we also observed a significantly elevated memory and effector CD8+ T-cell number in very young CMV+ individuals, who are by definition likely to be infected with CMV for a relatively short period (table 1). Also, the number of effector memory and effector CD8+ T-cells did not increase over age (fig. 2C,D). This suggests an increase in central memory CD8+ T cells shortly after infection, after which the number stays stable. It has previously been shown that CMV specific CD8+ T cells reside for a large part in the central memory and effector subset (13) and that the phenotype of CMV specific CD8+ T cells shifts more towards terminally differentiated during aging (14). Published data show that, at least during the first four months of CMV infection, effector CD8+ T-cell numbers expand and reach an individual set point in children (3). This could mean that a large number of CMV specific effector and

effector memory CD8^{+} T cells are formed early after infection and during chronic infection these cells are maintained.

We only observed a difference in Ki67 expressing cells between CMV+ and CMV- individuals in the effector CD8^{+} T-cell subset of children (fig. 3). It has been reported that expression levels of Ki67 rise in CMV specific CD8^{+} T cells shortly after primary infection of infants, after one year however, they have returned to the level of the total CD8^{+} T-cell pool (15). In CMV+ children, which are more likely to have been infected recently, we possibly observe exactly this phenomenon. Adult individuals are more likely to have been infected for a prolonged period and therefore to have normalized Ki67 expression on CD8^{+} T cells.

Given the results of our study and previously published data, we strongly recommend that subset defining cell surface markers, age and CMV serostatus are matched for the study populations of interest, when studying cell numbers within the CD8^{+} T-cell compartment.

REFERENCE LIST

1. Almanzar G, Schwaiger S, Jenewein B, et al. Long-term cytomegalovirus infection leads to significant changes in the composition of the CD8+ T-cell repertoire, which may be the basis for an imbalance in the cytokine production profile in elderly persons. J Virol **2005 Mar**;79(6):3675-83.

2. Chidrawar S, Khan N, Wei W, et al. Cytomegalovirus-seropositivity has a profound influence on the magnitude of major lymphoid subsets within healthy individuals. Clin Exp Immunol **2009 Mar**;155(3):423-32.

3. Kuijpers TW, Vossen MT, Gent MR, et al. Frequencies of circulating cytolytic, CD45RA+CD27-, CD8+ T lymphocytes depend on infection with CMV. J Immunol **2003 Apr** 15;170(8):4342-8.

4. Looney RJ, Falsey A, Campbell D, et al. Role of cytomegalovirus in the T cell changes seen in elderly individuals. Clin Immunol **1999 Feb**;90(2):213-9.

5. Miles DJ, Sanneh M, Holder B, et al. Cytomegalovirus infection induces T-cell differentiation without impairing antigen-specific responses in Gambian infants. Immunology **2008 Jul**;124(3):388-400.

6. Cannon MJ, Schmid DS, Hyde TB. Review of cytomegalovirus seroprevalence and demographic characteristics associated with infection. Rev Med Virol **2010 Jul**;20(4):202-13.

7. Fagnoni FF, Vescovini R, Mazzola M, et al. Expansion of cytotoxic CD8+. Immunology **1996 Aug**;88(4):501-7.

8. Provinciali M, Moresi R, Donnini A, Lisa RM. Reference values for CD4+ and CD8+ T lymphocytes with naive or memory phenotype and their association with mortality in the elderly. Gerontology **2009**;55(3):314-21.

9. Wikby A, Johansson B, Olsson J, Lofgren S, Nilsson BO, Ferguson F. Expansions of peripheral blood CD8 T-lymphocyte subpopulations and an association with cytomegalovirus seropositivity in the elderly: the Swedish NONA immune study. Exp Gerontol **2002 Jan**;37(2-3):445-53.

10. Naeger DM, Martin JN, Sinclair E, et al. Cytomegalovirus-specific T cells persist at very high levels during long-term antiretroviral treatment of HIV disease. PLoS One **2010**;5(1):e8886.

11. Vescovini R, Biasini C, Fagnoni FF, et al. Massive load of functional effector CD4+ and CD8+ T cells against cytomegalovirus in very old subjects. J Immunol **2007 Sep 15**;179(6):4283-91.

12. Khan N, Hislop A, Gudgeon N, et al. Herpesvirus-specific CD8 T cell immunity in old age: cytomegalovirus impairs the response to a coresident EBV infection. J Immunol **2004 Dec 15**;173(12):7481-9.

13. Appay V, Dunbar PR, Callan M, et al. Memory CD8+ T cells vary in differentiation phenotype in different persistent virus infections. Nat Med **2002 Apr**;8(4):379-85.

14. Hadrup SR, Strindhall J, Kollgaard T, et al. Longitudinal studies of clonally expanded CD8 T cells reveal a repertoire shrinkage predicting mortality and an increased number of dysfunctional cytomegalovirus-specific T cells in the very elderly. J Immunol **2006 Feb 15**;176(4):2645-53.

15. Miles DJ, van der Sande M, Jeffries D, et al. Cytomegalovirus infection in Gambian infants leads to profound CD8 T-cell differentiation. J Virol **2007 Jun**;81(11):5766-76.

CHAPTER 7

A GENERALIZED MATHEMATICAL MODEL TO ESTIMATE T- AND B-CELL RECEPTOR DIVERSITIES USING AMPLICOT

Irina Baltcheva[‡Δ], Ellen Veel[†Δ], Thomas Volman[†], Dan Koning[†],
Anja Brouwer[†], Jean-Yves Le Boudec[‡], Kiki Tesselaar[†],
Rob J. de Boer[§], José A. M. Borghans[†]

[‡]Laboratory for Computer Communications and Applications, École Polytechnique Fédérale de Lausanne, Switzerland
[†]Department of Immunology, University Medical Center Utrecht, Utrecht, The Netherlands
[§]Department of Theoretical Biology, Utrecht University, Utrecht, The Netherlands
[Δ]These authors contributed equally to this study

ABSTRACT

The efficiency of the adaptive immune system is dependent on the diversity of T- and B-cell receptors, which is created by random rearrangement of receptor gene segments. AmpliCot is an experimental technique that allows the measurement of the diversity of the T- and B-cell repertoire. This procedure has the advantage over other cloning and sequencing techniques of being time- and expense-effective. In previous studies, receptor diversity, measured with AmpliCot, has been inferred assuming a second-order kinetics model. The latter implies that the relation between diversity and concentration x time (Cot) values is linear. We show that a more detailed model, involving heteroduplex and transient-duplex formation, leads to significantly better fits of experimental data and to non-linear diversity-Cot relations. We propose an alternative fitting procedure, which is straightforward to apply and which gives an improved description of the relationship between Cot values and diversity.

7

MATHEMATICAL MODELING OF AMPLICOT

INTRODUCTION

The diversity of T and B-cell receptors (TCRs and BCRs) is a hallmark of the adaptive immune system, and is responsible for the specific recognition and the defense against a wide variety of pathogens. The structural diversity of BCRs and TCRs is achieved by somatic gene-segment rearrangements and random nucleotide additions or deletions (1). The estimation of the effective size of the human TCR repertoire, both in health and disease, is a fundamental question in immunology. Using single molecule DNA sequencing, it was estimated that the number of unique TCRβ CDR3 sequences in a healthy adult is 3-4,000,000 (2).

Several experimental techniques have been used to measure the diversity of the TCR or BCR repertoire. Immunoscope (or Spectratype) provides qualitative insights into the repertoire's diversity in terms of clone sizes (3;4); high-throughput DNA sequencing exhaustively enumerates the different clonotypes that are present in a sample, thus providing a more detailed picture of the repertoire (5-9). Such deep sequencing techniques are very expensive, can be very difficult to interpret because of sequencing and amplification errors, and can therefore not always be applied on large scale. AmpliCot has been introduced as an alternative approach, allowing for the measurement of the diversity of DNA samples through quantification of the re-hybridization speed of denatured PCR products (10;11). It has the advantage over cloning and (deep) sequencing methods to be time- and expense-effective.

The AmpliCot experiment is based on the so-called "Cot analysis" (12), according to which the time required for a DNA sample to re-anneal (expressed in terms of the product concentration x time, "Cot") is related to the diversity of the sample. To estimate the diversity of a DNA sample from its annealing curve, Baum and McCune (10) proposed to analyse the Cot values at which, e.g., 50% of the sample is annealed ($Cot_{0.5}$ values). The authors suggested that the relation between $Cot_{0.5}$ values and diversity is linear, which is indeed true if the annealing obeys second-order kinetics. Accordingly, it is assumed that only perfectly complementary pairs of DNA can associate, i.e., the possibility of heteroduplex formation is neglected. A recent study reported a systematic fluorescence loss at diversities exceeding 4×10^3 (13). Annealing curves of samples with diversity 10^6 and higher did not reach the 50% annealing point, which made the determination of a $Cot_{0.5}$ value impossible. One explanation that was proposed is that the low concentration of highly similar sequences results in the formation of heteroduplexes (13).

Driven by these observations, we investigated how to deal with heteroduplex formation and its consequences for the interpretation of AmpliCot data. In what follows, we formally define the previously used model, i.e., second-order kinetics, and we propose a more detailed model which considers the DNA annealing in two steps and takes into account the formation of transient duplexes and heteroduplexes. We then compare the ability of both models to fit AmpliCot annealing time-series. In doing so, we take advantage of the information contained in the entire annealing curves, rather than just the $Cot_{0.5}$ value. We use our model to derive what to our knowledge is a new formula describing the relation between Cot values and diversity. This formula is a generalization of the linear relation based on second-order kinetics. We show that the generalized Cot expression accurately reproduces Cot values of highly diverse samples and leads to better interpretation of experimental data. Finally, we propose a diversity estimation algorithm that is simple to use and that can account for heteroduplex formation.

MATERIALS AND METHODS

AmpliCot Assay. Samples containing PCR-amplified or artificially synthesized oligonucleotides were mixed with SYBR green fluorescent dye, which binds to double-stranded DNA. To determine the specific melting point for each analysis, an aliquot of the double stranded DNA (dsDNA) product (either a PCR product or a double stranded oligomer product) was melted by gradually increasing the temperature at which the change in SYBR green fluorescence intensity peaked. The annealing temperature for each sample was subsequently set to be 3 °C lower than its melting temperature. For AmpliCot analyses, three aliquots of the mixture were placed in a 96-well plate as the annealing samples and a reference, respectively. The premelting step consisted of measuring the baseline fluorescence of the samples and reference at annealing temperature (fig. 1A). Subsequently, the temperature was increased to 95 °C for 2 min to aim at total dissociation of the dsDNA strands, whereas the reference stayed at annealing temperature (melting step). The fluorescence intensity of the samples strongly decreased during the melting step as the double-stranded DNA de-hybridized. During the annealing step, the temperature of the samples was set back to annealing temperature and the time-varying fluorescence intensity was measured every 5 - 20 s (fig. 1A). For any given total concentration, the resulting reannealing speed is expected to be dependent on the diversity of the sample, because in samples of high diversity, each sequence is present at a low concentration.

Experimental Data. We tested our new mathematical model using four experimental data sets (see table 1): the original oligonucleotide data set of Baum & McCune (10), two new data sets with diversities ranging from 1 to 48 and from 10 to 40, and the recently published data set of Baum et al. (14) that includes highly diverse samples.

Oligonucleotides that were used to create data sets 2 and 3 (table 1) were synthesized according to the following format:

GCTGGCGCAGAAATATACAGGTCGGACCTCAGCTG-(**NNNN**)$_4$CCTCAGCACCTCC

in which NNNN represents one of the eight nucleotide combinations AATC, ATCA, TCTA, CAAA, TTAC, TACT, ACAT or CTTT (Eurofins MWG Operon, Huntsville, AL). Samples of the desired diversities were created by mixing the required amount of oligonucleotides at equimolar ratios. To slow down the annealing kinetics of the low diversity samples, some samples were diluted (table 1). There are two equivalent alternatives for handling concentration differences between samples. The first one is to adjust the annealing data by using Cot scaling (multiplication of time with the sample's concentration (Cot values)). The second consists of adjusting the concentration differences in the model equations by scaling the DNA association rates (Eqs. 1 and 2).

Heteroduplex formation. We tested whether heteroduplexes fluoresce less than homoduplexes, which may explain why highly diverse samples in which heteroduplex formation occurs tend to attain lower levels of fluorescence than homogeneous samples. The oligonucleotides used for these tests were synthesized according to the following format (Eurofins MWG Operon).

Main strand:

GCTGGCGCAGAAATATACAGGTCGGACCTCAGCTGTTACTTACACATCAAACCTCAGCACCTCCGCC

Complementary strand:

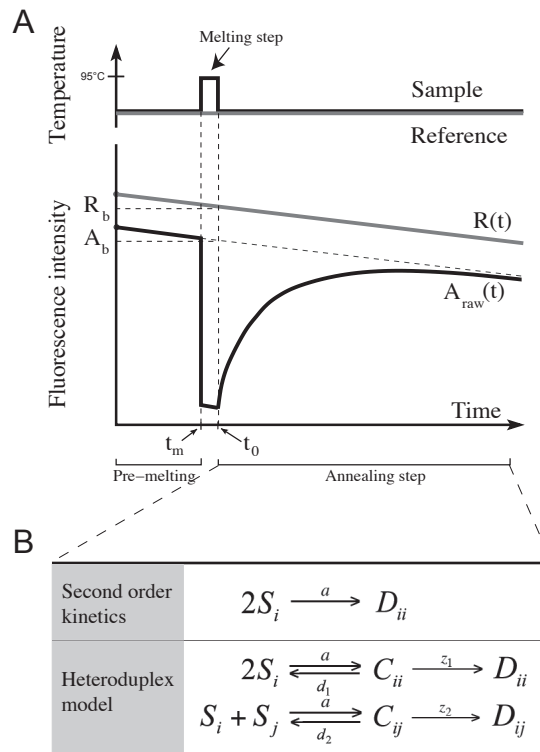GGCGGAGGTGCTGAGGTTTGATGTGTAAGTAACAGCTGAGGTCCGACCTGTATATTTCTGCGCCAGC

Figure 1. The AmpliCot assay and model. A. Samples containing PCR-amplified TCR genes or oligonucleotides are placed on both extremities of a 96-well plate as the samples and the reference. The baseline fluorescence intensity of samples and reference is measured at annealing temperature (premelting step). Samples are then melted at 95 °C and their fluorescence drops (melting step). After 2 min. of melting, the temperature of the samples is quickly set back to annealing temperature to allow for reannealing of DNA strands (annealing step). $A_{raw}(t)$ and $R(t)$ are, respectively, the fluorescence intensities of the samples and reference at time t (minutes), or at the start of the annealing step (A_b and R_b, respectively). B. Two possible models of the biochemical reactions occurring during the annealing step of AmpliCot. Second-order kinetics (*top line*) is the minimal model in which only homoduplexes are formed. The heteroduplex model (*bottom line*) considers the reaction in more detail. The association occurs in two steps (a first encounter, followed by a zipping reaction), and includes the possibility of heteroduplex formation.

Table 1. Four data sets of known diversity templates used in the analysis

Data set	Diversities	Nb. of replicates	Dilution factor
1 (10)	n = 1, 2, 5, 10, 30, 48, 96	1	Same for all n
2	n = 1, 4, 8, 16, 32, 48	2 (n = 1, 4, 8, 16) 1 (n = 32, 48)	1:4 (n = 1, 4) 1:2 (n = 8, 16, 32, 48)
3	n = 10, 20, 30, 40	2	Same for all n
4 (14)	n = 1, 4, 16, 64, 128, 512, 896, 1568, 2744, 4900, 8750, 15,625, 25,000	3	Same for all n

Three mismatches:
GGCGGAGGTGCTGAGGTTTGATGTGTAAGTAACATACGAGGTCCGACCTGTATATTTCTGCGCCAGC
Five mismatches:
GGCGGAGGTGCTGAGGTTTGATGTGTAAGTAACTTACCAGGTCCGACCTGTATATTTCTGCGCCAGC

These oligonucleotides were directly mixed at high concentrations with SYBR green dye and subjected to the AmpliCot procedure. For these experiments, samples were melted at 95 °C and subsequently annealed at 40 °C. We chose this annealing temperature because under these nonstringent conditions both homoduplexes and heteroduplexes will be formed (15;16).

Model. We considered two models describing the biochemical reaction of the annealing step of AmpliCot: second-order kinetics and the heteroduplex model (fig. 1B). We assumed that samples contain a large amount of DNA and that the material is well-mixed, so both models could be described by ordinary differential equations. The main difference between the models is the level of detail incorporated in the description of the underlying biochemical reaction.

Second-order Kinetics. Second-order kinetics is the simplest model describing AmpliCot (fig. 1B). It describes the association (at rate a) of two perfectly complementary single DNA strands under the assumption that the encounter of two complementary strands is the rate limiting step, and that the subsequent hybridization is fast compared to the former process. Under these assumptions, the hybridization of DNA is a second-order reaction (10). Consider a DNA sample of diversity n. Let S_i be the concentration of single-stranded DNA (ssDNA) molecules of type i, where, for simplicity, a certain ssDNA and its complementary strand are both denoted by i. Consequently, D_{ii} is the concentration of homoduplexes of type $i, i = 1, \ldots, n$. The following differential equations describe the second-order kinetics model: (Eq. 1)

$$\frac{dS_i}{dt} = -2aS_i^2$$

$$\frac{dD_{ii}}{dt} = aS_i^2$$

Let $t_0 = 0$ be the beginning of the annealing phase of AmpliCot and let T be the total concentration of DNA strands in a sample (i.e. twice the concentration of dsDNA pre-melting). Let f_i be the proportion of ssDNA of type i at the beginning of the annealing phase. Because a small fraction of DNA molecules may remain in the double-stranded form, we let α be the proportion of melted molecules at t_0 ($\alpha \in [0, 1]$). Thus, the initial conditions are $S_i(0) = \alpha f_i T$, and $2D_{ii}(0) = (1 - \alpha)f_i T, i = 1, \ldots, n$.

Heteroduplex Model. The heteroduplex model (fig. 1B) takes into account the fact that hybridization involves two distinct processes: the association of short, homologous sites on two single strands, followed by a reversible hybridization (17). Two perfectly complementary single strands S_i form a partially hybridized homoduplex C_{ii}. Two partially complementary

strands S_i and S_j can for a partially hybridized heteroduplex C_{ij} (where $j \neq i$). Partially hybridized homoduplexes (resp. heteroduplexes) can dissociate at rate d_1 (respectively, d_2), or hybridize completely at rate z_1 (respectively, z_2) to form the final product D_{ii} (respectively, D_{ij}, $j \neq i$). Note that $C_{ij} = C_{ji}$ and $D_{ij} = D_{ji}$. The differential equations describing the change in time of the above-mentioned concentrations are: (Eq. 2)

$$\frac{dS_i}{dt} = -2aS_i^2 - aS_i \sum_{j \neq i} S_j + 2d_1C_{jj} + d_2 \sum_{j \neq i} C_{ij},$$

$$\frac{dC_{ii}}{dt} = aS_i^2 - (d_1 + z_1)C_{ii},$$

$$\frac{dC_{ij}}{dt} = aS_iS_j - (d_2 + z_2)C_{ij},$$

$$\frac{dD_{ii}}{dt} = z_1C_{ii},$$

$$\frac{dD_{ij}}{dt} = z_2C_{ij}.$$

We assume that the melting process is fast compared to the re-annealing, and that the melting temperature is so high that no re-hybridization is occurring during the melting phase. Under these assumptions, the sample contains only ssDNA or unmelted dsDNA homoduplexes at the beginning of the annealing phase. The initial conditions for the above system are thus $S_i(0) = \alpha f_iT$, $2D_{ii}(0) = (1 - \alpha) f_iT$, $C_{ii}(0) = C_{ij}(0) = D_{ij}(0) = 0$, where $i = 1, \ldots, n$, $j \neq i$, and $\alpha \in [0, 1]$. Note that the heteroduplex model is a generalization of second-order kinetics, when setting $d_1 = d_2 = z_2 = 0$ and $z_1 \rightarrow \infty$ in the heteroduplex model (Eq. 2), one obtains the second-order kinetics model (Eq. 1).

Annealing Kinetics. From the above model definitions, we define the kinetics of fluorescent molecules, $F(t)$. We assume that the latter are proportional to the concentration of double-stranded molecules at time t. In the case of second-order kinetics (SOK), (Eq. 3)

$$F^{SOK}(t) = 2 \sum_{i=1}^{n} D_{ii}(t) = T - \sum_{i=1}^{n} S_i(t).$$

In the case of the heteroduplex model, we let heteroduplexes have a decreased fluorescence intensity compared to homoduplexes (see Results below). This is modeled by weighting their level of fluorescence by a factor $\varphi \in [0, 1]$. The concentration of fluorescent molecules under the heteroduplex model is hence defined as (Eq. 4)

$$F(t) = 2\left(\sum_{i=1}^{n} D_{ii}(t) + \varphi \sum_{i=1}^{n-1} \sum_{j=i+1}^{n} D_{ij}(t)\right).$$

From the above expression (Eq. 4), we define the theoretical annealing curve, $A(t)$, as the proportion of fluorescent material in a sample, i.e., $A(t) = F(t)/T$, where T is the total concentration of DNA strands in a sample. We present here three expressions of the annealing kinetics: with $A(t)$ we denote the solution of the heteroduplex model; $A^{SOK}(t)$ denotes the solution of the second-order kinetics model (i.e. special case of $A(t)$); and $A(t)$, the annealing kinetics of the experimental data.

To obtain a closed form solution of $A(t)$ and $A^{SOK}(t)$, we solved the ODE systems analytically (Eqs. 1 and 2) for the case where all DNA species have the same concentration in the sample, i.e., under the equal molarity assumption (see Appendix 1 for the definition of the result mean-field systems). The equimolarity assumption makes the level of diversity (n) a parameter of the system. Moreover, to solve the heteroduplex model analytically, we applied a quasi-steady state assumption for the transient complexes (see Appendix 2). The above transformations and the definition of $F(t)$ in Eq. 4 yield the expression: (Eq. 5)

$$A(t:n) = \frac{F(t)}{T} = \left(\alpha - \frac{\alpha}{1 + 2\frac{a}{n}\left(\xi_1 + \xi_2\left(\frac{n-1}{2}\right)\right)\alpha T t} \right)$$

$$x \left(\frac{\xi_1 + \varphi\xi_2\left(\frac{n-1}{2}\right)}{\xi_1 + \xi_2\left(\frac{n-1}{2}\right)} \right) + (1 - \alpha),$$

where $\varepsilon_1 = z_1/(z_1 + d_1)$, $\varepsilon_2 = z_2/(z_2 + d_2)$ and n has been highlighted as an argument of the function $A(\cdot)$. Note that $A(t; n) \, \varepsilon \, [1 - \alpha, 1]$. The expression $A^{SOK}(t)$ is a particular case of Eq. 5 and is obtained by setting $\varepsilon_1 = 1$ and $\varepsilon_2 = 0$ in Eq. 5: (Eq. 6)

$$A^{SOK}(t; n) = \frac{F^{SOK}(t)}{T} = 1 - \frac{\alpha}{1 + 2\frac{a}{n}\alpha T t}$$

To obtain the annealing kinetics from the raw experimental data, the experimental data were first normalized by correcting for the baseline fluorescence discrepancies of the reference and the sample and by correcting for the time-dependent fluorescence decline (fig. 1): (Eq. 7)

$$A^{data}(t; n) = \frac{R_b}{A_b}\left(\frac{A_{raw}(t)}{R_{(t)}} \right)$$

where A_b and R_b are the fluorescence intensities of the sample and the reference at the start of the annealing step, which were estimated as the mean of the last ten measurements of the pre-melting phase, assuming that the melting phase was short enough to ensure little loss of fluorescence during melting.

Cot values and annealing kinetics. The acronym "Cot" stands for concentration x time (12). In terms of our model, Cot = Tt. Cot values were used in the original AmpliCot paper (10) in order to compare the annealing speed of samples with different DNA concentrations.

Let $s = Tt$ be a Cot value. The annealing kinetics can be expressed as a function of the Cot value s, by replacing the product Tt with the new variable s in Eqs. (5) and Eq.: (Eq. 8)

$$A(s:n) = \left(\alpha - \frac{\alpha}{1 + 2\frac{a}{n}\left(\xi_1 + \xi_2\left(\frac{n-1}{2}\right)\right)\alpha s} \right)$$

$$\times \left(\frac{\xi_1 + \varphi\xi_2\left(\frac{n-1}{2}\right)}{\xi_1 + \xi_2\left(\frac{n-1}{2}\right)} \right) + (1 - \alpha),$$

(Eq. 9)

$$A^{SOK}(s;n) = 1 - \frac{\alpha}{1 + 2\frac{a}{n}\alpha s}$$

Model fitting. The models (Eq. 6 and Eq. 5) were fitted to experimental data (Eq. 7) using a least squares procedure (implemented in MATLAB 7.10.0, The MathWorks, Natick, MA), applied to the log-transformed annealing curves. The 95% confidence intervals on parameter values were computed using 999 bootstrap replicates of each original data set. The bootstrap was done by sampling points $(t_i, A_{raw}(t_i))$ from the raw annealing curves with replacement. The bootstrap replicates were fitted in the same way as the original data set. The confidence intervals were computed using order statistics of the bootstrap distribution (18).

RESULTS

Heteroduplexes give a lower fluorescence signal than homoduplexes. It was previously observed that samples of very high diversity may not reach the 50% annealing point (13). One hypothesis that would explain these observations states that the low concentration of perfectly complementary strands inside a huge excess of highly similar sequences results in the rapid formation of heteroduplexes, which will give a lower SYBR green fluorescence signal than homoduplexes (19;20). This would result in over-estimation of the diversity of a given sample. Indeed, when we mixed oligonucleotides that were either perfectly complementary or contained three or five mismatches (i.e., a mismatch of 5% or 7.5% of the oligonucleotide length, respectively) at a temperature (40°C) well below their melting points, we observed the formation of heteroduplexes with a lower fluorescence intensity than homoduplexes (fig. 2). The fluorescence level of the sample decreased as the number of mismatches in the complementary strand increased. These results show that heteroduplex formation may significantly influence the results of an AmpliCot experiment.
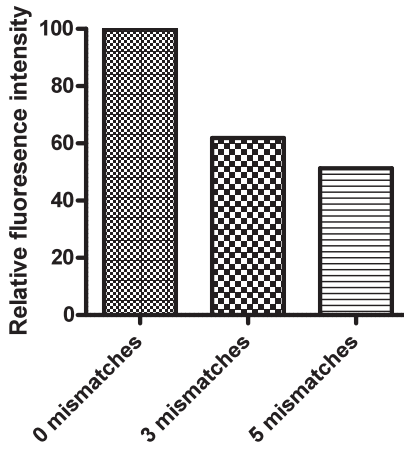
Figure 2. Heteroduplexes have a lower fluorescence intensity than homoduplexes. Formation of double stranded DNA products was analyzed at an annealing temperature of 40 °C for ssDNA samples with 0, 3 or 5 nucleotide mismatches. The fluorescence signal of two complementary strands (homoduplex) was set to 100% and the fluorescence intensity of heteroduplexes was expressed as a percentage of the fluorescence intensity of homoduplexes.

Generalized expression for Cot values as function of diversity (Cot$_p$(n)). The relation between Cot (concentration x time) values and diversity is important for the correct interpretation of the AmpliCot assay. Cot values of templates of known diversity are used to calibrate the assay, and are the benchmark for the inter- or extrapolation to unknown diversities. The procedure proposed in the original AmpliCot paper (10) presumes the validity of second-order kinetics, i.e., it assumes that no heteroduplexes or temporary complexes are formed. We present here a mathematical expression that describes how Cot values depend on the diversity of the sample (n). The expression is based on the relaxed assumption that the annealing kinetics behave according to the heteroduplex model (Eq. 2), which is a generalization of second-order kinetics. Let s^* be the Cot value for which a fraction p of a sample has annealed. We computed the formula presented hereafter by setting $A(s^*; n) = p$ in Eq. 8 and by solving for s^*. We call the generalized Cot expression $\mathrm{Cot}_p(n) = A^{-1}(s^*; n)$ (Eq. 10). Here the fraction annealed, p, is considered as a parameter and the diversity, $n \geq 1$, is the independent variable, for (Eq. 10)

$$\text{Generalized Cot} = \mathrm{Cot}_p(n) = \frac{1}{2a\alpha}\left(\frac{\alpha - (1 - p)}{\xi_1(1 - p) + \xi_2[(1 - p) + \alpha(\varphi - 1)]\left(\frac{n-1}{2}\right)}\right)n,$$

Where $\varepsilon_1 = z_1/(z_1+d_1)$ (respectively. $\varepsilon_2 = z_2/(z_2+d_2)$) is the proportion of homoduplexes (resp. heteroduplexes) that hybridize completely. A list of all parameters is provided in table 2. The expression of $\mathrm{Cot}_p(n)$ in the case of second-order kinetics can be derived either from Eq. 10 by setting $\varepsilon_1 = 1$ and $\varepsilon_2 = 1$, or by finding the value s^* for which $A^{SOK}(s^*) = p$ in Eq. 6: (Eq. 11)

$$\mathrm{Cot}_p^{SOK}(n) = \frac{1}{2a\alpha}\left(\frac{\alpha}{1 - p} - 1\right)n.$$

Importantly, the latter expression is linear in n, whereas the generalized Cot expression (Eq. 10) is a rational (nonlinear) function of n.

Table 2. Parameters, their meaning, and typical ranges

Parameter	Meaning	Range	Typical value
a	Association rate of two single DNA strands	>0	-
d_1	Dissociation rate of a partially hybridized homoduplex	>0	-
d_2	Dissociation rate of a partially hybridized heteroduplex	>0	-
z_1	Hybridization rate of a homoduplex	>0	-
z_2	Hybridization rate of a heteroduplex	>0	-
ξ_1	Composite parameter = $z_1/(z_1 + d_1)$	[0,1]	Close to 1
ξ_{12}	Composite parameter = $z_2/(z_2 + d_2)$	[0,1]	Close to 0
α	Proportion of melted molecules at start of annealing	[0,1]	>0.5
φ	Weight factor for the fluorescence of heteroduplexes	[0,1]	>0.5
n	Diversity	>0	-
p	Annealing proportion	[0,1]	-
T	Total concentration of single DNA strands in a sample	>0	-
A_b	Baseline fluorescence of a sample	>0	-
R_b	Baseline fluorescence of a reference	>0	-

Some parameters can differ in each experiment; in that case, typical values are not provided.

To illustrate the difference between the dynamics of second-order kinetics and the heteroduplex model, we plotted the annealing kinetics of both models for one set of parameter values and three diversities (fig. 3A). Although the diversity increases 10-fold between the curves (n = 10, n = 100, n = 1000), the annealing speed (reflected, in the Cot 50% value) in the case of the heteroduplex model does not decrease 10-fold, as it does under second-order kinetics, because the function $\text{Cot}_{0.5}(n)$ of Eq. 10 exhibits a concave (saturating) shape (fig. 3B). Note that the discrepancies between both Cot curves are small for low diversities, but the deviation from linearity becomes more apparent as diversity increases. Indeed, the higher the diversity, the more heteroduplexes are expected to be formed. Note that for n = 1, the heteroduplex model ($\text{Cot}_p(n)$, Fig. 3B) reveals a slightly higher Cot value even though heteroduplexes cannot be formed. This is due to the formation of temporary complexes (C_{ii}) in this model that delay the annealing process.

Annealing time-series data: heteroduplex model fits significantly better than second-order kinetics. To compare the validity of both models, we fitted Eqs 5 and 6 to the time-series of data sets 1 - 3 (table 1). The fits of both models to the annealing curves are depicted in fig. 4 where, due to space limitation, only three diversities per data set are presented. The fits of the full data sets can be found in Section S1 in the Supporting Material; the corresponding best-fitting parameters and their confidence intervals are given in section S2 in the Supporting Material. Note that the horizontal axes of the annealing curves are given in time units. We corrected for concentration differences in the data by adjusting the DNA association rate a in the model (a was multiplied by T, the estimated total ssDNA concentration in a sample, which, under the quasi-steady-state assumption, is equivalent to using a Cot scale in the data).
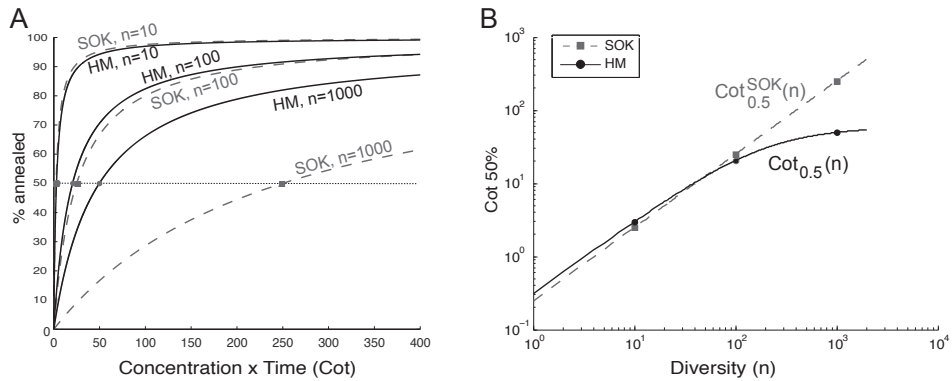
Figure 3. Second-order kinetics (SOK) and the heteroduplex model (HM) exhibit different annealing kinetics and diversity-Cot relations. A. Annealing kinetics as function of Cot values for three diversities (n = 10, n = 100, n = 1000) and both models (SOK: *dashed*; HM: *solid*). The chosen parameter values are similar to the best-fitting parameters for data set 1 (fig. 4): a = 2, ε_1 = 0.8, ε_2 = 0.009, φ = 0.97, α = 1, T = 1. B. Cot 50% values were computed using Eq. 10 (*solid*) and Eq. 11 (*dashed*) and were plotted as function of diversity for the same parameter values as in panel A. The relation between diversity and Cot values is linear under second-order kinetics, whereas the heteroduplex model reveals a saturating $\mathrm{Cot}_{0.5}(n)$ relation. Note that for n = 1, both models reveal slightly different Cot values even though heteroduplexes cannot be formed. This is due to transient duplex formation.

Visual inspection of these fits revealed a small difference between the performance of both models on the data set 1 (fig. 4A). The models clearly differ in fitting the time course of data set 2 (fig. 4B), where second-order kinetics was unable to reproduce the correct curvature and the apparent asymptotic value of the data, especially for high diversities. Similarly, second-order kinetics failed to give the correct asymptote value in the fit of data set 3 (fig. 4C). A formal statistical analysis, accounting for the different number of parameters in each model (likelihood ratio test for nested models, based on the x-square distribution (18)), indicated that the improvement brought by the heteroduplex model is significant for all three data sets (p-value < 10^{-3}).

Cot values as a function of diversity: heteroduplex model captures non-linear relationship, second order kinetics does not. Although the heteroduplex model gave a significantly better fit to all three AmpliCot time-series data, in some cases the visual difference between the fit of the second-order kinetics and the heteroduplex model was not very large. Small differences in the fit to the full annealing curve may, however, lead to large differences in the estimated Cot value, especially for higher Cot values that fall in the saturating part of the annealing curve. We therefore investigated the relationship between Cot values and the diversity n under second-order kinetics and the heteroduplex model. We used data sets 1 - 3 to estimate Cot 50% and Cot 80% values ($\mathrm{Cot}_p^{\mathrm{data}}(n)$, p = {0.5, 0.8}), which we plotted against diversity n (fig. 5). For comparison, we also computed $\mathrm{Cot}_p(n)$ and $\mathrm{Cot}_p^{\mathrm{SOK}}(n)$, p = {0.5, 0.8}, using Eqs. 10 and 11, given the best-fit parameters to each full data set (Table S1), described in the previous section.
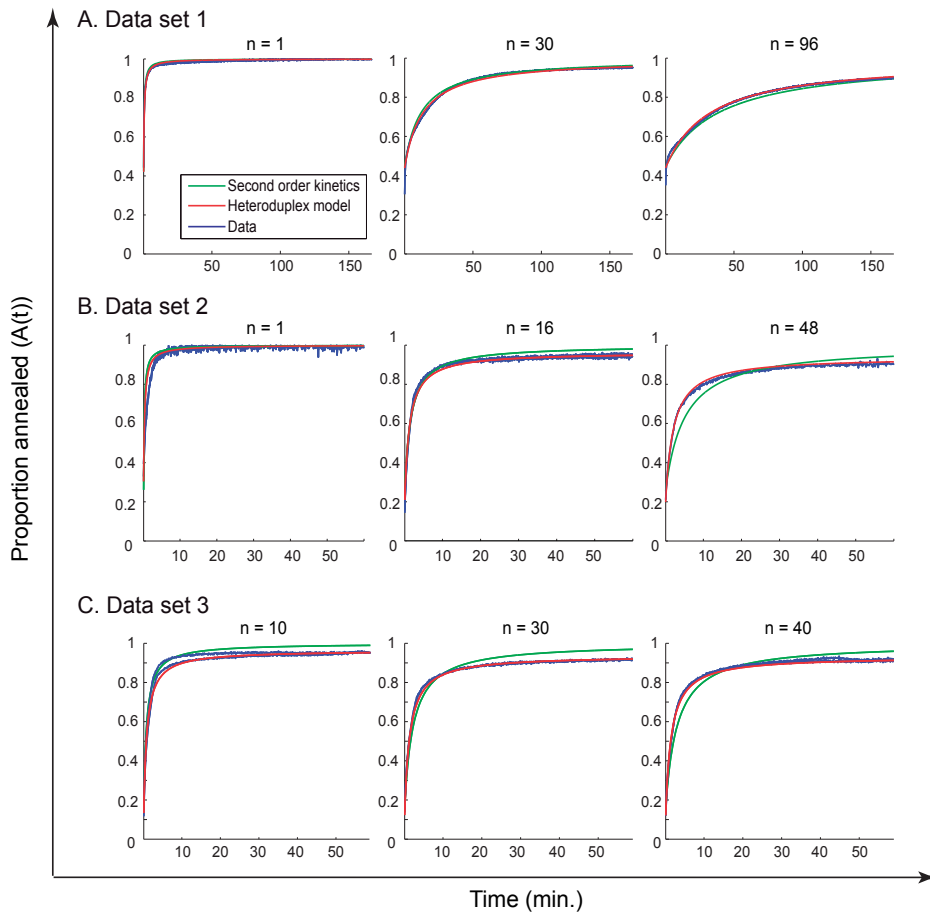
Figure 4. Best-fits of data sets 1 - 3 (A-C) for known diversity templates. (with the lowest, an intermediate and the diversities of each data set shown; all other diversities are given in section S1 in the Supporting Material) (*Solid blue*) Data sample (one or two replicates). (*Dashed green*) Best-fit of the second-order kinetics model (Eq. 6). (*Dashed-dotted red*) Best-fit of the heteroduplex model (Eq. 5). For the best-fitting parameters and their confidence intervals, see table S1 in the Supporting Material. The heteroduplex model results in a significantly better fit to the data than the second-order kinetics model (p-value < 10^{-3} for the three data sets).

Interestingly, Cot values that were directly estimated from the experimental data (Cot_p^{data}) presented a clear deviation from linearity (for all data sets) and exhibited a concave shape, similar to the one predicted by the heteroduplex model. As a result, Cot_p (n) curves were in general better captured by the heteroduplex model ($Cot_p(n)$) than by second-order kinetics (Cot_p^{SOK} (n)). The only exception is the description of Cot 50% values of data set 1, which is poor for both models (fig. 5A), because the Cot 50% value could hardly be read-out for this data set. The results of fig. 5 suggest that, in general, Cot values based on the generalized $Cot_p(n)$ expression (Eq. 10) yield more accurate diversity estimates than those based on second-order (Cot_p^{SOK} (n), Eq. 11).
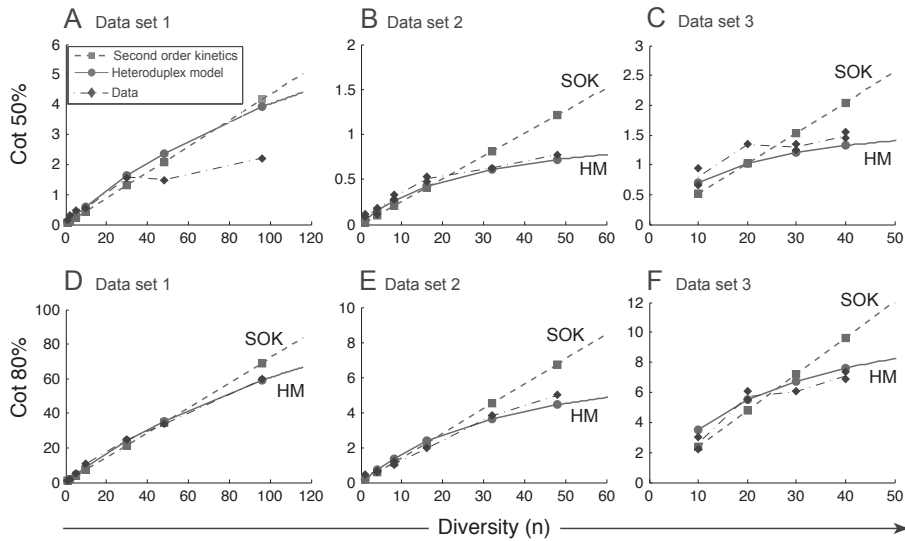
Figure 5. The generalized (nonlinear) Cot$_p$(n) expression reproduces Cot values of the experimental data better than second-order kinetics. The behavior of Cot 50% (*A-C*) and Cot 80% (*D-F*) as function of diversity was computed under both models: second-order kinetics (■ Eq. 11) and the heteroduplex model (●, Eq. 10). The best-fitting parameters of the time-series fits (table S1) were used. Cot 50% and 80% of the experimental data are also plotted (♦). The difference between both models is amplified as diversity increases. Connecting lines are shown to help the visualization of the trend.

Heteroduplex model also captures nonlinear trend of highly diverse samples. Driven by our finding that Cot values are better described with the heteroduplex model, we assessed our new formula for Cot$_p$(*n*) by fitting it directly to diversity-Cot relationships of data sets 1, 2 and 4, without first fitting the annealing time-series data. We omitted data set 3 because it contains too few different diversities to fit the five parameters of the generalized Cot expression. On the contrary, the recently published data set 4 (14) contains diversities that differ by several orders of magnitude and is thus particularly well suited for testing our new formula.

In fig. 6 are depicted the fits of Eq. 10 and Eq. 11 to the Cot 50% and 80% values of the different data sets. The annealing duration in data set 4 was too short to compute Cot 80% values, so we used Cot 70% annealing points instead. Note that the data of panels *A*, *B*, *D* and *E* of fig. 6 are the same as the data in the corresponding panels of fig. 5. Similarly to data sets 1-3, Cot values of data set 4 revealed a clear deviation from linearity at high diversities. Such deviation is clearly observed in all data sets and is well captured by the Cot expression based on the heteroduplex model (Eq. 10), in contrast to the Cot expression based on second-order kinetics (Eq. 11). Note that a convex shape was observed for Cot 50% values of data set 4, whereas Cot 70% and Cot 80% values exhibited a concave curvature. Both were well captured by the generalized Cot expression (fig. 6 C,F). Indeed, Eq. 10 is a rational function of diversity and hence allows for the reproduction of both convex and concave shapes. These correspond, respectively, to both asymptote-bounded arms of the function. To test whether the heteroduplex model (Eq. 10) fits the observed Cot values significantly better than second-order kinetics (Eq. 11), we applied a
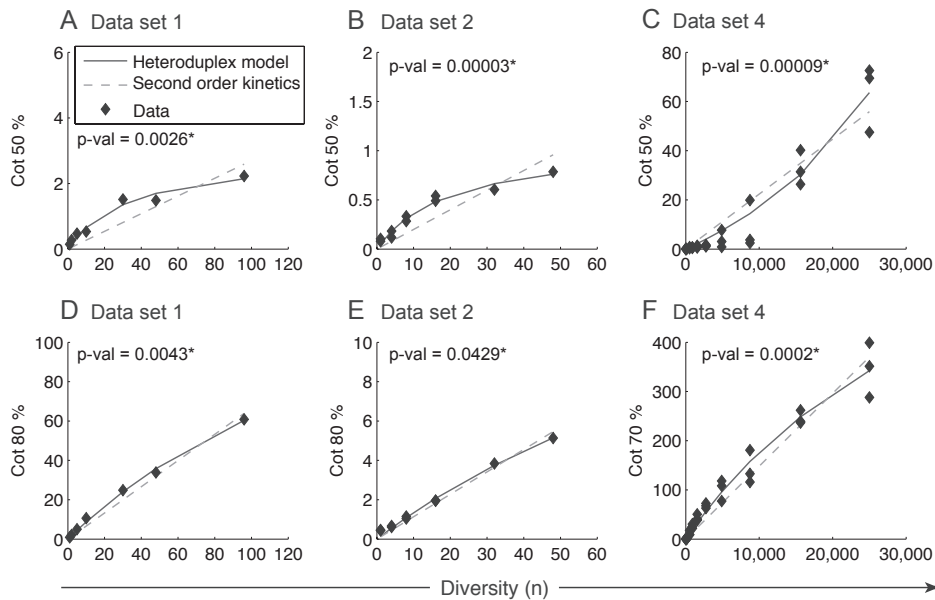
MATHEMATICAL MODELING OF AMPLICOT

Figure 6. Generalized (nonlinear) Cot$_p$(n) expression (Eq. 10) reproduces the diversity-Cot 50% and 80% relationships of data sets 1, 2 and 4 (A-F) better than the Cot$_p$(n) expression (Eq. 11). The Cot expression based on the heteroduplex model (*solid line*) and the Cot expression based on second-order kinetics (*dashed line*) were fitted to Cot 50% or Cot 80% values (*diamonds*), without calibrating the model on time-series annealing data. The highest Cot value assessable in data set 4 was Cot 70%. The best-fitting parameters to the data can be found in table S2 and Section S3 of the Supporting Material. The *p*-values of a likelihood ratio test for nested models are indicated in each panel. The fit of the generalized Cot expression was considered significantly better than the fit of Cot[SOK]*p* at level 95% when the *p*-value was <0.05 (indicated by*).

likelihood ratio test for nested models (18). Statistical significance was reached for all fits (see *p*-values in the *upper left corners* of each panel of fig. 6). Hence, in addition to better describing time-series annealing data, the heteroduplex model is also better at fitting Cot values directly, especially for highly diverse samples, such as those of data set 4.

Generalized Cot analysis: diversity estimation procedure. We formally define here an alternative to the original Cot analysis for the interpretation of AmpliCot experimental data. Our method allows the estimation of an unknown diversity from a library of known diversities and provides a more general alternative to the original method (10). The method consists of four steps. We suggest to use not only one, but several annealing proportions for better calibration. Second, the raw annealing data of the templates with known diversity are normalized to estimate the Cot$_p$ values necessary for the calibration of the generalized Cot expression. Third, the parameter values of Eq. 10 are determined by fitting this equation to Cot values of the data (for all predetermined annealing proportions). Finally, the unknown diversity is estimated by using the inverse of the calibrated Cot$_p$(*n*) relation and the measured Cot value of the sample to assess. The algorithm of our diversity estimation procedure is given below.

Diversity Estimation Algorithm:

1. Choose an appropriate set of values of *p* (annealing proportions).
2. Normalize the raw data using Eq. 7 and estimate the Cot_p values of the templates with known diversity.
3. Fit the parameters (a, α, ε_1, ε_2, φ) of the generalized Cot expression (Eq. 10) to the Cot data of the templates of known diversity.
4. Using the Cot value of the sample with unknown diversity, estimate its diversity from the generalized Cot curve fitted above.

DISCUSSION

A framework for better understanding and analysis of AmpliCot data. By means of mathematical modeling, we developed a general framework for the understanding and interpretation of AmpliCot data. We showed that the initially assumed underlying model, second-order kinetics (10), might not always be the best way to describe the DNA annealing kinetics. This was revealed by the model-fit of annealing time-series data and by the deviation from linearity of the Cot-diversity relation. We developed an alternative, the heteroduplex model, which describes the underlying biochemical reaction in further detail and reproduces the non-linear nature of Cot values as a function of diversity.

In the original AmpliCot paper, the authors assumed a linear relation between Cot values and calibrating diversities (10). We showed that this linear relation is indeed correct under second-order kinetics, i.e., in the absence of heteroduplexes and temporary duplexes (Eq. 11). However, under the heteroduplex model, the generalized $Cot_p(n)$ expression is not linear. Indeed, Eq. 10 is a rational function of n. Intuitively, the possibility of formation of partially fluorescent heteroduplexes results in a faster annealing for a given diversity and concentration. Instead of only binding to perfectly matching strands, some DNA molecules may associate to partially complementary molecules. The resulting heteroduplexes still contribute to the observed fluorescence but to a lesser extent, as we showed experimentally (fig. 2).

The presence of heteroduplexes with lower fluorescence levels can also explain the observation of Schütze et. al (13) who noted that reannealed samples did not reach their preanneal fluorescence intensity, even after correction for the fluorescence decline due to dye degradation. We also considered two alternative explanations for this phenomenon. The first hypothesis is that no heteroduplexes are formed, but homoduplexes may constantly associate and dissociate because the annealing temperature is very close to the melting temperature. We fitted such a model to the data and although it accounted for the above-mentioned loss of fluorescence, it did not explain the early time-course of the annealing curves (results not shown) and it yielded a significantly lower quality of fit compared to the heteroduplex model. The second alternative explanation that we tested is that the intensity of the SYBR green dye is diminished after melting. However, this explanation did not account for the observed dependence on diversity of the fluorescence loss. The heteroduplex formation leading to a lower SYBR green signal was therefore the most likely explanation.

Generic and easy-to-use diversity estimation procedure. We propose what to our knowledge is a novel procedure allowing the estimation of a sample's diversity from a library of known calibration diversities. Our procedure is based on the result that the heteroduplex model is the one that best describes AmpliCot data. The advantage of this new method over the second-order kinetics-based approach is that our method encompasses both underlying models. Indeed, the Cot expression of Eq. 10 is a generalization of the expression based on second-order kinetics. Therefore, it can be applied both to samples that exhibit few or no heteroduplexes (10;14), as well as to samples in which heteroduplex formation is suspected (13). The data itself will determine the degree of deviation from linearity (if any) of the diversity - Cot relation. Our new method is simple to use, as it requires the manipulation of one single formula (Eq. 10). It is also computationally efficient (complexity similar to the one of the second-order kinetics-based method), because it is directly calibrated on Cot values.

Limitations. When using our diversity estimation procedure, one should be careful in the parameter calibration step based on Cot values. Being a rational function of diversity, the generalized Cot expression (Eq. 10) has one vertical and one horizontal asymptote. When extrapolating unknown diversities that are expected to be different from the calibration set, one should be aware that the horizontal asymptote may render the estimation impossible. For example, this could happen if the calibrated parameters result in an asymptote below the Cot value of the sample with unknown diversity. To circumvent such problems, one could alternatively use the time-series data to calibrate parameters of the heteroduplex model in step 3 of the estimation procedure. The larger amount of information contained in time-series data is expected to result in more robust parameter estimates, and may reduce the number of calibrating diversities that are needed to make a sound estimation.

Applications. The correct calibration of AmpliCot is crucial for the estimation of an unknown diversity. If one uses a linear approximation by assuming second-order kinetics, the diversity estimation may be biased, as revealed by our nonlinear fits of the heteroduplex model to experimental data. In their recent articles, Baum et al. (11;14) proposed a method for estimating the absolute number of unique TCRβ chain rearrangements in a blood sample. AmpliCot is part of this integrated method and the assay was used to estimate the absolute diversity of several independent VβJβ pairs of CD4$^+$ naive T cells. The overall procedure resulted in highly reproducible estimates, but the authors consistently reported lower diversities than expected. Instead of the anticipated 100,000 or 200,000 cells with unique TCR sequences, the authors measured approximately two-fold lower diversities (fig. 5 of Baum et al. (11)). The authors suggested several reasons for this discrepancy: the potential existence of expanded clones, the phenotype reversion of atypical memory cells, and the higher probability of occurrence of some TCR rearrangements (11), which all seem entirely plausible. Our analysis of the calibration set published by Baum et al. (11) (data set 4) revealed a clear deviation from linearity (fig. 6, C and F) that, in the case of Cot 50%, could be another reason for the underestimation of the true diversity.

Conclusion. In summary, we show that deviations from linearity are well represented by the heteroduplex model. The use of a linear model could lead to under- or overestimation of unknown diversities, which could be improved by the use of the heteroduplex model.

APPENDIX 1: MEAN FIELD MODELS

The mean field models take advantage of the fact that all DNA strands in the sample are present in equal concentration in the sample. This equimolarity assumption allows to reduce the dimension of the ordinary differential equations and to render them independent of diversity.

Mean-field second-order kinetics. Let

$$t = \sum_{i=t}^{n} S_i(t) \text{ and } D(t) = \sum_{i=1}^{n} D_{ii}(t).$$

If all DNA strands are present in equimolar concentrations in the mixture, we have $S_i(t) = S_j(t)$, $\forall t$. Therefore, $S(t) = nS_i(t)$, $D(t) = {}_nD_{ii}(t)$ and the ODE system of Eq. 1 becomes (Eq. 12)

$$\frac{dS}{dt} = -2a\frac{S^2}{n},$$

$$\frac{dD}{dt} = a\frac{S^2}{n},$$

where we have used the fact that $nS_i = S/n$. The initial conditions are

$$S(0) = \alpha T \text{ and } 2D(0) = (1 - \alpha)T,$$

and the fluorescent molecules are

$$F(t) = 2D(t)$$

Mean-field heteroduplex model. Assuming equimolar concentrations of each species, we define the following quantities: (Eq. 13)

$$S(t) = \sum_{i=1}^{n} S_i(t) = nS_1(t),$$

$$C(t) = \sum_{i=1}^{n} C_{ii}(t) = nC_{11}(t),$$

$$H(t) = \sum_{i=1}^{n-1} \sum_{j=i+1}^{n} C_{ij}(t) = \frac{n(n-1)}{2}C_{12}(t),$$

$$J(t) = \sum_{i=1}^{n-1} \sum_{j=i+1}^{n} D_{ij}(t) = \frac{n(n-1)}{2} D_{12}(t),$$

$$D(t) = \sum_{i=1}^{n} C_{ii}(t) = nD_{11}(t),$$

where indices 1 and 2 have been chosen arbitrarily to design one species. *S(t)* denotes ssDNA, *C(t)*, partially hybridized homoduplexes, *H(t)*, partially hybridized heteroduplexes, *J(t)*, final product heteroduplexes, and *D(t)*, the final homoduplexes. The differential equations of Eq. 2 can be written in terms of the above variables as (Eq. 14)

$$\frac{dS}{dt} = -a\,(n+1)\frac{S^2}{n} + 2d_1 C + 2d_2 H,$$

$$\frac{dC}{dt} = a\,\frac{S^2}{n} - (d_1 + z_1)C,$$

$$\frac{dH}{dt} = a\,\left(\frac{n-1}{2}\right)\frac{S^2}{n} - (d_2 + z_2)H,$$

$$\frac{dJ}{dt} = z_2 H,$$

$$\frac{dC}{dt} = z_1 C,$$

with initial conditions

$$S(0) = \alpha T,$$

$$2D(0) = (1 - \alpha)T,$$

$$C(0) = H(0) = J(0)$$

and fluorescent molecules

$$F(t) = 2(D(t) + \varphi J(t)).$$

APPENDIX 2: MODEL SOLUTION

Second-order Kinetics. The solution of the ODE system of Eq. 12 with initial conditions

$$S(0) = \alpha T \text{ and } 2D(0) = (1 - \alpha)T$$

Is

$$S(t) = \frac{\alpha T}{1 + 2\frac{a}{n}\alpha T t}$$

$$D(t) = \frac{1}{2}\left(1 - \frac{\alpha}{1 + 2\frac{a}{n}\alpha T t}\right)T.$$

Heteroduplex model. We present here an analytical solution of the heteroduplex model of Eq. 14 under a quasi-steady state condition. If the association/dissociation rates a, d_1, d_2 of transient complexes $C(t)$ and $H(t)$ are large compared to the final duplex formation rates z_1 and z_2, we can assume that the transient complexes quickly reach a steady-state. By setting their corresponding time-derivatives to 0, we get (Eq. 15)

$$C = \frac{a}{n(d_1 + z_1)}S^2,$$

(Eq. 16)

$$H = \frac{a}{n(d_2 + z_2)}\left(\frac{n-1}{2}\right)S^2.$$

By inserting Eqs. 15 16 in the initial system (Eq. 14), we get: (Eq. 17)

$$\frac{dS}{dt} = -2K(n)S^2,$$

$$\frac{dJ}{dt} = \frac{a}{n}\left(\frac{z_2}{d_2 + z_2}\right)\left(\frac{n-1}{2}\right)S^2,$$

$$\frac{dD}{dt} = \frac{a}{n}\left(\frac{z_1}{d_1 + z_1}\right)S^2,$$

Where (eq 18)

$$K(n) = \frac{a}{n}\left(\frac{z_1}{d_1 + z_1} + \frac{z_2}{d_2 + z_2}\left(\frac{n-1}{2}\right)\right).$$

By using the initial conditions, we obtain the following solution of Eq. 17: (Eq. 19)

$$S(t) = \frac{\alpha T}{1 + 2K(n)\alpha T t},$$

$$J(t) = \frac{a}{n}\left(\frac{z_2}{d_2 + z_2}\right)\left(\frac{n-1}{2}\right)\frac{1}{2K(n)}\left(\alpha T - S(t)\right),$$

$$D(t) = \frac{a}{n}\left(\frac{z_1}{d_1 + z_1}\right)\frac{1}{2K(n)}\left(\alpha T - S(t)\right) + \left(\frac{1-\alpha}{2}\right)T.$$

MATHEMATICAL MODELING OF AMPLICOT

REFERENCE LIST

1. Goldsby RA, Kindt TJ, Osborne BA, Kuby J. Immunology. W.H. Freeman and company, New York, **2003**.

2. Robins HS, Campregher PV, Srivastava SK, et al. Comprehensive assessment of T-cell receptor beta-chain diversity in alphabeta T cells. Blood **2009 Nov 5**;114(19):4099-107.

3. Currier JR, Robinson MA. Spectratype/immunoscope analysis of the expressed TCR repertoire. Curr Protoc Immunol **2001 May**;Chapter 10:Unit.

4. Pannetier C, Cochet M, Darche S, Casrouge A, Zoller M, Kourilsky P. The sizes of the CDR3 hypervariable regions of the murine T-cell receptor beta chains vary as a function of the recombined germ-line segments. Proc Natl Acad Sci U S A **1993 May 1**;90(9):4319-23.

5. Boyd SD, Marshall EL, Merker JD, et al. Measurement and clinical monitoring of human lymphocyte clonality by massively parallel VDJ pyrosequencing. Sci Transl Med **2009 Dec 23**;1(12):12ra23.

6. Freeman JD, Warren RL, Webb JR, Nelson BH, Holt RA. Profiling the T-cell receptor beta-chain repertoire by massively parallel sequencing. Genome Res **2009 Oct**;19(10):1817-24.

7. Mardis ER. Next-generation DNA sequencing methods. Annu Rev Genomics Hum Genet **2008**;9:387-402.

8. Shendure J, Ji H. Next-generation DNA sequencing. Nat Biotechnol **2008 Oct**;26(10):1135-45.

9. Wang C, Sanders CM, Yang Q, et al. High throughput sequencing reveals a complex pattern of dynamic interrelationships among human T cell subsets. Proc Natl Acad Sci U S A **2010 Jan 26**;107(4):1518-23.

10. Baum PD, McCune JM. Direct measurement of T-cell receptor repertoire diversity with AmpliCot. Nat Methods **2006 Nov**;3(11):895-901.

11. Baum PD, Young JJ, McCune JM. Measurement of absolute T cell receptor rearrangement diversity. J Immunol Methods **2011 May 31**;368(1-2):45-53.

12. Britten RJ, Kohne DE. Repeated sequences in DNA. Hundreds of thousands of copies of DNA sequences have been incorporated into the genomes of higher organisms. Science **1968 Aug 9**;161(3841):529-40.

13. Schutze T, Arndt PF, Menger M, et al. A calibrated diversity assay for nucleic acid libraries using DiStRO--a Diversity Standard of Random Oligonucleotides. Nucleic Acids Res **2010 Mar**;38(4):e23.

14. Baum PD, Young JJ, Zhang Q, Kasakow Z, McCune JM. Design, construction, and validation of a modular library of sequence diversity standards for polymerase chain reaction. Anal Biochem **2011 Apr 1**;411(1):106-15.

15. Ishii K, Fukui M. Optimization of annealing temperature to reduce bias caused by a primer mismatch in multitemplate PCR. Appl Environ Microbiol **2001 Aug**;67(8):3753-5.

16. Sipos R, Szekely AJ, Palatinszky M, Revesz S, Marialigeti K, Nikolausz M. Effect of primer mismatch, annealing temperature and PCR cycle number on 16S rRNA gene-targetting bacterial community analysis. FEMS Microbiol Ecol **2007 May**;60(2):341-50.

17. Wetmur JG, Davidson N. Kinetics of renaturation of DNA. J Mol Biol **1968 Feb 14**;31(3):349-70.

18. Le Boudec JY. Performance evaluation of computer and communication systems. EPFL Press, Lausanne **2010 Jan 1**.

19. Colborn JM, Byrd BD, Koita OA, Krogstad DJ. Estimation of copy number using SYBR Green: confounding by AT-rich DNA and by variation in amplicon length. Am J Trop Med Hyg **2008 Dec**;79(6):887-92.

20. Schneeberger C, Speiser P, Kury F, Zeillinger R. Quantitative detection of reverse transcriptase-PCR products by means of a novel and sensitive DNA stain. PCR Methods Appl **1995 Feb**;4(4):234-8.

21. Carpenter J, Bithell J. Bootstrap confidence intervals: when, which, what? A practical guide for medical statisticians. Stat Med **2000 May 15**;19(9):1141-64.

SUPPORTING MATERIAL

S1. Fit of Time-Series Data. The best-fit parameters of both second-order kinetics and the heteroduplex model to the time-series data sets 1-3 are given in fig. S1, fig. S2 and fig. S3.

S2. Best-Fit Parameters: Time-Series Data. The best-fit parameters of both models fitted to the different time-series data of fig. S1, fig. S2 and fig. S3 are given in table S1.

For all data sets the association rate a is lower under the heteroduplex model than under second-order kinetics, whereas the proportion α of melted molecules at was higher under the heteroduplex model than under second-order kinetics. Since $\xi_1 = \frac{z_1}{(d_1 + z_1)}$ was above 0.5, i.e., the zipping rate z_1 was larger than the dissociation rate d_1, transient homoduplexes have a higher probability to permanently hybridize than to dissociate. Because $\xi_2 = \frac{z_2}{(d_2 + z_2)} < 0.5$, transient heteroduplexes tend to dissociate rather than to hybridize completely.

Of interest are the quantitative differences between the best-fit parameters of the three data sets. First, the proportion of melted molecules α is larger for data sets 2 and 3 than for data set 1. Possibly, more time elapsed between the effective start of the annealing phase and the first measurement in data set 1. Second, we observed that ξ_2 in data set 1 is one order of magnitude smaller than in the other data sets. This means that in data set 1, only a few heteroduplexes were formed. Indeed, the closer ξ_2 is to 0, the larger d_2 (the dissociation of transient heteroduplexes) is compared to z_2 (the zipping of heteroduplexes). Finally, the fluorescence of heteroduplexes in the first data set is only slightly lower than the fluorescence of homoduplexes ($\Phi \approx 0.97$), whereas in data sets 2 and 3, it is about 90% of that of homoduplexes ($\Phi \approx 0.9$). This difference can be caused by the structural difference of the oligonucleotides used in the three data sets.
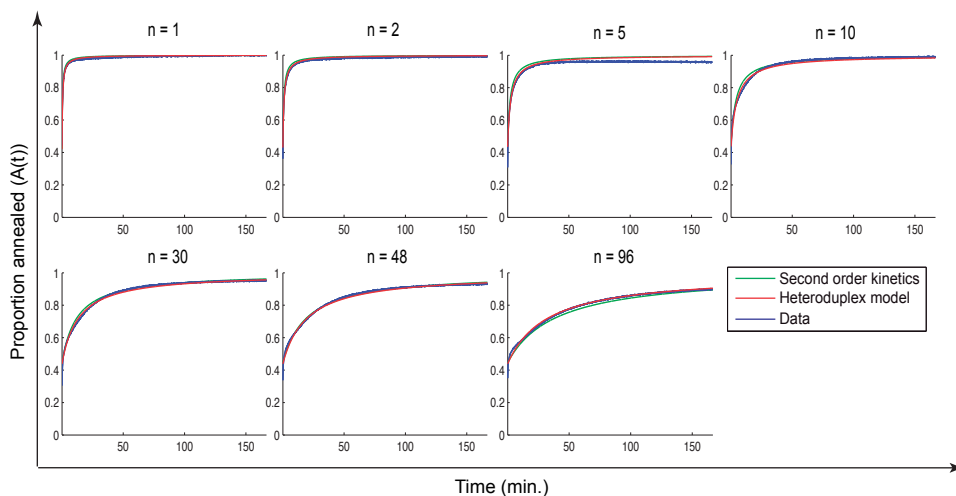

Figure S1. Best-fit of Baum&McCune's data ((10), fig.2a) for known diversity templates (each panel. Blue: experimental data. Green: best-fit of the second-order kinetics model. Red: best-fit of the heteroduplex model. For the best-fit parameters and confidence intervals, see Table S1. The heteroduplex model fits significantly better than second-order kinetics (p-value $< 10^{-3}$).

Table S1. Best-fit reaction rates and 95% confidence intervals (CI)

Model	Param.	Data set					
		1		**2**		**3**	
		Value	95% CI	Value	95% CI	Value	95% CI
	ML	35 577		10 835		7051	
SOK	a	2.2160	[2.1835, 2.2535]	12.9887	[12.3851, 13.6816]	7.9439	[7.6179, 8.2326]
	α	0.5532	[0.5462, 0.5605]	0.7435	[0.7123, 0.7741]	0.8423	[0.8210, 0.8588]
	ML	39 444		13 635		11 343	
	a	2.1719	[1.7439, 3.7591]	9.3091	[9.0372, 16.4313]	6.5503	[3.9625, 9.5867]
HM	α	0.5608	[0.5524, 0.5697]	0.8180	[0.7795, 0.8497]	0.8930	[0.8715, 0.9443]
	ξ_1	0.7962	[0.4639, 1.0000]	0.9994	[0.5195, 1.0000]	0.6275	[0.3813, 0.9982]
	ξ_2	0.0093	[0.0052, 0.0112]	0.0923	[0.0521, 0.0946]	0.0884	[0.0534, 0.1397]
	φ	0.9703	[0.9482, 0.9946]	0.8915	[0.8824, 0.8970]	0.8969	[0.8912, 0.9051]

Each model was fitted to the annealing data of data sets 1-3 (fig. S1, fig. S2, fig. S3) by minimizing the sum of squared errors (on log scale). ML is the maximum likelihood of the best-fit. $\xi_1 = \frac{\xi_1}{(z_1 + d_1)}$ and $\xi_2 = \frac{\xi_2}{(z_2 + d_2)}$. The confidence intervals (in parenthesis next to the parameter values) were computed using 999 bootstrap replicates (21). SOK: second-order kinetics, HM: heteroduplex model.

Figure S2. Best-fit of data set 2 for known diversity templates (each panel). Blue: data sample (two replicates). Green: best-fit of second-order kinetics. Red: best-fit of the heteroduplex model. For the best fit parameters and confidence intervals, see Table S1. The heteroduplex model fits significantly better than second-order kinetics (p-value < 10^{-3}).
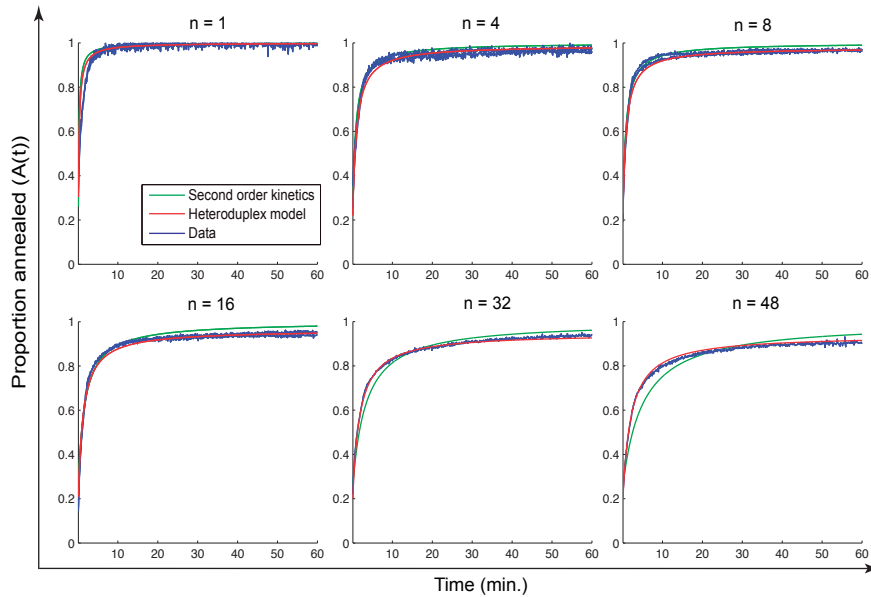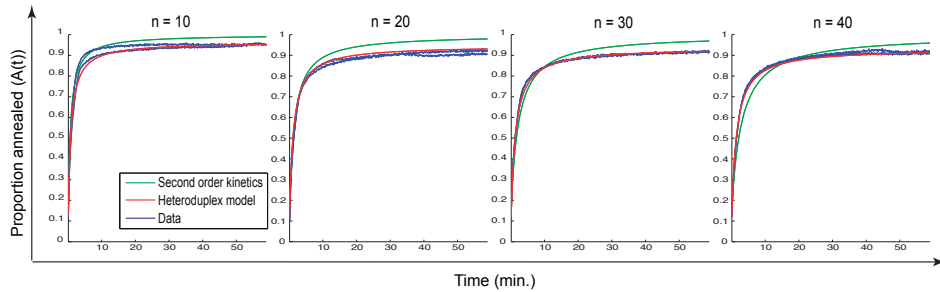
Figure S3. Best-fit of data set 3 for known diversity templates (each panel). Blue: data sample (two replicates). Green: best-fit of second-order kinetics. Red: best-fit of the heteroduplex model. For the best-fit parameters and confidence intervals, see Table S1. The heteroduplex model fits significantly better than second-order kinetics (p-value $< 10^{-3}$).

S3. Best-Fit Parameters: Cot Data. Table S2 compares the best-fit parameters of both models fitted to annealing data (AD, as in table S1), or to Cot 50% or 80% values (as in fig. 6). Note that we did not fit Cot values of data set 3 because of the low number of different diversities in this data set. Similarly, we did not fit annealing curves of data set 4 because this data set was used as a validation set to our diversity prediction procedure. The fitted parameters are rather different according to the method used (annealing data vs Cot values). This was expected in the case of second-order kinetics because parameters a and α are not identifiable in Eq. 11. The discrepancies observed between the fits of Cot 50% and Cot 80% values highlight the importance of the choice of an annealing percent. The data (and consequently the best-fit parameters) exhibited very different properties according to which point was chosen (Fig. 6). Fitting the annealing curves (time-series data) has the advantage of being independent of the choice of an annealing percentage

Table S2. Comparison of the best-fit parameters as fitted on time-series annealing data (AD, as in table S1), or directly on Cot 50% or 80% values (fig. 6 of main text)

Model	Param.	Data set								
		1			2			3		
		AD	Cot 50%	Cot 80%	AD	Cot 50%	Cot 80%	AD	Cot 50%	Cot 70%
SOK	a	2.2160	6.3647	2.2549	12.9887	3.8716	13.1807	7.9439	7.0568	67.2213
	α	0.5532	0.5748	0.7276	0.7435	0.5542	0.4998	0.8423	0.5056	0.7451
HM	a	2.1719	5.1001	2.9702	9.3091	4.6209	13.1994	6.5503	380.9901	55.0737
	α	0.5608	0.7122	0.5644	0.8180	0.6100	0.5074	0.8930	0.9283	1.0000
	ξ_1	0.7962	0.7121	0.5957	0.9994	0.7440	0.8045	0.6275	0.9998	0.8003
	ξ_2	0.0093	0.0381	0.0301	0.0923	0.0923	0.0120	0.0884	0.0001	0.0003
	φ	0.9703	0.6664	0.6790	0.8915	0.7653	0.7918	0.8969	0.2860	0.7617

Each model was fitted to the data by minimizing the sum of squared errors between Cot values and Eq. 10 (HM: heteroduplex model) or Eq. 11 (SOK: second-order kinetics).

CHAPTER

GENERAL DISCUSSION

8

In this thesis we studied the alterations that occur in the human T-cell compartments during chronic viral infections. We investigated the dynamics, activation status and phenotypical characteristics of different T-cell subsets in HIV infected individuals and during CMV infection. Here, our findings are placed in a broader perspective.

DOES THE CD4⁺ T-CELL COMPARTMENT OF HIV INFECTED INDIVIDUALS NORMALIZE DURING cART?

It is over 15 years since combination antiretroviral therapy (cART) was introduced to treat human immunodeficiency virus (HIV) infection. After the introduction of cART several patterns of response have been observed in patients with different stages of disease. With cART, the majority of individuals that adhere to treatment show a good response as defined by the decrease of HIV viral load to undetectable levels and immunologic reconstitution with a complete normalization of the CD4⁺ T-cell compartment (1). Upon suppression of virus replication during cART, two phases of CD4⁺ T-cell reconstitution can be distinguished. In the first 2 - 3 months after the start of cART, the number of CD4⁺ T cells increases primarily due to redistribution of naive and CD27⁺ memory CD4⁺ T cells from the tissues to the blood and secondary lymph nodes (2-4). The second phase of CD4⁺ T-cell reconstitution may take several years and involves the regeneration of the naive pool (1;2;5), which leads to an increased diversity of the CD4⁺ T-cell pool (6). This reconstitution of naive CD4⁺ T-cell numbers has been suggested to occur due to thymic production, because the number of signal joint T-cell receptor excision circles (TREC) per microgram CD4⁺ T-cell DNA rises in accordance with the rise in CD4⁺ T-cell numbers (7). However, there is convincing evidence against this, which shows that the TREC content of naive CD4⁺ T cells increases during HAART and correlates with declining naive T cell division rates, but not with increasing naive T-cell numbers (8). With this in mind, the increase in naive CD4⁺ T cells is more likely to depend on more than one factor, such as normalization of naive T-cell proliferation and death rates, to a certain degree redistribution of naive CD4⁺ T cells from tissues and also thymic production (8). Most individuals show a good immunologic response to virus suppression by HAART by increasing their CD4⁺ T-cell numbers substantially, however a certain degree of inter-individual variability can be observed. For instance, some subjects with only a modest virologic response occasionally have large rises of CD4⁺ T-cell numbers, whereas others with undetectable viral load show only a small increase in CD4⁺ T-cell numbers. In approximately 20% of cases, the so-called immunological non-responders (INR), good virus control is associated with poor CD4⁺ T-cell recovery (9-14). In these cases, initial CD4⁺ T-cell redistribution often occurs, which allows a rapid but moderate gain in CD4⁺ T-cell numbers. This, however, is followed by a plateau or even a decline in CD4⁺ T-cell numbers instead of the expected increase (15).

WHY DO SOME INDIVIDUALS SHOW NO IMMUNOLOGICAL RESPONSE TO CART, DESPITE SUFFICIENT SUPPRESSION OF HIV REPLICATION?

In **chapter 3** we analyzed T-cell turnover in INR on cART. We observed that CD4⁺ T cells of INR have a short life span compared to CD4⁺ T cells of healthy individuals and immunological

responders (IR) (**chapter 2 and chapter 3**) (fig. 1). A recently published study analyzed the number of CD4$^+$ recent thymic emigrants in INR retrospectively and compared these to immunological responders (IR) (16). They showed consistently lower CD31 expression on naive CD4$^+$ T cells of INR, measured from the start of treatment until 36 months thereafter (16). In addition, this publication showed that levels of apoptosis within CD4$^+$ T cells of INR were similar to those of IR (16). Li et al. (2011) therefore concludes that low thymic output is the main cause for insufficient CD4$^+$ T-cell gain in INR. We, however, find that a shortened life span plays an important role as well. In **chapter 3** we show that INR to cART have a very high turnover of the CD4$^+$ T-cell compartment, which is unfavorable for reconstitution of CD4$^+$ T-cell numbers in those individuals.

Since analysis of T-cell turnover using deuterated water labeling is a more sensitive technique, compared to measurement of CD31 expression, we believe that the main cause for insufficient CD4$^+$ T-cell reconstitution in INR is increased turnover of these cells. However, reduced thymic output may also contribute.
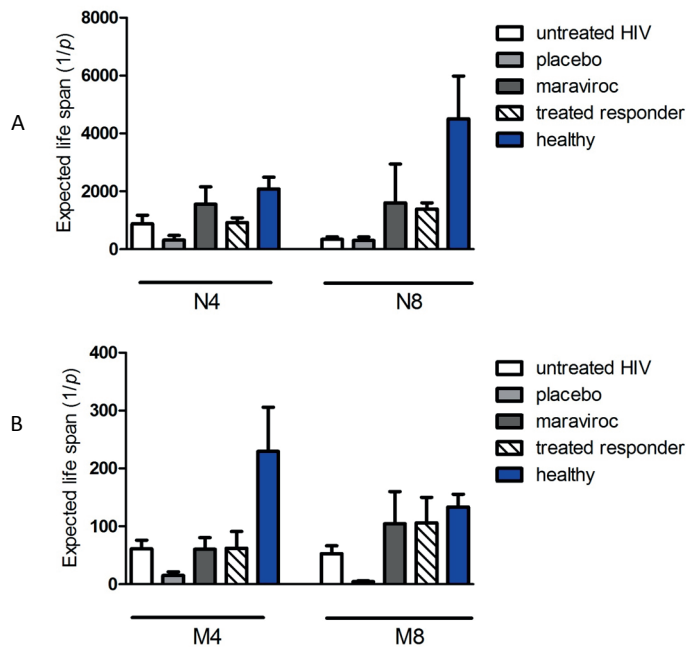
Figure 1. Estimated T-cell life spans in healthy and HIV-infected individuals. Estimated life spans of A) naive and B) memory CD4$^+$ and CD8$^+$ T cells in untreated HIV-infected individuals (white bars), immunological non-responder placebo-treated (light grey bars), immunological non-responder Maraviroc-treated (dark grey bars, immunological responder (dashed bars) HIV infected cART treated individuals and healthy (blue bars) individuals.

DO IMMUNOLOGICAL NON-RESPONDERS BENEFIT FROM SUPPLEMENTING cART WITH MVC?

Maraviroc (MVC) is an HIV entry inhibitor, which selectively blocks the CCR5 receptor. A significant increase in CD4$^+$ T-cell numbers, but no difference in virological efficacy, was observed between MVC treated and placebo treated individuals in a randomized trial (Pfizer study 1029), evaluating MVC vs. placebo in antiretroviral experienced patients with dual tropic (D/M) or indeterminate HIV. The reproducibility and mechanism underlying this increase in CD4$^+$ T-cell numbers in patients using MVC is currently unknown. A CD4$^+$ T-cell increase, even with no effect on virus replication, is potentially interesting for INR, since suppression of HIV replication is substantial in these individuals and they would hence probably not benefit from an agent that aims at better control of virus replication. In order to confirm the effect of MVC intensification on CD4$^+$ T-cell increase and to gain insight in the mechanism behind it, we performed a large, 48-week, double blind, placebo-controlled clinical trial, which is described in **chapter 4**. Surprisingly, we observed that after 48 weeks of MVC treatment intensification, CD4$^+$ T-cell numbers did not significantly increase in the arm of INR that were treated with MVC, compared to INR that were given placebo. Others also reported no increase in CD4$^+$ T-cell numbers upon MVC treatment (17-21). Furthermore, a recent publication shows that IR, for whom the treatment regimen was intensified with MVC did not significantly increase their CD4$^+$ T-cell numbers (22). Whether CD4$^+$ T-cell numbers increase upon MVC treatment without an effect in virus replication is thus still under debate.

Next to CD4$^+$ T-cell numbers, we studied T-cell activation during MVC treatment. The percentage of activated CD4$^+$ T cells decreased slightly in both treatment arms. In a recent publication, the activation of CD4$^+$ T cells has been reported to decrease shortly after treatment intensification with MVC, however, it increased again after 12 weeks (23). This could be explained by increased CCR5 expression upon MVC treatment, which was observed *in vitro* in (24) and in **chapter 4**. Interestingly, the percentage of activated CD8$^+$ T cells increased with 2% in 48 weeks in the placebo arm, but not in the MVC arm (**chapter 4**). Apparently treatment with MVC prevents CD8$^+$ T-cell activation in cells that would otherwise have become activated. The density of CCR5 molecules on the surface of CD4$^+$ T cells has been shown to be positively correlated with the activation state of CD8$^+$ T cells (25), which is in line with our observation that CCR5 expression on CD4$^+$ T cells as well as CD8$^+$ T cell activation does not increase upon treatment with MVC (**chapter 4**).

Based on the results of our study we cannot conclude that immunological non-responders benefit from treatment intensification with MVC. The current challenge is to determine if, and if so, for which specific patients MVC treatment intensification would be beneficial.

THE EFFECT OF MVC ON T-CELL TURNOVER AND LIFE SPAN

In addition to T-cell numbers and immunological parameters, we used D$_2$O labeling to study the expected life span of CD4$^+$ T cells in INR during MVC treatment intensification in the same randomized setting (described in **chapter 3**). We did not expect the life span of CD4$^+$ T cells to be affected by treatment with MVC, since CD4$^+$ T-cell numbers remained stable throughout the

study protocol. Surprisingly, however, we observed a longer life span of CD4+ T cells in the MVC group, compared to the placebo group (**Chapter 3**). The question thus remains why, despite an increased life span, CD4+ T-cell numbers did not increase in the MVC group. An altered balance between T-cell activation and apoptosis may alter CD4+ T-cell dynamics but leave numbers unchanged. However, in line with the results comparing from our large 48-week clinical trial, we did not observe a significant difference in either CD4+ T-cell activation or CD4+ T-cell apoptosis between the MVC- and placebo treated patients who were included in the labeling study (**chapter 3**). A difference in T-cell distribution between tissue, blood and lymphoid organs may also explain why CD4+ T-cell numbers did not increase in the blood in INR during MVC treatment intensification. Although a recent study showed that the addition of MVC to the treatment regimen of recipients of allogeneic hematopoietic stem-cell transplantation reduced CCL5 and induced lymphocyte trafficking directly ex vivo (26), which would argue against increased migration of CD4+ T cells to the tissue upon treatment with MVC and rather favour a hypothesis where CD4+ T cells accumulate in the blood. Less migration to the tissues could be beneficial for HIV infected patients because it would result in less immunopathology there. However, for the deletion of the HIV reservoir in the tissues it may not be favorable to prevent T cells from migrating to these sites. Even if there is no increase in absolute CD4+ T-cell numbers, a decreased turnover may result in a better functionality of the CD4+ T-cell compartment due to more quiet steady state and less replicative senescence. HIV infected individuals could therefore benefit from MVC treatment intensification in the long run, however further studies are necessary to confirm our results and to investigate the clinical benefits.

WHY DO CD8+ T-CELL NUMBERS NOT NORMALIZE DURING cART?

It has been shown that the CD4+ T-cell compartment has the ability to completely normalize during long-term successful cART (1). In **chapter 5** we investigated whether this also holds for the CD8+ T-cell compartment. In contrast to CD4+ T-cell numbers, we observed that absolute CD8+ T-cell numbers did not normalize after long-term suppressive cART, but instead were still elevated. Memory and effector CD8+ T-cell numbers were particularly high after 5 years of successful CART. In contrast, naive CD8+ T-cell numbers, which have been described to be decreased upon the start of cART (27), had normalized completely. Apparently, naive CD8+ T cells have the ability to fully reconstitute after long-term treatment. Using deuterium labeling, we have estimated the average life span of CD8+ T cells during successful cART. Naive CD8+ T cells of HIV infected individuals that receive successful cART had a significantly longer life span than those of untreated HIV infected individuals (fig. 1). However, the average life span of naive CD8+ T cells in HIV infected individuals on successful cART was still shorter than that of healthy individuals (**chapter 2**). Therefore, we conclude that the naive CD8+ T-cell compartment benefits from successful, long-term cART, but complete normalization does not occur.

Longitudinal analyses showed a decline in central- and effector memory CD8+ T-cell numbers during long-term cART, although this decline was very modest, considering the 5 year time span in which it was measured. We expected a more substantial decrease, since the driving force behind CD8+ memory T-cell expansion, HIV replication, had been suppressed and

memory T cells are generally short lived (**chapter 2** (28)). Interestingly, the life span of memory T cells in HIV infected individuals that respond well to cART is nearly identical to that of healthy individuals (fig. 1 and **chapter 2**). It could thus be that, in the absence of HIV replication, a new dynamic balance has formed in the CD8$^+$ memory compartment that is comparable to that of a healthy individual, in which cells are maintained and even slightly increase as an individual ages. Although memory CD8$^+$ T cells have a half-life of only 244 days in healthy individuals (28) the CD8$^+$ T-cell population as a whole could still be maintained due to renewal of cells. Memory T-cell populations have been described to, potentially, be very long-lived (29;30). Given the above, it is not likely that memory CD8$^+$ T-cell numbers have the ability to completely normalize in the long run.

To explain the slow nature of the decrease in memory CD8$^+$ T cell numbers during cART we investigated whether the memory pool could be partially maintained by activation. Markers of T-cell activation have been shown to be overexpressed on CD8$^+$ T cells during untreated HIV infection (31-33). In **chapter 5**, we showed that the fraction of activated and Ki67 expressing CD8$^+$ T cells was not elevated in HIV infected individuals after long-term cART. Another factor of influence could be an accumulation of senescent CD8$^+$ T cells, which have weak proliferative capacity and short telomeres due to replicative senescence and have been described to be resistant to apoptosis (34;35). We observed that the effector memory CD8$^+$ T cell pool of HIV infected individuals after long-term cART contained a larger fraction of senescent T cells than that of healthy individuals. Despite an expansion of senescent CD8$^+$ T cells we did not find that individuals after long-term cART had decreased numbers of apoptotic cells compared to healthy individuals. Activation, senescence and apoptosis are thus not likely to be responsible for the CD8$^+$ T-cell maintenance we observed.

Changes in the T-cell compartment of HIV infected individuals are often compared to changes that occur during aging. HIV infection has therefore been described as accelerated immunological aging. One characteristic of immunological aging is accumulation of highly differentiated effector CD8$^+$ T cells. This is observed in uninfected aging individuals (28), as well as untreated HIV infection (29). We observed that effector CD8$^+$ T-cell numbers in IR increased during long-term cART. When we analyzed the viral load below 50 copies per ml, we found HIV replication below this limit in very few individuals. Also, we found no correlation between HIV replication below 50 copies per ml and CD8$^+$ T-cell number. We therefore conclude that HIV itself is not likely to be the driving force behind effector CD8$^+$ T-cell accumulation during cART. An alternative explanation would be that other antigens, for instance those that also cause accumulation of effector CD8$^+$ T cells in the elderly, drive this accumulation. If this is the case, effector CD8$^+$ T cells will remain elevated, even in the absence of HIV replication.

DO OTHER CHRONIC INFECTIONS AFFECT CD8$^+$ T-CELL DYNAMICS DURING cART?

Persistent viruses, other than HIV, may be responsible for the maintenance of memory and effector CD8$^+$ T cells in HIV infected, cART treated, individuals. The incidence of the herpes viruses Epstein-Barr virus, human herpes virus 8 (HHV8) and cytomegalovirus (CMV) has been shown to be higher in HIV infected individuals compared to healthy individuals (36). Not only

was the incidence shown to be higher, also reactivations, as measured by antibody titers, occurred in 20 – 30% of HIV infected individuals that responded well to cART (36), whereas reactivation of herpes viruses is very rare in healthy individuals. EBV DNA load has been shown to be significantly higher in HIV infected individuals on cART than in healthy individuals (37). The intensity of EBV CD8+ T-cell responses was shown to be relatively low, compared to the intensity of HIV CD8+ T-cell responses during untreated HIV infection. However, treatment with cART resulted in a significantly reduced number of HIV specific CD8+ T cells, whereas CD8+ T-cell responses against EBV were increased during cART (38). CD8+ T-cell responses against HHV8 have also been described to be increased during cART, resulting in lower HHV8 viral titers (39-41). However, whether the increase in EBV and HHV8 specific CD8+ T-cell responses contributes substantially to the dynamics of the total CD8+ T-cell pool remains unclear. In addition, it has been shown that HIV infected individuals on cART, with undetectable viral loads, have exceptionally high numbers of CMV specific effector CD8+ T cells (42). Levels of CMV specific effector CD8+ T cells in HIV infected individuals during cART are comparable to those in the very elderly, only they occur at much younger ages (42). Since the incidence of CMV in HIV infected individuals is significantly increased, compared to the general population (36) it could well be that infection with CMV is an important factor driving CD8+ T-cell differentiation towards the effector phenotype in HIV infected individuals during long-term cART. In **chapter 6** we describe that CMV does so in healthy individuals. Not only does CMV affect CD8+ T-cell differentiation toward the effector phenotype in healthy individuals, it also has a marked influence on CD8+ T-cell differentiation toward the memory phenotype. In **chapter 6** we used a large cohort of two hundred and eighty seven healthy individuals, both children and adults, to investigate whether CMV seroprevalence affects absolute CD8+ T-cell numbers. Effector and effector memory CD8+ T-cell numbers were elevated in CMV seropositive individuals compared to CMV seronegative individuals, in both children and adults. The rate at which the effector memory CD8+ T-cell number increased with age was not different between CMV seronegative and CMV seropositive individuals. Furthermore, children that were CMV seropositive, already at a very young age, had high effector and effector memory CD8+ T-cell numbers, suggesting that CMV induces an instant rise in effector and effector memory CD8+ T-cells and thereafter these cells are maintained. After the initial expansion, the effector and effector memory CD8+ T-cell pools are not necessarily expanded further due to CMV. This could also apply for HIV infected individuals during cART, in whom CMV has probably had a profound influence on CD8+ T-cell differentiation during untreated HIV when individuals are generally immunocompromised to a certain degree. After initiation of cART, HIV infected individuals that respond well to therapy become more immunocompetent and are better able to control CMV. Memory and effector CD8+ T cells that have formed during untreated HIV could then still be maintained, but not expanded further.

AMPLICOT; A TOOL TO MEASURE T-CELL DIVERSITY

This thesis mainly focuses on T-cell numbers and dynamics, however, to efficiently combat (chronic) infections, a sufficiently diverse T-cell receptor (TCR) repertoire is crucial as well. Next generation sequencing techniques allow in depth analysis of the complete TCR repertoire

in individuals blood samples (43-46). These techniques, however, are very costly and time consuming. In **chapter 7**, we performed an in depth analysis to improve the AmpliCot method (47). AmpliCot is a fast and inexpensive tool to measure TCR diversity (48-50). In **chapter 7** we propose a detailed model, involving heteroduplex and transient-duplex formation that leads to significantly better fits of experimental ampliCot data. We propose that the AmpliCot technique is very suitable to investigate whether T-cell diversity changes over time. It could, for instance be applied to measure TCR diversity of CD4^{+} T cells during treatment intensification with MVC, described in **chapter 4**. It will be informative to know whether TCR diversity has changed, this would shed more light on the potential benefits of treatment with MVC. Also, for future experiments, the AmpliCot technique could elucidate whether the CD8^{+} T-cell expansions that we observed in HIV infected individuals in **chapter 5** and in CMV seropositive individuals in **chapter 6** are caused by a few dominant, or many non-dominant antigens. This would, at least in part, clarify whether a single virus, or a few dominant epitopes of a virus are responsible for the majority of the CD8^{+} T-cell expansions. Taken together, the ampliCot technique, combined with our improved model for interpretation of experimental data, is a potentially very useful technique to investigate certain subjects of this thesis in more depth.

CONCLUDING REMARKS

8

In this thesis we have shown that complete reconstitution of the T-cell compartment during cART is not achieved in the majority of HIV infected individuals. Patients that are unable to reconstitute their CD4^{+} T-cell compartment during cART do not benefit from short-term treatment with MVC in terms of CD4^{+} T-cell gain. T-cell turnover does seem to normalize after MVC treatment, but it is currently unclear whether that is actually beneficial for the patients. Larger studies are necessary to identify specific patient groups that could profit from MVC treatment. Longer studies could elucidate whether long-term beneficial effects of MVC treatment in INR occur. Furthermore, individuals that do reconstitute their CD4^{+} T-cell compartment still have a vastly expanded CD8^{+} T-cell compartment after more than 5 years of successful cART. CMV, and other viruses that affect healthy individuals during aging, potentially play an important role in the maintenance of CD8^{+} T cells during cART. Further studies, for instance analyzing the fraction of CMV specific CD8^{+} T cells are necessary to shed more light on the maintenance of CD8^{+} T cells during successful cART treatment of HIV infected individuals. We did not find an indication for normalization of the CD8^{+} T-cell compartment in the long run. In conclusion, the introduction of cART treatment significantly improves the survival and the quality of life of HIV infected individuals, however, to achieve complete normalization of the T-cell compartment there is still a need for improvement of cART.

REFERENCE LIST

1. Vrisekoop N, van GR, de Boer AB, et al. Restoration of the CD4 T cell compartment after long-term highly active antiretroviral therapy without phenotypical signs of accelerated immunological aging. J Immunol **2008 Jul 15**;181(2):1573-81.

2. Carcelain G, Blanc C, Leibowitch J, et al. T cell changes after combined nucleoside analogue therapy in HIV primary infection. AIDS **1999 Jun 18**;13(9):1077-81.

3. Hazenberg MD, Otto SA, Wit FW, Lange JM, Hamann D, Miedema F. Discordant responses during antiretroviral therapy: role of immune activation and T cell redistribution rather than true CD4 T cell loss. AIDS **2002 Jun 14**;16(9):1287-9.

4. Renaud M, Katlama C, Mallet A, et al. Determinants of paradoxical CD4 cell reconstitution after protease inhibitor-containing antiretroviral regimen. AIDS **1999 Apr 16**;13(6):669-76.

5. Autran B, Carcelain G, Li TS, et al. Positive effects of combined antiretroviral therapy on CD4+ T cell homeostasis and function in advanced HIV disease. Science **1997 Jul 4**;277(5322):112-6.

6. Gorochov G, Neumann AU, Kereveur A, et al. Perturbation of CD4+ and CD8+ T-cell repertoires during progression to AIDS and regulation of the CD4+ repertoire during antiviral therapy. Nat Med **1998 Feb**;4(2):215-21.

7. Douek DC, McFarland RD, Keiser PH, et al. Changes in thymic function with age and during the treatment of HIV infection. Nature **1998 Dec 17**;396(6712):690-5.

8. Hazenberg MD, Otto SA, Cohen Stuart JW, et al. Increased cell division but not thymic dysfunction rapidly affects the T-cell receptor excision circle content of the naive T cell population in HIV-1 infection. Nat Med **2000 Sep**;6(9):1036-42.

9. Benveniste O, Flahault A, Rollot F, et al. Mechanisms involved in the low-level regeneration of CD4+ cells in HIV-1-infected patients receiving highly active antiretroviral therapy who have prolonged undetectable plasma viral loads. J Infect Dis **2005 May 15**;191(10):1670-9.

10. Florence E, Lundgren J, Dreezen C, et al. Factors associated with a reduced CD4 lymphocyte count response to HAART despite full viral suppression in the EuroSIDA study. HIV Med **2003 Jul**;4(3):255-62.

11. Grabar S, Le M, V, Goujard C, et al. Clinical outcome of patients with HIV-1 infection according to immunologic and virologic response after 6 months of highly active antiretroviral therapy. Ann Intern Med **2000 Sep 19**;133(6):401-10.

12. Kelley CF, Kitchen CM, Hunt PW, et al. Incomplete peripheral CD4+ cell count restoration in HIV-infected patients receiving long-term antiretroviral treatment. Clin Infect Dis **2009 Mar 15**;48(6):787-94.

13. Marziali M, De SW, Carello R, et al. T-cell homeostasis alteration in HIV-1 infected subjects with low CD4 T-cell count despite undetectable virus load during HAART. AIDS **2006 Oct 24**;20(16):2033-41.

14. Torti C, Cologni G, Uccelli MC, et al. Immune correlates of virological response in HIV-positive patients after highly active antiretroviral therapy (HAART). Viral Immunol **2004**;17(2):279-86.

15. Guihot A, Bourgarit A, Carcelain G, Autran B. Immune reconstitution after a decade of combined antiretroviral therapies for human immunodeficiency virus. Trends Immunol **2011 Mar**;32(3):131-7.

16. Li T, Wu N, Dai Y, et al. Reduced thymic output is a major mechanism of immune reconstitution failure in HIV-infected patients after long-term antiretroviral therapy. Clin Infect Dis **2011 Nov**;53(9):944-51.

17. Cuzin L, Trabelsi S, Delobel P, et al. Maraviroc intensification of stable antiviral therapy in HIV-1-infected patients with poor immune restoration: MARIMUNO-ANRS 145 study. J Acquir Immune Defic Syndr **2012 Dec 15**;61(5):557-64.

18. Hunt PW, Shulman NS, Hayes TL, et al. The immunologic effects of maraviroc intensification in treated HIV-infected individuals with incomplete CD4+ T-cell recovery: a randomized trial. Blood **2013 Jun 6**;121(23):4635-46.

19. Rusconi S, Adorni F, Vitiello P. Maraviroc (MVC) as Intensification Strategy in Immunological Non-responder HIV-infected Patients with Virologic Success on HAART. EACS, Belgrade, Abstract PS1/7 **2011 Oct 12**.

20. Stepanyuk O, Chiang TS, Dever LL, et al. Impact of adding maraviroc to antiretroviral regimens in patients with full viral suppression but impaired CD4 recovery. AIDS **2009 Sep 10**;23(14):1911-3.

21. Wilkin TJ, Lalama CM, McKinnon J, et al. A pilot trial of adding maraviroc to suppressive antiretroviral therapy for suboptimal CD4(+) T-cell recovery despite sustained virologic suppression: ACTG A5256. J Infect Dis **2012 Aug 15**;206(4):534-42.

22. Vitiello P, Brudney D, MacCartney M, et al. Responses to switching to maraviroc-based antiretroviral therapy in treated patients with suppressed plasma HIV-1-RNA load. Intervirology **2012**;55(2):172-8.

23. Gutierrez C, Diaz L, Vallejo A, et al. Intensification of antiretroviral therapy with a CCR5 antagonist in patients with chronic HIV-1 infection: effect on T cells latently infected. PLoS One **2011**;6(12):e27864.

24. Arberas H, Guardo AC, Bargallo ME, et al. In vitro effects of the CCR5 inhibitor maraviroc on human T cell function. J Antimicrob Chemother **2013 Mar**;68(3):577-86.

25. Portales P, Psomas KC, Tuaillon E, et al. The intensity of immune activation is linked to the level of CCR5 expression in human immunodeficiency virus type 1-infected persons. Immunology **2012 Sep**;137(1):89-97.

26. Reshef R, Luger SM, Hexner EO, et al. Blockade of lymphocyte chemotaxis in visceral graft-versus-host disease. N Engl J Med **2012 Jul 12**;367(2):135-45.

27. Roederer M, Dubs JG, Anderson MT, Raju PA, Herzenberg LA, Herzenberg LA. CD8 naive T cell counts decrease progressively in HIV-infected adults. J Clin Invest **1995 May**;95(5):2061-6.

28. Vrisekoop N, den B, I, de Boer AB, et al. Sparse production but preferential incorporation of recently produced naive T cells in the human peripheral pool. Proc Natl Acad Sci U S A **2008 Apr 22**;105(16):6115-20.

29. Co MD, Kilpatrick ED, Rothman AL. Dynamics of the CD8 T-cell response following yellow fever virus 17D immunization. Immunology **2009 Sep**;128(1 Suppl):e718-e727.

30. Hammarlund E, Lewis MW, Hansen SG, et al. Duration of antiviral immunity after smallpox vaccination. Nat Med **2003 Sep**;9(9):1131-7.

31. Gaines H, von Sydow MA, von Stedingk LV, et al. Immunological changes in primary HIV-1 infection. AIDS **1990 Oct**;4(10):995-9.

32. Hazenberg MD, Stuart JW, Otto SA, et al. T-cell division in human immunodeficiency virus (HIV)-1 infection is mainly due to immune activation: a longitudinal analysis in patients before and during highly active antiretroviral therapy (HAART). Blood **2000 Jan 1**;95(1):249-55.

33. Prince HE, Kleinman S, Czaplicki C, John J, Williams AE. Interrelationships between serologic markers of immune activation and T lymphocyte subsets in HIV infection. J Acquir Immune Defic Syndr **1990**;3(5):525-30.

34. Posnett DN, Edinger JW, Manavalan JS, Irwin C, Marodon G. Differentiation of human CD8 T cells: implications for in vivo persistence of CD8+. Int Immunol **1999 Feb**;11(2):229-41.

35. Spaulding C, Guo W, Effros RB. Resistance to apoptosis in human CD8+ T cells that reach replicative senescence after multiple rounds of antigen-specific proliferation. Exp Gerontol **1999 Aug**;34(5):633-44.

36. Lennette ET, Busch MP, Hecht FM, Levy JA. Potential herpesvirus interaction during HIV type 1 primary infection. AIDS Res Hum Retroviruses **2005 Oct**;21(10):869-75.

37. Ling PD, Vilchez RA, Keitel WA, et al. Epstein-Barr virus DNA loads in adult human immunodeficiency virus type 1-infected patients receiving highly active antiretroviral therapy. Clin Infect Dis **2003 Nov 1**;37(9):1244-9.

38. Dalod M, Dupuis M, Deschemin JC, et al. Broad, intense anti-human immunodeficiency virus (HIV) ex vivo CD8(+) responses in HIV type 1-infected patients: comparison with anti-Epstein-Barr virus responses and changes during antiretroviral therapy. J Virol **1999 Sep**;73(9):7108-16.

39. Bourboulia D, Aldam D, Lagos D, et al. Short- and long-term effects of highly active antiretroviral therapy on Kaposi sarcoma-associated herpesvirus immune responses and viraemia. AIDS **2004 Feb 20**;18(3):485-93.

40. Sullivan SG, Hirsch HH, Franceschi S, et al. Kaposi sarcoma herpes virus antibody response and viremia following highly active antiretroviral therapy in the Swiss HIV Cohort study. AIDS **2010 Sep 10**;24(14):2245-52.

41. Wilkinson J, Cope A, Gill J, et al. Identification of Kaposi's sarcoma-associated herpesvirus (KSHV)-specific cytotoxic T-lymphocyte epitopes and evaluation of reconstitution of KSHV-specific responses in human immunodeficiency virus type 1-Infected patients receiving highly active antiretroviral therapy. J Virol **2002 Mar**;76(6):2634-40.

42. Naeger DM, Martin JN, Sinclair E, et al. Cytomegalo-virus-specific T cells persist at very high levels during long-term antiretroviral treatment of HIV disease. PLoS One **2010**;5(1):e8886.

43. Freeman JD, Warren RL, Webb JR, Nelson BH, Holt RA. Profiling the T-cell receptor beta-chain repertoire by massively parallel sequencing. Genome Res **2009 Oct**;19(10):1817-24.

44. Robins HS, Campregher PV, Srivastava SK, et al. Comprehensive assessment of T-cell receptor beta-chain diversity in alphabeta T cells. Blood **2009 Nov 5**;114(19):4099-107.

45. Robins HS, Srivastava SK, Campregher PV, et al. Overlap and effective size of the human CD8+ T cell receptor repertoire. Sci Transl Med **2010 Sep 1**;2(47):47ra64.

46. Warren RL, Freeman JD, Zeng T, et al. Exhaustive T-cell repertoire sequencing of human peripheral blood samples reveals signatures of antigen selection and a directly measured repertoire size

of at least 1 million clonotypes. Genome Res **2011 May**;21(5):790-7.

47.   Baltcheva I, Veel E, Volman T, et al. A generalized mathematical model to estimate T- and B-cell receptor diversities using AmpliCot. Biophys J **2012 Sep 5**;103(5):999-1010.

48.   Baum PD, McCune JM. Direct measurement of T-cell receptor repertoire diversity with AmpliCot. Nat Methods **2006 Nov**;3(11):895-901.

49.   Baum PD, Young JJ, McCune JM. Measurement of absolute T cell receptor rearrangement diversity. J Immunol Methods **2011 May 31**;368 (1-2):45-53.

50.   Baum PD, Young JJ, Schmidt D, et al. Blood T-cell receptor diversity decreases during the course of HIV infection, but the potential for a diverse repertoire persists. Blood **2012 Apr 12**;119(15):3469-77.
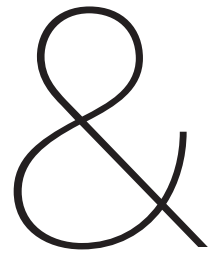
8

GENERAL DISCUSSION

APPENDICES

&

NEDERLANDSE SAMENVATTING

HET IMMUUNSYSTEEM

T cellen. Het immuunsysteem is belangrijk voor de bescherming van het lichaam tegen pathogenen, zoals virussen, bacteriën en schimmels. Bij deze taak is een diverse verzameling cellen betrokken. Lymfocyten, een type witte bloedcel, zijn een belangrijke component van het immuunsysteem. Zij dragen ertoe bij dat pathogenen onschadelijk gemaakt worden. Van de lymfocyten zijn voor dit proefschrift vooral de $\alpha\beta$ T cellen van belang. Er bestaan twee soorten $\alpha\beta$ T cellen, namelijk de CD4$^+$ T cellen en de CD8$^+$ T cellen, die verschillende functies uitoefenen. CD4$^+$ T cellen zijn met name belangrijk voor het onschadelijk maken van extracellulaire pathogenen, zoals bacteriën. CD8$^+$ T cellen zijn meer gericht op het doden van intracellulaire pathogenen, zoals virussen.

Ontwikkeling van T cellen. Voorlopers van T cellen worden aangemaakt in het beenmerg, waarna zij naar de thymus migreren voor verdere ontwikkeling. T cellen betreden de thymus als CD4$^-$CD8$^-$ cellen en kunnen zich uiteindelijk ontwikkelen tot $\alpha\beta$ CD4$^+$ of CD8$^+$ T cellen. Deze ontwikkeling kan opgedeeld worden in een aantal processen, te beginnen met VDJ recombinatie, waarbij delen van het T-cel receptor (TCR) gen bijna willekeurig worden gecombineerd. Hierdoor krijgt vrijwel iedere T cel een unieke TCR, waarmee een potentieel grote verscheidenheid aan ziekteverwekkers kan worden herkend.

Activatie en differentiatie van T cellen. Eenmaal in het perifere lymfestelsel zal een T cel blijven circuleren tot het een lichaamsvreemd eiwit (antigeen) herkend. Indien een T cel nog geen antigeen heeft herkend wordt deze naïef genoemd. Wanneer er een interactie plaatsvindt tussen een TCR en lichaamsvreemd antigeen, wordt de T cel geactiveerd. Deze zal dan differentiëren tot een effector T cel. Om een effectieve respons te kunnen genereren vermeerderen geactiveerde T cellen zich, dit wordt clonale expansie genoemd. Na de clonale expansie, wanneer het pathogeen verdreven is, vindt een contractiefase plaats. Het overgrote deel van de effector T cellen sterft af en de cellen die overblijven worden geheugen (memory) cellen. Deze memory cellen kunnen snel in actie komen wanneer hetzelfde pathogeen een volgende keer het lichaam binnendringt.

CHRONISCHE VIRALE INFECTIES

HIV. Een van de meest bekende chronische infecties is human immunodeficiency virus (HIV) infectie. Personen met klinische symptomen van AIDS doken voor het eerst op in de Verenigde Staten in 1981. Het virus dat dit nieuwe syndroom veroorzaakte werd in 1983 gevonden en HIV genoemd. HIV infecteert specifiek CD4$^+$ T cellen en veroorzaakt activatie van een groot gedeelte van het immuunsysteem. Hiermee tast het de functie van het immuunsysteem ernstig aan. Het immuunsysteem is niet in staat het HIV-virus te elimineren, daarom blijft het levenslang in het lichaam aanwezig. Tijdens de eerste weken van de infectie wordt een CD8$^+$ T-cel respons tegen het virus gevormd en deze respons blijft aanwezig zolang het virus zich repliceert.

Vanwege continue clonale expansie nemen effector en memory CD8$^+$ T cellen tijdens een HIV infectie in aantal toe. CD4$^+$ T cellen vormen ook een respons tegen HIV, maar deze neemt een aantal maanden na primaire infectie af. Tijdens HIV infectie dalen CD4$^+$ T cellen in aantal. Deze afname wordt veroorzaakt door eliminatie van virus-geïnfecteerde cellen door CD8$^+$ T cellen, door directe effecten van het HIV virus op CD4$^+$ T cellen en door de geactiveerde staat waarin het immuunsysteem verkeerd. Doordat CD8$^+$ T cellen in staat zijn het virus redelijk adequaat te controleren blijven HIV geïnfecteerde personen vaak lange tijd vrij van symptomen. HIV heeft echter een hoge mutatiesnelheid, waardoor het de CD8$^+$ T cellen op den duur te slim af is. Hierdoor stijgt de hoeveelheid virusdeeltjes in het bloed en nemen de CD4$^+$ T cellen sneller in aantal af. Op een bepaald punt starten HIV geïnfecteerden met anti-HIV therapie, die combination anti-retroviral therapy (cART) wordt genoemd. Een groot deel van de patiënten die hun medicatie trouw gebruiken laat hierop een goede respons zien. Dit betekenent dat het aantal virusdeeltjes in het bloed daalt en de CD4$^+$ T cellen in aantal toenemen.

CMV. Een andere, veel voorkomende, chronische infectie is cytomegalovirus (CMV) infectie. CMV is een humaan herpesvirus dat na infectie levenslang in het lichaam aanwezig blijft. Gezonde personen ervaren geen symptomen van CMV infectie en naar schatting wordt 50 tot 90% van de bevolking tijdens het leven met dit virus geïnfecteerd. CD8$^+$ T cellen zijn erg belangrijk bij het onder controle houden van dit virus. Tijdens de chronische fase van de infectie bevindt CMV zich grotendeels in een sluimertoestand, waarin het geen detecteerbare schade veroorzaakt. Reactivatie van het virus komt bijna uitsluitend voor in personen met een verslechterd immuunsysteem.

DIT PROEFSCHRIFT

Chronische virale infecties leggen een grote druk op het immuunsysteem, zoals hierboven beschreven voor HIV en CMV. Het is voor de patiënt van belang om het immuunsysteem zo gezond mogelijk te houden om te voorkomen dat klinische symptomen van de infectie zich openbaren. Zelfs wanneer er geen klinische symptomen optreden kan het immuunsysteem zodanig veranderen dat andere infecties minder effectief kunnen worden bestreden. Hierom is het belangrijk de veranderingen die plaatsvinden in het immuunsysteem tijdens chronische virale infecties te karakteriseren, alsmede de oorzaak ervan te achterhalen. Ook is het van belang verschillen tussen personen in respons op een virus, of op therapie gericht op het onderdrukken ervan, in kaart te brengen. Door inzicht in deze processen kunnen mogelijk nieuwe therapieën worden ontwikkeld die ervoor zorgen dat virussen beter gecontroleerd kunnen worden en schade aan het immuunsysteem beperkt blijft.

T-cel dynamiek in HIV geïnfecteerde personen. Om te begrijpen welke processen verantwoordelijk zijn voor het verlies van CD4$^+$ T cellen tijdens HIV infectie is het belangrijk om een kwantitatief inzicht te krijgen in de levensduur van deze cellen. In hoofdstuk 2 doen wij onderzoek naar de dynamiek van T cellen in HIV geïnfecteerde personen die (nog) niet worden behandeld met cART en vergelijken deze met gezonde personen en HIV geïnfecteerde personen die succesvol worden behandeld met cART (immunologische responders). We

vonden dat de levensduur van T cellen in onbehandelde HIV geïnfecteerde personen tenminste drie maal korter is dan in gezonde personen. De levensduur van T cellen in HIV geïnfecteerde personen die worden behandeld met cART is nog steeds korter dan die in gezonde personen, maar wel beduidend langer dan in personen die niet met cART worden behandeld. Ondanks dat het aantal CD4$^+$ T cellen tijdens behandeling met cART toeneemt tot normaalwaarden blijft de levensduur van deze cellen dus verkort. Dit betekent dat er waarschijnlijk in een behandelde HIV geïnfecteerde een andere balans tussen aanmaak en sterfte van T cellen bestaat dan in gezonde personen.

T-cel dynamiek en immunologische parameters in HIV geïnfecteerde personen tijdens behandeling met Maraviroc. Hoewel een grote groep HIV geïnfecteerde personen door middel van cART het virus onderdrukt en een stijging in het aantal CD4$^+$ T cellen laat zien, zijn er ook personen bij wie de therapie niet dit beoogde effect heeft. Ongeveer 20% van alle HIV geïnfecteerden die worden behandeld met cART is wel in staat het virus te onderdrukken, maar laat desondanks geen stijging in het aantal CD4$^+$ T cellen zien. Deze personen worden immunologische non-responders genoemd. In hoofdstuk 3 en 4 doen wij onderzoek naar Maraviroc, een relatief nieuw geneesmiddel dat het binnendringen van HIV in een cel blokkeert. Er zijn aanwijzingen dat dit geneesmiddel, onafhankelijk van virus-onderdrukking, een stijging in het aantal T cellen kan bewerkstelligen. Dit is potentieel interessant voor de bovengenoemde immunologische non-responders. In hoofdstuk 4 onderzoeken wij immunologische parameters in een 48 weken durende, dubbelblinde, placebo-gecontroleerde klinische studie met Maraviroc. We bekijken onder meer het aantal CD4$^+$ en CD8$^+$ T cellen gedurende de studie, activatie, proliferatie, translocatie van microbiële producten uit de darm, celdood en het percentage recent geproduceerde CD4$^+$ T cellen. Ondanks de bovengenoemde aanwijzingen liet onze studie geen verschil in het aantal CD4$^+$ T cellen zien tussen personen die Maraviroc gebruikten en de placebo groep. Opmerkelijk was dat wij wel minder celdood detecteerden in zowel CD4$^+$ T cellen als CD8$^+$ T cellen in de Maraviroc groep. Ook vonden wij een hoger percentage recent geproduceerde CD4$^+$ T cellen in de Maraviroc groep. Voor geen van de andere onderzochte parameters vonden wij een verschil. In hoofdstuk 3 onderzoeken wij de levensduur van T cellen in een kleinere groep personen binnen de bovengenoemde klinische studie. We vonden dat behandeling met Maraviroc resulteert in een langere levensduur van T cellen die dicht in de buurt komt van de levensduur van deze cellen in gezonde personen. Het is opvallend dat wij, ondanks de langere levensduur van CD4$^+$ T cellen in de Maraviroc groep, geen stijging in het aantal CD4$^+$ T cellen zien. Een mogelijke verklaring hiervoor zou kunnen zijn dat zowel de aanmaak als de sterfte van cellen verandert door het gebruik van Maraviroc en dat deze processen elkaar opheffen. Ook zou de distributie van T cellen tussen het bloed en andere plaatsen in het lichaam een rol kunnen spelen aangezien in deze studie uitsluitend het bloed wordt gemonitord.

CD8$^+$ T-cel aantallen in HIV geïnfecteerde personen tijdens cART. Voorgaande studies hebben laten zien dat het CD4$^+$ T-cel compartiment in staat is volledig te normaliseren tijdens langdurige behandeling met cART. In hoofdstuk 5 onderzoeken wij of het CD8$^+$ T-cel compartiment, dat door langdurige druk van het HIV virus in omvang is toegenomen, ook volledig kan

normaliseren tijdens cART. Wij vonden dat, in tegenstelling tot het CD4+ T-cel compartiment en het naïeve CD8+ T-cel compartiment, de memory en effector CD8+ T-cel compartimenten niet normaliseerden in aantal, maar verhoogd bleven. Met longitudinale analyses hebben wij onderzocht of er in deze compartimenten gedurende de periode van behandeling met cART veranderingen in celaantal optraden. Dit onderzoek liet zien dat memory cellen tijdens cART wel in aantal afnamen, maar vooral in het eerste jaar van behandeling. Het uitblijven van verdere daling van memory CD8+ T-cel aantal werd niet veroorzaakt door T-cel activatie door HIV of door een verstoorde celdood. De meest waarschijnlijk verklaring voor het verhoogde aantal CD8+ memory T cellen is dat, tijdens onbehandelde HIV, ook CD8+ T-cel responsen zijn opgewekt tegen andere pathogenen dan HIV zelf. Deze pathogenen zijn mogelijk nog in het lichaam aanwezig en onderhouden het CD8+ T-cel compartiment, waardoor normalisatie wordt voorkomen. CMV is hiervoor een heel waarschijnlijke kandidaat.

CD8+ T-cel aantallen in CMV geïnfecteerde personen. Referentiewaarden voor absolute CD8+ T-cel aantallen zijn gepubliceerd in verschillende cohorten, maar hierbij is nooit onderscheid gemaakt tussen CMV geïnfecteerde (CMV+) personen en personen die niet met CMV zijn geïnfecteerd (CMV-). In hoofdstuk 6 laten wij zien dat er aanzienlijke verschillen bestaan tussen het CD8+ T-cel compartiment van CMV+ en CMV- personen. Memory en effector CD8+ T-cel aantallen waren significant verhoogd in CMV + personen. Opvallend was dat heel jonge CMV+ kinderen, die per definitie nog niet lang met het virus geïnfecteerd zijn, al zeer sterk verhoogde CD8+ memory en effector T-cel aantallen hadden. De verandering in CD8+ T-cel aantallen over de leeftijd verschilde echter niet tussen CMV+ en CMV- personen. Dit suggereert dat infectie met CMV zorgt voor een plotselinge toename in CD8+ memory en effector T cellen en dat deze vervolgens worden onderhouden. Met de bovenstaande resultaten in ogenschouw genomen is het erg belangrijk om CMV status te controleren wanneer CD8+ T-cel aantallen van groepen gezonde personen worden vergeleken in wetenschappelijke studies.

AmpliCot. Voor het genereren van een goede T-cel respons is het belangrijk een divers T-cel repertoire te hebben, zodat veel verschillende pathogenen herkend kunnen worden. Er zijn verschillende technieken beschikbaar om TCR diversiteit te meten, maar deze hebben allemaal als nadeel zeer tijdrovend of kostbaar te zijn of maar een relatief klein gedeelte van het repertoire te kunnen analyseren. Enige jaren geleden is een nieuwe techniek ontwikkeld, AmpliCot. Bij deze techniek wordt gebruik gemaakt van TCR DNA, dat als dubbelstrengs molecuul voorkomt. Deze strengen passen exact op elkaar. Wanneer dit DNA verhit wordt raken de twee strengen los van elkaar en bij afkoelen zullen ze weer een dubbelstrengs molecuul vormen. Dit proces kan worden gemonitord. De tijd die nodig is om een DNA heel monster, na het uit elkaar smelten, weer dubbelstrengs te laten worden is een maat voor de TCR diversiteit van een monster. Immers, hoe meer unieke DNA moleculen er zijn, hoe lastiger het is om de passende 'partner' te vinden.

Een mathematisch model om T-cel receptor diversiteit te benaderen met AmpliCot. In reeds gepubliceerde studies werd receptor diversiteit, gemeten met AmpliCot, afgeleid met behulp van een model waarbij tweedegraads kinetiek werd aangenomen. In hoofdstuk 7

laten wij zien dat een gedetailleerder model, waarbij rekening wordt gehouden met de formatie van heteroduplexen en tijdelijke duplexen, het proces beter beschrijft. Onze methode zorgt voor meer inzicht in de AmpliCot methode en leidt tot betere interpolatie van onbekende diversiteiten.

Conclusies. In dit proefschrift hebben wij laten zien dat complete normalisatie van het T-cel compartiment tijdens cART bij de meeste HIV geïnfecteerde personen niet plaatsvindt. Voor immunologische non-responders is het gebruik van Maraviroc geen geschikte therapie om CD4^{+} T-cel aantallen te laten stijgen. De levensduur van T cellen lijkt wel te normaliseren door gebruik van Maraviroc, maar het is niet duidelijk of dit voor de patiënt een werkelijk voordeel oplevert. Grotere studies zouden patiëntengroepen kunnen identificeren die wel specifiek van behandeling met Maraviroc kunnen profiteren en langere studies zouden kunnen vaststellen of er voordelige lange termijn effecten zijn van gebruik van Maraviroc. Verder hebben we laten zien dat HIV geïnfecteerde personen die wel hun CD4^{+} T-cel aantal een normaliseren tijdens cART, nog steeds een verhoogd aantal CD8^{+} T cellen hebben na langdurige behandeling. CMV en andere virussen waar de meeste personen tijdens normale veroudering aan blootgesteld worden zouden een belangrijke rol kunnen spelen in het onderhouden van deze CD8^{+} T cellen tijdens cART. In conclusie heeft de introductie van de cART behandeling de overlevingskansen en de levenskwaliteit van HIV geïnfecteerde personen significant verbeterd, echter, er is nog steeds grote ruimte voor verbetering, met name om complete normalisatie van het T-cel compartiment te bereiken.

&

CURRICULUM VITAE

Ellen Veel werd op 9 maart 1982 geboren te Alkmaar. Na het behalen van het havo diploma in 1999 heeft zij een aantal jaar als gediplomeerd apothekersassistente gewerkt. In 2001 is zij gestart met de opleiding Biochemie aan Hogeschool Inholland. Als onderdeel van deze studie liep zij stage aan de afdeling Immunologie van het Institute for Biomedical Aging research te Innsbruck, Oostenrijk onder supervisie van Prof. dr. B. Grubeck-Loebenstein en D. Herndler-Brandstetter, MSc. Na het behalen van haar diploma startte zij in 2005 met haar masteropleiding Celbiologie aan de Vrije Universiteit te Amsterdam. Onderzoeksstages voor deze opleiding werden uitgevoerd aan de afdeling Moleculaire Carcinogenese van het Nederlands Kanker Instituut, onder supervisie van Dr. R.L. Beijersbergen en drs. A.W. Fabius en aan het La Jolla Institute for Allergy and Immunology te La Jolla, Verenigde Staten, onder supervisie van Prof. dr. S.P. Schoenberger en Dr. R. Arens. Na het behalen van het masterdiploma startte zij in april 2008 met haar promotieonderzoek aan de afdeling Immunologie van het UMC Utrecht onder begeleiding van en Dr. K. Tesselaar en Dr. J.A.M. Borghans in de groep van Prof. dr. F. Miedema. De resultaten van dat onderzoek zijn beschreven in dit proefschrift.

Sinds 2012 is zij werkzaam als Regulatory Affairs Associate bij Disphar International BV te Baarn.

&

CURRICULUM VITAE

LIST OF PUBLICATIONS

Baltcheva I*, Veel E*, Volman T, Koning D, Brouwer A, Le Boudec J-Y, Tesselaar K, De Boer RJ, Borghans JAM. A Generalized Mathematical Model to Estimate T- and B-cell Receptor Diversities Using Amplicot. *Biophysical Journal 2012 Sept;103(5):999-1010*

Herndler-Brandstetter D, Veel E, Laschober GT, et al. Non-regulatory CD8+CD45RO+CD25+ T-lymphocytes may compensate for the loss of antigen-inexperienced CD8+CD45RA+ T-cells in old age. *Biol Chem 2008 May;389(5):561-8*

Herndler-Brandstetter D, Schwaiger S, Veel E, et al. CD25-expressing CD8+ T cells are potent memory cells in old age. *J Immunol 2005 Aug 1;175(3):1566-74*

Veel E, Drylewicz J, Van Lelyveld SFL, Westera L, Otto SA, Van Oort A, Gaiser K, Spierenburg G, De Kroon I, Hoepelman AIM, Borghans JAM, Tesselaar K. cART Intensification with Maraviroc Decreases T-cell Turnover in HIV-1 Immunological Non Responders. *Submitted for publication*

Veel E, Mudrikova T, Van Gent R, Otto SA, Wensing AMJ, Hoepelman AIM, Borghans JAM, Tesselaar K. Memory CD8 T cells are persistently increased in successfully treated HIV patients even after long-term cART. *Manuscript in preparation*

Veel E, Van Gent R, Westera L, Bloemers BL, Otto SA, Ruijsink B, Rabouw H, Borghans JAM, Tesselaar K. Delineating the numbers of the CD8$^+$ T cell compartment: the effect of age and CMV serostatus. *Manuscript in preparation*

Vrisekoop N, Veel E, Van Gent R, Mugwagwa T, Drylewicz J, Van Lelyveld SFL, De Boer AB, Otto SA, Ruiter AFC, Ackermans MT, Vermeulen JN, Huidekoper HH, Gaiser K, Sauerwein HP, Prins JM, Miedema F, De Boer RJ, Tesselaar K, Borghans JAM. Quantification of naive and memory T-cell turnover during HIV-1 infection. *Manuscript in preparation*

Van Lelyveld SFL, Veel E*, Drylewicz J*, Otto SA, Borghans JAM, Richter C, Soetekouw R, Prins JM, Brinkman K, Mulder JW, Kroon F, Wensing AMJ, Nijhuis M, Tesselaar K, Hoepelman AIM, and the MIRS study group. Maraviroc Intensification in Patients with Suboptimal Immunological Recovery Despite Virological Suppressive cART: a 48-week, Placebo-controlled Trial. *Manuscript in preparation*

DANKWOORD

Vier jaar lang zwoegen in het lab en daarna nog heel wat avonden en weekenden achter de computer. Nu ben ik beland bij het allerlaatste stukje van dit proefschrift, het dankwoord. Velen hebben een bijdrage geleverd aan de totstandkoming van dit werk, een aantal van hen wil ik hierbij graag bedanken.

Toen ik in november 2007 mijn sollicitatiebrief op de bus deed had ik geen idee in wat voor groep ik eventueel terecht zou komen. Groep Frank/Kiki/José bleek een plezierige, inspirerende omgeving waarin ik me altijd vrij voelde mijn ideeën te ventileren. Frank, mijn promotor, al in mijn eerste jaar stapte je over naar de raad van bestuur. Ik heb je zodoende maar kort als groepsleider mogen meemaken. Wel hadden we ieder kwartaal de 'vrijdag lunchbespreking' waar ik altijd zeer geënthousiasmeerd en geïnspireerd raakte. Bedankt voor je motivatie, input en voor het feit dat je mijn promotor bent. Groep Frank werd later groep Kiki/José. Co-promotoren, ik heb jullie beiden als zeer fijne begeleiders ervaren. Bedankt voor jullie bijdrage tijdens alle besprekingen. Kiki, voor zowel technisch advies als theoretische input kon ik bij je terecht. Je wist me altijd naar het onderzoek te laten kijken van een kant die ik zelf nog niet had ontdekt. José, jouw taalgevoel is mijn stukken zeer ten goede gekomen! Ook wil ik je bedanken voor je positieve blik. Steeds als ik dacht dat het in vier jaar echt niet af ging komen kwam ik toch weer vol vertrouwen bij je vandaan.

De rest van groep Kiki/José (Sigrid, Julia, Steven, Vera, Liset, Anita, Thomas en Rogier) enorm bedankt voor al jullie input tijdens de wekelijkse werkbesprekingen. Sigrid, zonder jouw, hulp zou mijn promotie zeker twee keer zou lang hebben geduurd. Aan letterlijk ieder hoofdstuk heb je een bijdrage geleverd. Enorm bedankt voor alle tijd en energie die je daarin gestoken hebt! Julia, many thanks for the mathematical input! Chapter 2, 3 and 4 would not have existed without your help. Steven, bedankt voor de goede samenwerking op het MIRS project. Het zijn twee mooie stukken geworden. Vera en Liset, ook jullie zijn aan de laatste loodjes bezig. Veel succes nog even, ik kijk uit naar jullie boekjes.

Ook mijn studenten mag ik natuurlijk niet vergeten. Anja, je hebt veel tijd gestoken in het Amplicot project, gelukkig heeft het toch een mooi paper opgeleverd. Ramona, thank you very much for your contribution to the CMV study. Huib, ook jij hebt een bijdrage geleverd aan de CMV studie, heel erg bedankt daarvoor.

Zonder proefpersonen zou dit boekje uit heel wat minder hoofdstukken bestaan. Tania en Inge, ik wil jullie heel erg bedanken voor alle inclusies en het afnemen van materiaal.

Irina, when I started working on Amplicot I never envisioned ending up in Biophysical Journal... I very much enjoyed our collaboration and I learned a lot from all our discussions.

Gerrit en Koos, dankbaar ben ik voor alle uren die jullie met mijn materiaal achter de Aria hebben doorgebracht!

Ik kijk met veel plezier terug op mijn tijd in AIO kamer 3. Ex-kamergenoten, in de laatste samenstelling Thijs, Hilde, Peter, Cordula, Kristof, Kirsten, Wouter, Bart, Lodewijk en Marit, bedankt voor de gezelligheid.

Lieve vrienden en vriendinnen, jullie wil ik bedanken voor de nodige ontspanning (kopjes thee, etentjes, sinterklaasavondjes en vakanties...). Het heeft de jaren van de promotie een stuk lichter gemaakt!

Jasper en Armida, jullie heb ik leren kennen tijdens mijn stage. Ik vind het super dat we nog steeds vrienden zijn!

Emy, je bent mijn liefste vriendin, met jou kan ik alles delen. Bedankt dat je er bent, al bijna 20 jaar! Ik ben heel blij dat je vandaag naast me staat als paranimf.

Hans, Janny, Ed en Sabine, je schoonfamilie heb je niet voor het uitkiezen, maar ik heb het erg met jullie getroffen. Met de komst van Luca en straks zijn broertje of zusje wordt het er alleen maar leuker op.

Ver, mijn broer, al zou je niet zeggen dat wij dezelfde genen hebben, we kunnen het erg goed met elkaar vinden! Leuk dat je mijn paranimf wilt zijn. Lotte, never a dull moment met jou, het is altijd gezellig als we elkaar zien.

Pa en ma, bedankt voor alles wat jullie me altijd hebben gegund! Het heeft het studeren en promoveren voor mij een stuk makkelijker gemaakt. Ook wil ik jullie bedanken voor jullie voortdurende interesse in mijn werk. Ik hoop dat na het doorbladeren van dit boekje alles een beetje op z'n plaats valt.

Lieve Ben, je bent er nog maar pas en nu al niet meer weg te denken. Ik ben heel blij met je!

Lieve Bob, je bent mijn steun en toeverlaat, bij jou kan ik met alles terecht. Menig vrij uur is de afgelopen jaren in mijn promotie gaan zitten, bedankt voor je geduld en begrip hiervoor. Ook wil ik je bedanken voor alle mooie avonturen die we in onze vrije tijd samen hebben beleefd. Ons grootste avontuur is pas begonnen, het ouderschap! Ik kijk erg uit naar de jaren die nog voor ons liggen!